UNIVERSIDADE FEDERAL DE SÃO CARLOS
CENTRO DE CIÊNCIAS BIOLÓGICAS E DA SAÚDE
PROGRAMA DE PÓS-GRADUAÇÃO EM CIÊNCIAS AMBIENTAIS

CAMILA TAVARES PEREIRA

DINÂMICA CLIMÁTICA E COMPORTAMENTO TÉRMICO EM DISTINTAS LOCAL CLIMATE ZONES EM UMA CIDADE TROPICAL COSTEIRA

SÃO CARLOS -SP
2020

CAMILA TAVARES PEREIRA

DINÂMICA CLIMÁTICA E COMPORTAMENTO TÉRMICO EM DISTINTAS LOCAL CLIMATE ZONES EM UMA CIDADE TROPICAL COSTEIRA

Tese apresentada ao Programa de Pós-Graduação em Ciências Ambientais da Universidade Federal de São Carlos, como parte dos requisitos para a obtenção do título de Doutora em Ciências Ambientais[1].

Orientador: Prof. Dr. Vandoir Bourscheidt
Coorientador: Prof. Dr. Érico Masiero

São Carlos-SP
2020

UNIVERSIDADE FEDERAL DE SÃO CARLOS

Centro de Ciências Biológicas e da Saúde
Programa de Pós-Graduação em Ciências Ambientais

Folha de Aprovação

Defesa de Tese de Doutorado da candidata Camila Tavares Pereira, realizada em 25/03/2020.

Comissão Julgadora:

Prof. Dr. Érico Masiero (UFSCar)

Prof. Dr. Vandoir Bourscheidt (UFSCar)

Profa. Dra. Renata Bovo Peres (UFSCar)

Profa. Dra. Denise Helena Silva Duarte (USP)

Prof. Dr. Gustavo Zen de Figueiredo Neves (EESC/USP)

Prof. Dr. Victor Eduardo Lima Ranieri (EESC/USP)

AGRADECIMENTOS

A trajetória do doutorado foi realizada com a contribuição e participação de pessoas muito especiais.

Gostaria de agradecer meu orientador, Prof. Dr. Vandoir, pela forma como me ajudou a conduzir o trabalho, pela amizade, paciência, paçoca, por sempre achar tempo mesmo à distância e pela forma sutil de dizer quando algo estava muito errado ou muito ruim, ou ambos.

Agradeço ao meu coorientador, Prof. Dr. Érico, por aceitar embarcar junto nesta caminhada, pelas conversas, apoio e contribuições significativas no processo de aprendizagem.

Meu eterno agradecimento ao Prof. Dr. Gerald Mills, University College Dublin (Irlanda), por fazer parte do meu sonho. Go raibh maith agat pela orientação, carinho e apoio durante todo o intercâmbio.

Aos amigos da salinha, que me proporcionaram conhecimento vasto na arte de fazer café com a mesma medida, que fizerem manhãs e tardes menos solitárias. Obrigada mais que especial ao meu amigo Raul, não só pelo café, pão na chapa, paçoca, memes do Vandoir, mas também pelo apoio incondicional nas etapas de campo, por dominar o Qgis e passar pacientemente seu conhecimento para mim.

Gostaria de agradecer ao pessoal de Santos que não só viabilizaram a pesquisa, mas fizerem da coleta de campo momentos prazerosos, obrigada ao casal David e Adriana e a técnica Adriana da Universidade Católica de Santos. Ao secretário Gunther Graf, coordenador de Informações Urbanas da Secretaria de Desenvolvimento Urbano (Sedurb), por disponibilizar dados necessários para as simulações da tese. Da mesma forma, gostaria de agradecer e muito ao prof. Renan da Universidade Santa Cecilia (Santos) que não mediu esforços a todos os meus pedidos de ajuda (e foram muitos).

Aos técnicos e professores do Decam que me ajudaram de alguma forma no desenrolar do projeto.

Agradeço aqueles que me acompanham desde sempre e que estão no meu coração, minha família querida, em especial a minha mãe, pelas inúmeros sim quando eu precisei e pelo suporte, que sem esses não seria possível realizar o doutorado.

Tire as construções da minha praia
Não consigo respirar
As meninas de mini saia
Não conseguem respirar
Especulação imobiliária
E o petróleo em alto mar
Subiu o prédio eu ouço vaia"
(Lucro – Baiana System)

RESUMO

Tavares, C. P. – Dinâmica climática e comportamento térmico em distintas Local Climate Zones em uma cidade tropical costeira. 2020 – 101p: Tese (Doutorado) – Universidade Federal de São Carlos, Centro de Ciências Biológicas e da Saúde, Programa de Pós-Graduação em Ciências Ambientais, São Carlos – 2020.

Nas últimas décadas, reconhecendo os efeitos nocivos da urbanização na saúde humana, numerosos estudos vêm sendo realizados em cidades tropicais e subtropicais, principalmente no que diz respeito as Ilhas de Calor Urbano (ICU) e ao conforto térmico. Além disso, avanços na área da climatologia urbana aplicada foram feitos por meio da metodologia elaborada por Stewart e Oke (2012) ao classificar o ambiente em *Local Climate Zones* (LCZ). Nesta perspectiva, esta tese teve como objetivo avaliar a dinâmica e o comportamento térmico que diferentes LCZs, condicionadas pelos aspectos físicos, sociais e econômicos, têm sobre a formação e alteração do microclima da cidade de Santos (São Paulo). Para isso, adotaram-se vários métodos e ferramentas com a finalidade de produzir informações relevantes do clima da cidade. Desta forma, três principais abordagens foram analisadas e discutidas no decorrer da tese: a sazonalidade das ICU nas LCZs; a influência dos diferentes espaços urbanos na temperatura radiante média e de superfície; e o conforto térmico em distintas LCZs. A variabilidade temporal da ICU foi analisada com base em coleta de dados climáticos durante o verão e o inverno sob "condições meteorológicas ideais". Os resultados indicam dois comportamentos termais distintos da ICU nas LCZs. Durante o período noturno, os valores máximos da ICU foram observados na *compact high-rise building* (HRB), enquanto no período diurno, maiores magnitudes da ICU foram observadas na *compact low-rise* (CLR2), ambos mostrando a influência do fator de visão do céu e da vegetação na ICU. Em relação à segunda abordagem, a fim de observar a influência das morfologias urbanas na temperatura radiante média e na temperatura de superfície, duas metodologias foram empregadas: cálculo da temperatura de superfície e simulações do modelo urbano. A primeira foi obtida por meio do plugin Land Surface Temperature (QGIS – v2.8.9), e a segunda a partir do software The Solar *LongWave Environmental Irrandiance Geometry model* (SOLWEIG, v2019a – QGIS). Em ambas análises ficou evidente a contribuição da vegetação e do sombreamento dos edifícios na diminuição da temperatura radiante média e na temperatura de superfície. Na terceira abordagem, HRB e CLR2 foram escolhidas para análise do conforto térmico, utilizando o *Physiological Equivalent Temperature* (PET), calculado por meio do SOLWEIG. Destarte, ficou evidente a distinção socioespacial das LCZs formadas a partir da valoração dos espaços, principalmente pelo mercado turístico, o qual influência até hoje a infraestrutura urbana disponível em cada área. Espaços estes que foram determinantes para os níveis de conforto térmico observados durante o verão e o inverno nas duas LCZs. Assim, os resultados evidenciaram a situação crítica de stress térmico dos moradores da CLR2 principalmente durante o verão. De tal modo, a tese avançou tanto no enriquecimento teórico do clima urbano de uma cidade tropical costeira, assim como na questão de planejamento, ao discutir as variáveis que possam contribuir para a qualidade ambiental de cada LCZ.

Palavras-chave: Local Climate Zones; Ilhas de calor urbano; SOLWEIG; Temperatura radiante média; Temperatura de Superfície. Conforto térmico; Santos.

ABSTRACT

In recent decades, recognizing the harmful effects of urbanization on human health, numerous studies have been carried out in tropical and subtropical cities, mainly regarding Urban Heat Islands (UHI) and thermal comfort. In addition, advances in the field of applied urban climatology were made using the methodology developed by Stewart and Oke (2012), based on the classification of the environment in Local Climate Zones (LCZ). In this perspective, this thesis aimed to evaluate the dynamics and thermal behavior that different LCZs, conditioned by physical, social, and economic aspects, have on the formation and alteration of the microclimate in the city of Santos (São Paulo). For this, several methods and tools were adopted in order to produce relevant information about the city's climate. In this way, three main approaches were analyzed and discussed on the present thesis: the UHI seasonality in LCZs; the influence of different urban spaces on the surface and mean radiant temperature; and thermal comfort in different LCZs. The seasonal variability of the UHI was analyzed based on the collection of climatic data during summer and winter under "ideal weather conditions". The results showed two thermal behaviors distinct from the UHI in the LCZs. During the night time, maximum UHI values were observed in the compact high-rise building (HRB), while in the daytime, higher UHI magnitudes were observed in the compact low-rise (CLR2), both showing the influence of the sky view factor and vegetation in the UHI. Regarding the second approach, in order to observe the influence of urban morphologies on the mean radiant temperature and on the surface temperature, two methodologies were used: calculation of the surface temperature and simulations of the urban model. The first was obtained through the Land Surface Temperature plugin (QGIS - v2.8.9), and the second from The Solar LongWave Environmental Irrandiance Geometry model (SOLWEIG, v2019a - QGIS). In both analyzes, the contribution of vegetation and the shading of buildings were evident in the reduction of the mean radiant temperature and in the surface temperature. In the third approach, HRB and CLR2 were chosen for the analysis of thermal comfort, using the Physiological Equivalent Temperature (PET), calculated through SOLWEIG. Thus, the socio-spatial distinction of LCZs formed from the valuation of spaces was evident, mainly due to the tourism market, which influences the urban infrastructure available in each area until today. These spaces were decisive for the levels of thermal comfort observed during summer and winter in the two LCZs. Thus, the results showed the critical situation of thermal stress of CLR2 citizens, especially during the summer. In such a way, the thesis advanced both in the theoretical enrichment of the urban climate of a tropical coastal city and in the question of planning, when discussing the variables that may contribute to the environmental quality of each LCZ.

Keywords: Local Climate Zones; Urban Heat Island; SOLWEIG; Mean radiant temperature; land surface temperature; Thermal comfort; Santos.

LISTA DE FIGURAS

LISTA DE TABELAS

ABREVIATURAS E SIGNIFICADOS

Centro Nacional de Monitoramento e Alertas de Desastres Naturais - CEMADEN

Companhia Ambiental do Estado de São Paulo - CETESB

Instituto Brasileiro de Geografia e Estatística - IBGE

Instituto Nacional de Meteorologia - INMET

Local Climate Zones - LCZ

METeorological Aerodrome Report - METAR

Região Metropolitana da Baixada Santista - RMBS

SOlar and LongWave Environmental Irradiance Geometry model - SOLWEIG

World Urban Database and Access Portal Tools - WUDAPT

SUMÁRIO

ESTRUTURA DA TESE

A tese aborda como tema central os microclimas da cidade de Santos, mais especificamente a variação temporal, sazonal e espacial da dinâmica e do comportamento térmica em quatro áreas representativas da diversidade urbana e socioeconômica. A partir desse tópico, importantes discussões foram elaboradas nos artigos que, juntos, constroem a linha narrativa da tese, sendo esta composta por uma introdução, 3 artigos – que, de modo diferente e complementar, relacionam a especificidade de cada área, assim como a resposta térmica em diferentes escalas espaciais – e pelas considerações finais.

Na introdução do trabalho, um breve referencial histórico sobre clima urbano, Ilhas de calor e estudos sobre parametrizações de cenários são apresentados, bem como a proposta, as questões e os objetivos da tese. No final desta introdução também foi incluída a caracterização da área de estudo, a fim de auxiliar na compreensão do que foi discutido nos artigos.

O primeiro artigo, "Seasonal variation of canopy layer heat island at distinct Local Climate Zones in a tropical coastal city", consiste na análise e interpretação dos dados de temperatura do ar coletados em cinco áreas classificadas em Local Climate Zones (LCZ), segundo a proposta de Stewart e Oke (2012). A coleta de dados teve início no dia 17 de novembro de 2017 e finalizou no dia 18 de outubro de 2018. A partir desta, foi possível avaliar a sazonalidade das Ilhas de Calor segundo as propriedades urbanas de cada LCZ. Desta forma, identificou-se quais LCZs são mais suscetíveis a formação e intensificação deste fenômeno, tal como quais fatores contribuem para amenizá-lo.

O segundo artigo, "Analysis of Local Climate Zones and vegetation cover using land surface temperature and mean radiant temperature in a coastal city with a tropical climate", apresenta a variação espacial e temporal da temperatura radiante média (TRM) e da temperatura de superfície (TS) nas LCZs em um dia de alta radiação durante o verão na cidade de Santos (17 de dezembro de 2017). Para isso, utilizamos dois métodos de comparação, o primeiro relacionado à temperatura de superfície obtida pelo satélite LANDSAT 8, e o segundo por meio do modelo Solar and LongWave Environmental Irradiance Geometry (SOLWEIG), na mesma data descrita acima. Posteriormente, a variação diurna da temperatura radiante média e a influência da vegetação foram analisadas para todas as LCZs.

O terceiro artigo, "Socio-spatial inequality and its relationship to thermal (dis)comfort in two major Local Climate Zones in a tropical coastal city", apresenta a sazonalidade do microclima urbano por meio de duas abordagens, TRM e conforto térmico, em duas principais e distintas LCZs na cidade de Santos. Desta forma, destaca-se o processo de urbanização em ambas áreas e como este influenciou na formação de diferentes ambientes térmicos urbanos.

INTRODUÇÃO

O clima urbano é o produto das alterações que o homem provoca no ambiente natural. Por consequência, a população citadina é que sofre as influências das transformações climáticas locais. Segundo Landsberg (2006), há três causas básicas para as mudanças climáticas locais que podem ser provocadas pela urbanização. A primeira é a alteração na superfície, quando, por exemplo, uma floresta densa é substituída por um complexo de substâncias rochosas, como tijolos e concreto; naturalmente, locais úmidos, dentre eles, charcos e pântanos, são drenados e a rugosidade aerodinâmica é aumentada por obstáculos de variados tamanhos. A segunda causa consiste na produção de calor nas cidades, sendo este proporcionado pelo metabolismo da massa de seres humanos e animais, pelo calor liberado por indústrias, e ampliado nos anos recentes pela ampla expansão dos veículos com motores de combustão interna. Por fim, a terceira maior influência das cidades sobre o clima refere-se à transformação da composição atmosférica, frequentemente com algum deslocamento em relação às áreas densamente povoadas.

Um dos fenômenos mais documentados referentes as mudanças climáticas é a Ilha de Calor Urbana (ICU), com observações e dados de monitoramento das características deste fenômeno disponíveis desde o início do século anterior ou até antes (Santamouris, 2015). De acordo com Oke (1981), a formação da Ilha da ICU pode ser atribuída aos seguintes fatores:

- ❖ Modificação do balanço das radiações, sobretudo a retenção da radiação do infravermelho termal ao nível das ruas;
- ❖ Redução da evaporação e evapotranspiração devido à escassez de vegetação e extensão de superfícies impermeabilizadas;
- ❖ Diminuição da velocidade do vento (em razão da elevada rugosidade do espaço urbano) e, consequentemente, das transferências de calor sensível;
- ❖ Alteração da composição da atmosfera urbana;
- ❖ Produção de calor pelas atividades urbanas;
- ❖ Acúmulo de calor (e gradual liberação durante a noite) pelos edifícios e materiais de construção.

O aumento da intensidade da ICU pode afetar negativamente o bem-estar dos cidadãos de várias maneiras, como danos no sistema termo regulatório causados por estresse por calor, estresse cardiovascular, exaustão térmica, ataque cardíaco e doenças cardiorrespiratórias (Aflaki et al., 2017). Estudos realizados pela Organização Mundial de Saúde (OMS) e o

Programa das Nações Unidas para o Meio Ambiente (PNUMA) indicam que as condições de conforto térmico afetarão milhares de pessoas no futuro, uma vez que estão relacionadas ao clima e à forma de apropriação e interação com os espaços locais e/ou regionais (Observatório do Clima, 2009).

A título de exemplo, a onda de calor que atingiu Chicago em 1995 matou entre 550 e 800 pessoas. Da mesma forma, na Europa, a morte de 35.000 pessoas foi atribuída ao calor durante o verão de 2003 (Wang; Berardi; Akibari, 2015). Em 2010, na cidade de Santos, uma forte onda de calor ocorrida na primeira semana de fevereiro causou a morte de 32 pessoas idosas. As temperaturas atingiram 39°C com a sensação térmica de até 45°C (Lima, 2010 - O Estado de São Paulo).

Estudos sugerem que fenômenos extremos como estes estão se tornando cada vez mais frequentes por causa das mudanças climáticas (Nobre et al., 2010). As distintas condições adversas ao conforto e à segurança humana nos conglomerados urbanos em grande parte das cidades, em especial nas metrópoles, devem, portanto, se intensificar devido às mudanças climáticas locais e globais. São previstas repercussões como o aumento da vulnerabilidade do espaço construído e das populações, do custo de manutenção e adaptação da infraestrutura, dos espaços urbanos e das edificações, com efeitos socioeconômicos de diversas ordens, desde o detrimento de vidas humanas ao acréscimo do custo dos seguros dos bens localizados em determinadas áreas urbanas (Bueno et al., 2012).

Com o intuito de formular medidas mitigatórias para as condições atuais e futuras em relação ao clima urbano, diversos estudos vêm utilizando simulações por meio de diferentes modelos de estrutura urbana ou *Urban Canopy Model* (*e.g.* ENVI-met, SUEWS, SOLWEIG, RayMan). Além disso, por meio destes modelos é possível identificar quais são as respostas térmicas e as medidas mais eficazes para cada ambiente construído, levando em consideração alguns fatores condicionantes, sendo os principais: construção, pavimento, asfalto, tipo de superfície, vegetação, altura dos edifícios e o fator de visão do céu (FVC). Estas variáveis ambientais urbanas podem, até certo ponto, ser controladas pela atividade de planejamento e projeto, em ambas escalas, da cidade e do edifício, por meio das legislações de uso e ocupação do solo, códigos de edificações etc. (Duarte, 2015). Desta forma, podemos destacar diversos estudos que trabalharam com tais parametrizações em diferentes escalas do clima (Acero e Arrizabalaga, 2016; Alexander, Mills e Fealy, 2015; Emmanuel, Rosenlund e Johansson, 2007; Hammerberg et al., 2018; Järvi, Grimmond e Christen, 2011; O'malley et al., 2015; Rafael et al., 2017). No Brasil, importantes estudos foram feitos em relação à formação de microclimas segundo a morfologia urbana, muitos destes utilizando o modelo ENVI-met: Alves, Andrade e Nery (2011) em Salvador, Gusson (2014) em São Paulo, Masiero (2014) em São Jose do Rio

Preto, Krüger, Minella e Rasia (2010), e Schmitz (2014) em Curitiba, Soares et al., (2011) em João Pessoa.

SOLWEIG é outro programa vem ganhando destaque em estudos de simulações do clima urbano. Trata-se de um modelo computacional gratuito capaz de simular as variações espaciais da temperatura radiante média e fluxos 3D de radiação de ondas longas e ondas curtas. O SOLWEIG usa o modelo digital de superfície (*DSM)* e dados meteorológicos como dados primários de entrada e implementa algoritmos para o cálculo de outras variáveis, como Fator de Visão do Céu (*SVF*). Dessa maneira, ele pode lidar com o ambiente urbano real e calcular valores de *Tmrt* para um grande domínio espacial de uma maneira computacionalmente eficiente e rápida. Destarte, o SOLWEIG possui vantagens sobre outros modelos que consomem muito tempo, como o ENVI-met, ou que podem lidar apenas com pontos de interesse, como o RayMan (Chen et al., 2016). O SOLWEIG vem sendo empregado para simulações em diferentes cidades e ambientes urbanos (Chen et al., 2016; Chen, Lin e Matzarakis, 2014; Lau et al., 2016; Lindberg e Grimmond, 2011; Lindberg, Holmer e Thorsson, 2008). Além disso, constantes melhorias foram feitas no modelo, como a inclusão do efeito da vegetação (Lindberg e Grimmond, 2011) e do material de superfície (Lindberg, Onomura e Grimmond, 2016).
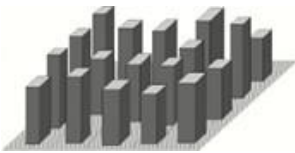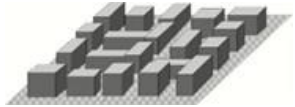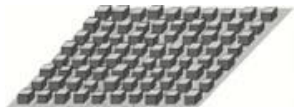
Neste contexto, apesar da cidade de Santos e a Baixada Santista como um todo, já terem sido alvo de importantes estudos em climatologia e parametrizações no contexto de mudança climática (Alfredini et al., 2013; Alfredini et al., 2014; Alfredini, Arasaki e Pezzoli, 2015; Young, 2016), até o momento não há estudos que relacionem e analisem as diferentes morfologias urbanas de Santos e sua influência na alteração do microclima no cenário atual a partir de dados de campo e simulações. Em relação ao município de Santos, segundo o Plano Diretor (2018), este é subdividido em sete macrozonas[2]: Leste, Centro, Noroeste, Morros, Continental 1 e 2, e Estuário. As macrozonas são formadas de acordo com suas características urbanas, ambientais, sociais e econômicas similares, assim como em relação à política de desenvolvimento urbano. Desta forma, áreas que representassem as diferentes condições tanto de estrutura urbana como socioeconômica situadas em diferentes macrozonas foram escolhidas para análise e posteriormente classificadas segundo a proposta de Stewart e Oke (2012) em *Local Climate Zones (LCZ)*. Stewart e Oke (2012) definem as LCZs como regiões de coberturas de superfícies uniformes, estrutura, material e atividades humanas que podem abranger centenas de metros a vários quilômetros em escala horizontal. Originalmente desenvolvido para

---
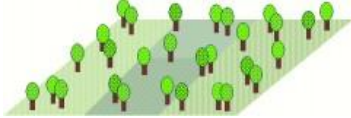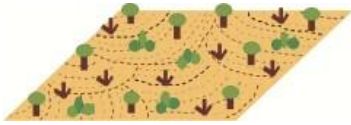
[2] Mapa disponível em:
https://www.santos.sp.gov.br/static/files_www/conteudo/planodiretor/LC%20821_2013_Plano%20Diretor_Anexo%20III_Macrozonas%20INSULAR%20%2B%20AC-A0.pdf

facilitar a comparação dos estudos observacionais das ICU e para fornecer um protocolo objetivo para medir a intensidade das mesmas, as LCZs são divididas em 17 classes, sendo 10 referentes a tipologia construtiva e 7 nos tipos de cobertura do solo (Tabela 1).

Tabela 1. Tipos de LCZ (Adaptado de Stewart e Oke, 2012).

LCZ	Tipologia construtiva	
1	Ocupação compacta e edificações elevadas	
2	Ocupação compacta e edificações médias	
3	Ocupação compacta e edificações baixas	
4	Ocupação aberta e edificações elevadas	
5	Ocupação aberta e edificações médias	
6	Ocupação aberta e edificações baixas	
7	Ocupação desordenada e edificações baixas	
8	Grandes compartimentos e edificações baixas	
9	Ocupação espaçada com edifícios isolados	

10	Zona industrial	
LCZ	**Tipo de cobertura do solo**	
A	Vegetação densa	
B	Vegetação esparsa	
C	Arbustos isolados	
D	Plantação rasteira	
E	Pavimento	
F	Solo exposto ou arenoso	
G	Corpos d'agua	

Para a classificação e mapeamento das LCZs para a cidade de Santos seguimos a metodologia disponível no World Urban Database and Access Portal Tools (WUDAPT). O WUDAPT é uma iniciativa global, que tem como objetivo preencher as lacunas de dados necessários para resolver os desafios globais das cidades e comunidades sustentáveis e como um guia para facilitar ações baseadas no clima (Mills et al., 2015; See et al., 2015). Diversos pesquisadores têm feito uso desta ferramenta em diferentes cidades ao redor do mundo, como em Hamburgo (Bechtel e Daneke, 2012), Glasgow (Emmanuel e Krüger, 2012), Szeged (Lelovics, 2014), Phoenix (Middel, 2014), Dublin (Alexander e Mills, 2014), Berlin (Mitraka, 2015), Hong Kong (Ren et. al., 2016), Kochi (Thomas et al., 2014), Delhi (Sharma et al., 2016),

Nagpur (Kotharkar e Bagade, 2018), Colombo (Perera e Emmanuel, 2016), Nanjing (Yang et al., 2018), São Paulo (Ferreira e Duarte, 2019) entre outras.

Segundo Perera e Emmanuel (2018), uma das principais dificuldades na aplicação do conhecimento do clima urbano no planejamento e tomada de decisões nos trópicos é a falta de dados, tanto em termos de elementos significativos da cobertura do uso da terra quanto em seus efeitos no clima local. Destarte, em vista das abordagens anteriores, este projeto tem como propósito avançar os estudos referentes ao clima urbano em multi escala, temporal e espacial, a fim de compreender quais fatores influenciam na alteração da temperatura do ar (Ta), na temperatura radiante média TRM como também no conforto térmico, na expectativa de propor medidas que colaborem no arrefecimento das áreas em questão. Diante desta perspectiva, a localização da área de estudo é representativa das principais condições geográficas de maior vulnerabilidade, uma vez que se situa em área costeira e apresenta típica morfologia urbana e verticalizações que interferem e alteram a dinâmica termal da cidade (Acero et al., 2013; Alcoforado et al., 2006; Prata, 2005). Dessa forma, podemos destacar principalmente as altas rugosidades ao longo da orla que impedem a penetração dos ventos ao centro da cidade, a impermeabilização do solo, a tendência ao uso de iluminação e climatização artificiais e informais, a infraestrutura e edificações frágeis e a intensa urbanização e densidade. Assim, esta proposta vem a enquadrar-se, a fim de aprofundar os estudos de ICU em cidades tropicais e oferecer subsídios adicionais que possam contribuir para mitigar ou melhorar os componentes do microclima urbano no cenário atual de Santos.

Questões da pesquisa

❖ Como se comporta o campo térmico em diferentes tipos de ambiente urbano em uma cidade litorânea?

❖ Qual a relação dessas áreas com o processo de urbanização?

❖ Existem alternativas, considerando os interesses públicos e privados, de amenizar os campos térmicos das diferentes áreas?

Objetivo geral

Este projeto tem como objetivo principal investigar qual o comportamento térmico e influências que diferentes LCZs, condicionadas pelos aspectos físicos, sociais e econômicos, têm sobre a formação e alteração do microclima da cidade de Santos.

Objetivos Específicos

❖ Avaliar componentes climáticos específicos (temperatura do ar, temperatura radiante média, fluxo do vento e radiação) em cinco diferentes LCZs na cidade de Santos em distintas sazonalidades.

❖ Determinar como os fatores condicionantes urbanos (volume de construção, arranjo espacial, espaços verdes, tipos de superfície) influenciam na formação de microclimas utilizando o modelo de simulação SOLWEIG.

❖ Averiguar o conforto térmico das LCZs levando em consideração as distintas formas de produção do espaço urbano.

❖ Avaliar como o cenário de aumento de gabarito estabelecido pelo Plano Diretor pode influenciar o microclima urbano da Macrozona Noroeste da cidade.

Área de estudo

A cidade de Santos (Figura 1) está geograficamente situada no litoral centro do Estado de São Paulo e configura um compartimento isolado na forma de baixada, com morros separados entre a serra e o oceano. Em 2018, Santos possuía uma população estimada de 432,957 mil habitantes (Instituto Brasileiro de Geografia e Estatística - IBGE, 2018). A partir de 1996, Santos foi incorporada como município da Região Metropolitana da Baixada Santista (RMBS), composta pela aglomeração e conurbação dos municípios de São Vicente, Cubatão, Praia Grande, Mongaguá, Itanhaém, Peruíbe, Bertioga e Guarujá (Zündt, 2006). A RMBS é um ambiente caracterizado pela influência direta dos fenômenos ocorridos em zona costeira. Observa-se cenários com baixa e alta densidade populacional, intensa urbanização, atividades industriais em larga escala, exploração turística, e ecossistemas complexos e de importante significado ambiental (IBGE, 2002).
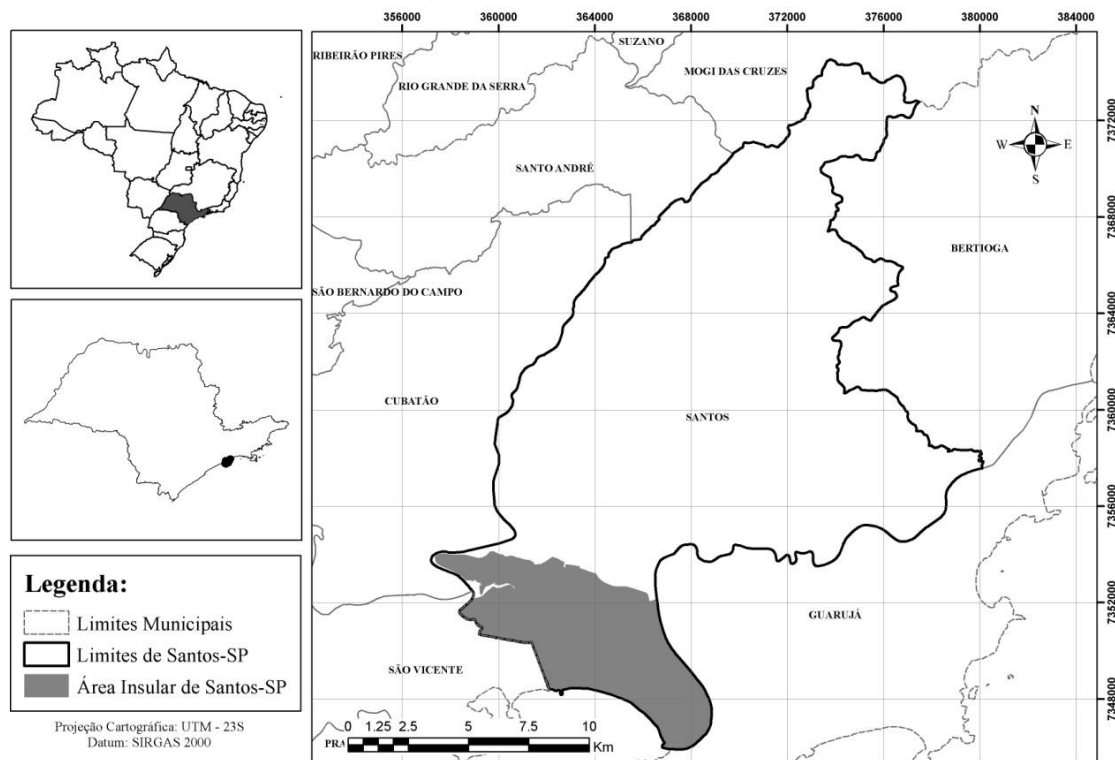
Figura 1 Localização da área insular de Santos, objeto de estudo do projeto.

Santos possui um clima típico do Atlântico Tropical, influenciado pela proximidade do oceano e suas preponderâncias nos padrões de circulação atmosférica, que tem função essencial nos elementos climáticos, como temperatura, precipitação e direção do vento. A temperatura média anual em Santos é de cerca de 21,9 °C, com uma diferença de 5 °C entre as estações de verão e inverno (Young, 2016). Em média, a cidade de Santos recebe cerca de 2500 milímetros de precipitação total anual concentrada nos meses de outubro a abril (75%) e um total mensal médio de 317 milímetros (Miller et al., 2012). Em relação ao padrão de ventilação, a alternância da brisa marítima e terrestre estabelece uma troca térmica permanente. Além disso, os ventos vindos de sul e sudeste, acompanhados pelas massas polares, são predominantes de abril a setembro, sendo responsáveis por carregar umidade para região e aumentar a nebulosidade (Prata, 2005). O outro padrão de ventos é o de noroeste, caracterizado pela chegada de frentes frias, e que causa mudanças no tempo, soprando com maior intensidade de maio a agosto. Em janeiro, ventos intensos de Noroeste trazem tempestades de verão (Afonso, 2001).

A Baixada Santista é a área de ocupação urbana mais antiga do Estado de São Paulo e uma das primeiras do Brasil colônia. Desde a sua formação, a região estava ligada às atividades portuárias. Alguns eventos relacionados à exportação de café, construção de portos e ferrovias contribuíram para o incipiente desenho urbano de Santos durante o século XIX. Nos primeiros anos do século XX, canais foram construídos em todo o lado oeste para saneamento e embelezamento dos caminhos pelo Engenheiro Sanitarista Saturnino Brito. Em meados do

referido século, dois fatores dicotômicos impulsionaram a expansão urbana de Santos. O primeiro relacionado à construção da rodovia Anchieta, que propiciou o processo de verticalização da orla, impulsionada pelo turismo de verão. Já o segundo, ligado ao processo de construção civil e ao porto, impulsionou a ocupação desordenada de moradores na zona noroeste do município, até então ambiente natural de banco de areia e manguezal. Muitos dos novos habitantes desta área vieram principalmente da região Nordeste do país. Esses fatores têm contribuído até agora no desenvolvimento dessas três áreas principais: (i) a região sudeste, localizada próxima à praia, na qual concentra a maior parte dos investimentos e dinamismo econômico; (ii) a área norte, que coincide com o antigo núcleo histórico; e (iii) a região noroeste, que concentra um grande número de assentamentos informais de baixa qualidade com moradores na sua maioria de baixa renda. O processo de intensa ocupação da cidade de Santos originou uma cadeia de impactos ambientais, marcada pela poluição industrial, portuária e domiciliar, acompanhada de grande adensamento urbano na orla e surgimento de assentamentos subnormais (Secretaria de Planejamento e Desenvolvimento Sustentável, 2011).

Seasonal variation of canopy layer heat island at distinct Local Climate Zones in a tropical coastal city

Abstract

This work examines the characteristics of the seasonal canopy layer heat island (UHI$_{UCL}$) in a medium-sized coastal city in the state of São Paulo using the Local Climate Zones approach. The present analysis is based on datalogger campaign conducted from 15th November 2017 to 11th October 2018, complemented by full meteorological data from two stations, one inside the urban area and other in the vicinities (used as a general reference). A careful analysis was conducted to select the more representative days (minimum cloudiness, homogeneous solar radiation, and no/low wind), and the resulting dataset was organized in two seasons: summer and winter. Based on the UHI intensity analysis, the results indicate that, during the night period, the temperature anomaly (UHI$_{UCL}$= LCZx - LCZy) is higher in the compact high-rise buildings and during the winter. During daytime, the maximum was found in compact low-rise building and for summer period, although strong variations where observed. Those variations seem to be related with the patterns of solar exposure, shading, and vegetation of each area, but may also be associated with the differences observed between the urban and rural station. This suggests that UHI intensity analysis during daytime strongly depends on complete meteorological information.

Keywords: Canopy layer heat island; Local Climate Zones; meteorological data.

1.   INTRODUCTION

The urban climate is the product of the alterations that human activities cause in the natural environment. Cities contribute to changes in climate and atmospheric composition on different scales: local, regional, and even globally (Oke et al., 2017). Cities are more vulnerable to the effects of these alterations due to the high concentration of people, settlements, and material goods (Georgeson et al., 2016). Therefore, it is in these regions, with a large concentration of people, that the original landscape is transformed most intensely, changing the local climate. In the last decades, by recognizing the harmful effects of urbanisation on human health and thermal comfort, numerous surveys have been done in tropical and subtropical cities, mainly regarding the Urban Heat Island (UHI). The importance of UHI in summer and hot climates lays especially on the thermal discomfort (and heat-related health issues) and air quality (Sailor & Dietsch, 2007).

There has been a growing interest in the UHI, especially in the Asia-Pacific regions, in cities like Colombo (Emmanuel, 2003; 2005a,b; Emmanuel & Johansson, 2006), Kuala Lumpur

(Tso, 1996; Morris et al., 2015), Singapore (Tso, 1996; Nicol, 1996; Wong et al., 2005; Chow & Roth, 2006; Roth & Chow, 2012), and Hong Kong (Giridharn et al., 2004, 2005; Nicol & Wong, 2005; Tan et al., 2016). On the other hand, there is a lack of studies on this matter in South America, which is suffering with a disproportionate actual (and projected) urban growth. Few studies were conducted in Argentina (Bejaran & Cammiloni, 2003; Camilloni & Barrucand, 2012), and more recently in Western Pacific cities like Andacollo (Crawford et al., 2018), Antofagasta, Lima, Guayaquil, and Valparaiso (Palme et al., 2016).

In Brazil, the urban climate trajectory began with the study conducted by Monteiro (1976) related to the conception of Urban Climate System. Since that, the surveys have been evolving and expanding to other interconnected areas, such as UHI, thermal comfort, micro-urban climate, and energy management. Some examples are the works of Lombardo (1984), Assis & Frota (1999), Amorim (2002), Ribeiro (2005), Souza (2007) and Duarte (2010, 2016). More detailed analyzes are, therefore, particularly important in assessing a city's efforts to promote UHI mitigation strategies, and thus the ability of policymakers and citizens to compare different options and predict possible effects (Wang, Berardi, and Akbari, 2015).

In this context, different activities have been promoting changes in the urban environment and in the microclimate of Santos, a coastal city on the southeast of Brazil. The summer tourism, the petrochemical complex, the regional construction activity, the exploration of oil and gas from Santos Basin, as well as the infrastructure linked to the Port of Santos are some examples of such activities (Kawashima et al., 2015). And the different urban patterns imposed by those activities imply in different effects on the UHI, which are usually evaluated through the so-called Local Climate Zones (LCZs) (Stewart & Oke, 2012). LCZ framework has been applied in tropical countries by various researchers, such as Kochi (Thomas et al., 2014), Delhi (Sharma et al., 2016) and Nagpur (Kotharkar & Bagade, 2018) in India, Colombo (Perera & Emmanuel, 2016) in Sri Lanka, Hong Kong (Siu & Kart, 2013) and Nanjing (Yang et al., 2018) in China, and Sao Paulo (Ferreira & Duarte, 2019) in Brazil. Therefore, the main goal of the study is to assess the (seasonal) thermal behavior of each LCZs in Santos and the factors that most influence it, focusing not only on heat island magnitudes but also on temperature daily variations between the sites, as well as on the shadow pattern. The climatic effects of the interaction between the main airflow patterns, urban characteristics, and location of different land use categories in Santos are discussed.

2.   STUDY AREA AND METHODS

2.1 Study area

Santos (Fig. 2), located on the Southern Brazilian Coast, is considered one of the most important municipalities in the State of Sao Paulo. Since its inception, the city has been linked to port activities. Some events related to coffee exportation and railway construction contributed to the incipient urban design of Santos during the 19th century. In the early years of the 20th century, canals were built by Saturnino Brito (sanitary engineer) across the west side to improve sanitation. In the middle of the century, two dichotomous factors drove Santos's urban sprawl. The first, related to the construction of the Anchieta highway and summer tourism, provided the process of verticalization of the waterfront. The second, linked to port labor, boosted the disorderly occupation of the northwest area. These factors have so far contributed to the development of three main areas in Santos city: (i) the southeastern region, located near the beach, where most investment and economic dynamism are concentrated; (ii) the northern area, which coincides with the old historical nucleus; and (iii) the northwest region, which concentrates a large number of informal settlements with mostly low-income residents (Bloch, Papachristodoulou, and Monroy, 2012).
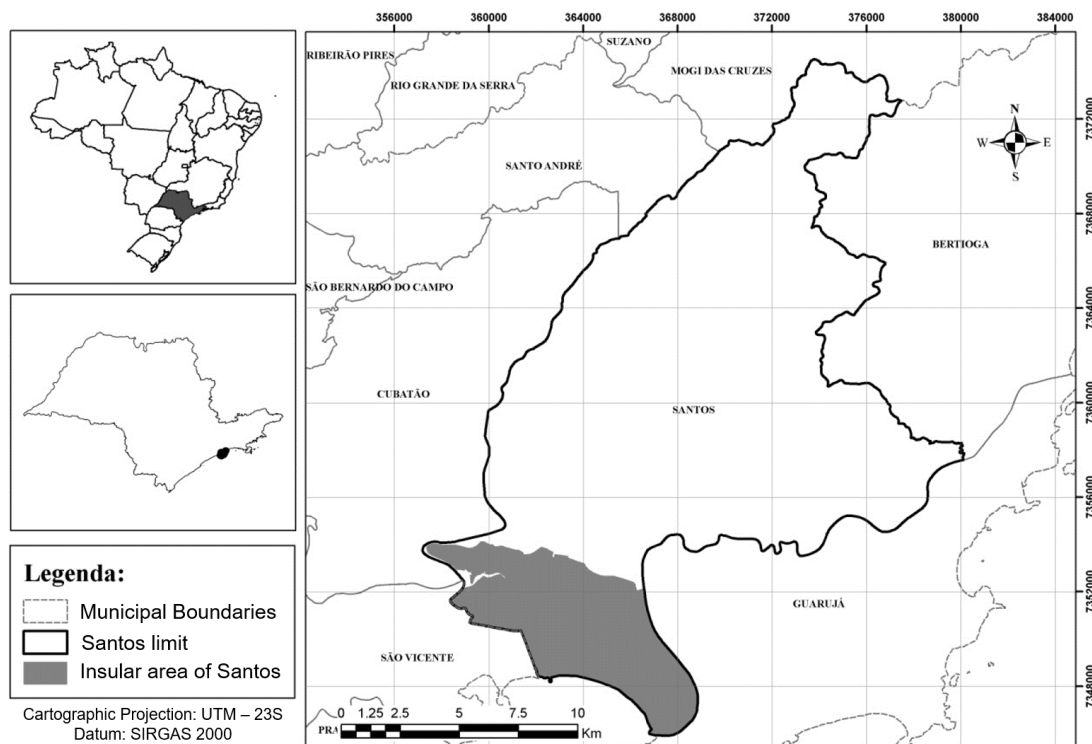
Figure 1. Location of the city of Santos, with emphasis on the island area, object of study.

.

According to Köppen's climate classification, Santos is within the Af class, characterized by a tropical rainy climate. Based on Miller et al., 2012, "the median annual temperature in Santos is around 21.9°C, with a difference of 5°C between summer and winter seasons. On average, Santos receives about 2500 mm of total annual precipitation concentrated from October to April (75%) and an average monthly total of 317 mm". Besides, the proximity of the Atlantic Ocean influences on atmospheric circulation patterns, which play an essential role in climate elements such as temperature, humidity, precipitation, and wind direction. Regarding the ventilation pattern, the alternation of the sea and land breeze establishes a permanent thermal exchange. The sea breeze blowing toward the mainland begins in the late morning and remains acting until the middle of the night when the land breeze starts to dominate until the early morning.

2.2. Local Climate Zones

This system was adopted in this study, with the sites characterized accordingly. The aim of the LCZ concept is to enhance the understanding and interpretation of air temperature differences within the urban context and to allow the communication and comparison of results among cities (Fenner et al., 2014). The landscape is represented by 17 LCZs, from which 15 are defined by surface structure and cover; and 2 by construction materials and anthropogenic heat emissions. The standard set is divided into "built types" 1–10, and "land cover types". Thus, this new classification leads to a more significant interpretation of UHI intensity through the temperature differences between LCZs and the reference station ($\Delta T = \text{LCZ}_{X-Y)}$ (Stewart & Oke, 2012). LCZ scheme was proposed to better account for the role that urban morphology plays in the UHI phenomenon and to provide a rich source of information about urban areas that is consistent and comparable among different cities (Bechtel et al., 2019). Our purpose here is not to evaluate the LCZ scheme but to use it to classify the observation sites and to understand the variations among them. The LCZ map was produced in agreement with WUDAPT methodology workflow (BechteL et al., 2015). It is based on three daytime LANDSAT 8 scenes (July 26th and November 15th, 2017 and August 30st, 2018), on training areas selected in Google Earth, and on the algorithm for Local Climate Zone classification within the System for Automated Geoscientific Analyses (SAGA) version 6.4. The classification algorithm is the so-called Random Forest classifier, which consists of integrated decision trees that classify each image pixel into one LCZ type. The LCZ map[3] spatial resolution is 100m (Fig. 3).

---

[3] See Bechtel et al., 2019 to assess more information about LCZ workflow and WUDAPT.
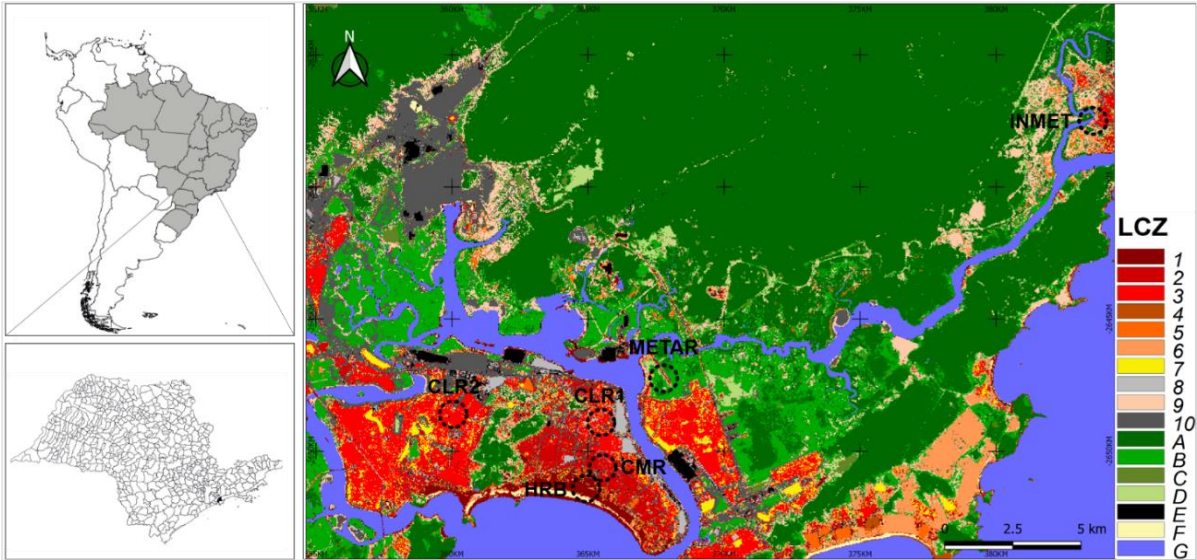
Figure 2. Santos - Local Climate Zone Classification. Circles, with radius of 500m, represents LCZs and three official stations used in this study: CETESB, METAR and INMET.

Based on the LCZ classification, our sites include compact high-rise, mid-rise and low-rise buildings. Compact high-rise building (HRB) is classified as LCZ1. Compact Mid-rise (CMR) and CETESB as LCZ2 and compact low-rise 1 and 2 as LCZ3 (Fig. 2). The reference station (INMET) was classified as sparsely built (LCZ9). The accuracy of the map was produced by Benjamin Bechtel, which showed Overall Accuracy (OA) of 0.78 and the Kappa coefficient was 0.75 (Fig. 4, left). The Weighted Accuracy (WA) (Fig. 4, right) illustrates a metric that accounts for similarity and dissimilarity between LCZs. For more information see Bechtel et al., 2019.
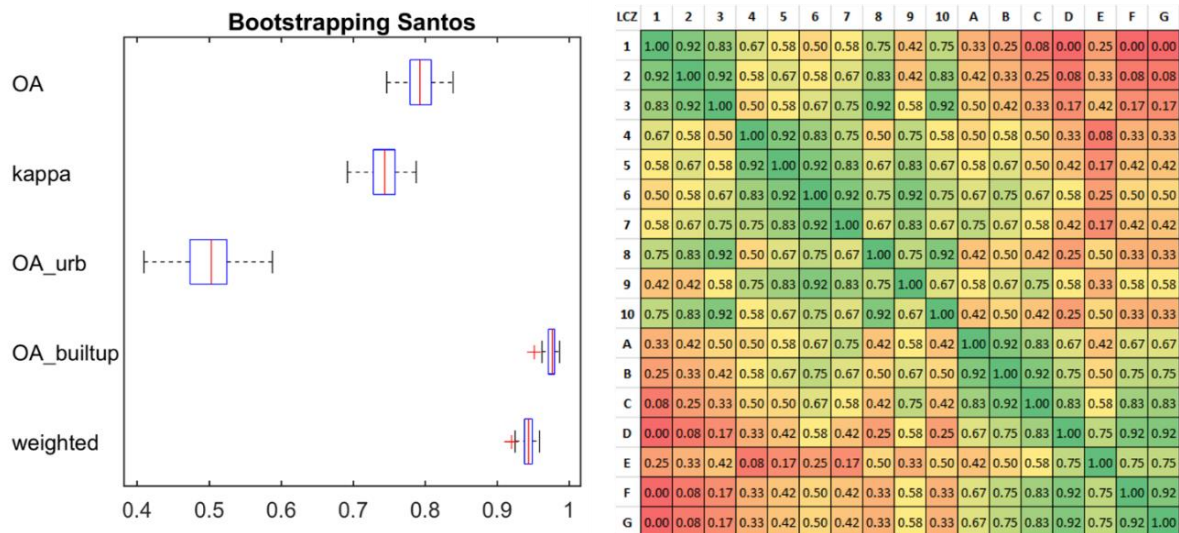
Figure 3. Bootstrapping results for Santos (left); Similarity of LCZ types applied to a weighted accuracy measure (right).

The OA_urb (Fig. 4, left) is the OA of urban-only reference polygons and thus indicates the quality for the urban classes. The OA_builtup is the overall accuracy of built vs. natural types only, ignoring their internal differentiation. WA is based on the climatic impact discussed in Stewart, Oke, and Krayenhoff (2014) and consists of up to twelve points for the properties openness, height, cover, and thermal inertia, penalizing confusion between dissimilar types more than between similar classes (Stewart, 2016 apud Bechtel et al., 2017). For instance, LCZ 1 is most alike the other two compact urban types (LCZs 2 and 3) and hereafter these pairs have higher weights than classes which are quite different, such as LCZ 1 and the natural types, as LCZ B. The weights are applied to the confusion matrix so that WA measures the accuracy of the LCZ map in terms of the expected thermal impact, rather than the percentage of predicted LCZ values that exactly match those in the reference areas (Bechtel et al., 2017).

2.3 Observation sites and daily shadow pattern

The analysis of Santos's microclimate was designed based on the LCZ classification (Stewart & Oke, 2012). Two weather stations and four data loggers[4] represent the variations of different built environments considering their forms, functions, historical processes, and valuation of space. In this way, INMET (National Meteorological Institute of Brazil) and CETESB (Environmental Company of the State of São Paulo) were chosen as official stations (Fig. 5). The first one, located in a relatively less occupied area beside a river, situated in Bertioga town (23 km from Santos), was considered as a reference station. The second, located in the middle of the city, was used to validate the data logger measurements. Four data loggers (HOBO Pro v2) distributed across the city were used to capture the response of air temperature and relative humidity for the different LCZ types. For temperature, the accuracy is 0.2°C for the range between 0° to 50°C with 0.02°C of resolution , and for relative humidity the resolution is 0.03% with an accuracy of +/- 2.5% between 10% and 90% RH (typical), to a maximum of +/- 3.5% out of this range. Other two stations were used only to obtain data from cloud cover and precipitation, i.e. METeorological Aerodrome Report (METAR) and National Center for Monitoring and Early Warning of Natural Disasters (CEMADEN), respectively.

---

[4] All data loggers were protected by the Solar Radiation Shield RSI. The solar radiation shield is recommended for temperature and relative humidity measurement accuracy in locations exposed to direct or reflected solar radiation.

Figure 4. Official stations: CETESB (left) and INMET (right).

Three data loggers are positioned in the central-south area, and another in the northwest of Santos urban area. CETESB was selected for validating the measured campaign. The first, compact high-rise building (HRB), located at the seafront, has the prevalence of high-rise commercial and residential buildings, characterized by flats ranging from 50 to 120 m. This area is densely built up on impermeable soils. In relation to green areas, planted trees and patches grass are observed in the horizontal beachfront park, in the drainage canal, and in the walkways. Moreover, it has a large flux of people and vehicles over the entire year, with a significant increase in summer holidays. The second, compact mid-rise building (CMR), located in a central-south area, is dominated by mid-rise commercial and residential buildings consisting of 3 – 9 floors. Other kinds of urban use are featured in this area, like low-rise residential buildings, warehouses, office blocks and open parking. Like the CMR's urban function, compact low-rise building 1 (CLR1), situated in a central-north portion of Santos, has some particularities that distinguish it from the former, like its position close to the harbor and the presence of smaller buildings. With respect to the green areas, CLR1 has less planted trees, but a considerable number of grass patches. Finally, compact low-rise 2 (CLR2), situated in the northwest side, is dominated by compact low-rise buildings (z = 10 - 14 m) and local markets. A relevant feature of this area is the occupation (starting in the 1950s) without a clear legal urban growth and sprawl regulation, resulting not only in tortuous but also narrow streets. Different from the others, the CLR2 has small quantities of urban parks characterized by both scarce trees and grass patches. Details about the sky view factor (SVF) for all LCZs are shown in Figure 6. The SVF was determined from the images generated by a fisheye lens, attached to a camera, and positioned 1,5m above the ground, aligned vertically upwards. The images were

further processed in the Rayman 1.2 computer program developed by Matzarakis (2009), based on recommendations of Matzarakis et al., (2010). Morphological characteristics of all sites are summarized in Table 1.

COMPACT HIGH-RISE BUILDING (LCZ1)
23°58'13.50"S 46°19'37.76"W
SVF = 0.133

COMPACT LOW-RISE BUILDING 1 (LCZ3)
23°56'46.85"S 46°19'19.06"W
SVF = 0.338

COMPACT MID-RISE BUILDING (LCZ2)
23°57'49.09"S 46°19'16.18"W
SVF = 0.357

COMPACT LOW-RISE BUILDING 2 (LCZ3)
23°56'34.96"S 46°22'31.46"W
SVF = 0.691
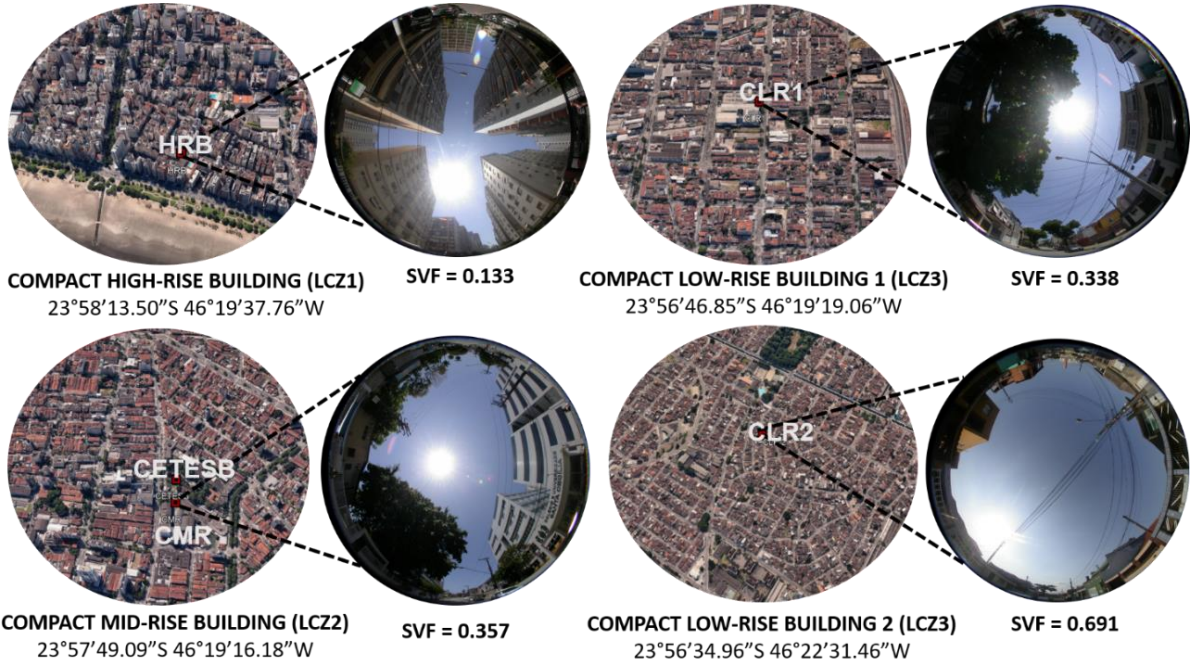
Figure 5. Sky view factor and general panorama for each LCZ: HRB (top left), CMR and CETESB (bottom left), CLR1 (top right) and CLR2 (bottom right). The red point shows data logger position and localization of the official station (CETESB).

Table 1 Description of morphological features of each official station used and LCZ analyzed in this study.

Site	Sensor Height (m)	Measured data	General urban features of site (within 500m radius)	General vegetation features of site (within 500m radius)	NDVI[5] (within 500m radius)	Coastline distance (km)
CETESB (official station)	3	Temp RH	Mid-rise commercial and residential buildings; shopping malls, universities, office blocks, schools.	Tress planted at irregular intervals on the sidewalks, small gardens spaces in front of houses and commercial buildings. Mature trees planted at regular intervals throughout the drainage canal.	0.27	1,24 (1,76 km from the drainage canal)
METAR (official station)	3	Cloud height Cloud cover	Located in the air base of Santos, it has a warehouse and a runway.	Mixture of bare, soil exposed, grass patches and Atlantic forest patches.	0.78	8,02 (0,7 km from river)
INMET (official station)	3	Temp Rainfall	Mixture of open low-rise residential buildings and warehouses.	Large amount of tress in the garden spaces of houses. Several grass patches and concentrated portions in the north, south and west of Atlantic Forest from site.	0.48	1,13 (0,1 km from the drainage canal)
HRB (DL[6])	4,5	Temp RH	Front of the beachfront has a mixture of both compact high-rise commercial buildings and residential flats, open car parks.	Mixture of open grass and irregular tress planted in the beachfront. Mature trees planted at regular intervals throughout drainage canal. Large amount of tress in sidewalks and in garden spaces of buildings.	0.23	0,16
CMR (DL)	2,5	Temp RH	Mid-rise commercial and residential buildings; shopping malls, universities, office blocks, schools, and municipal offices.	Tress planted at irregular intervals in sidewalks, small gardens spaces in front of houses and commercial buildings. Mature trees planted at regular intervals throughout the drainage canal.	0.27	1,12 (1,96 km from the drainage canal)
CLR1 (DL)	2,5	Temp RH	Mid-rise commercial and residential buildings; shopping malls, universities, office blocks, schools, warehouse, and parking lots.	Numerous small grass patches; Isolated trees in the sidewalks and gardens of houses and commercial buildings. Irregular and sparse trees throughout the drainage canal.	0.26	3,0 (1,2 km from the drainage canal)
CLR2 (DL)	2,5	Temp RH	Low-rise residential with a mixture of small business and plazas.	Numerous small grass patches; sparse trees at the sidewalks and municipal buildings. Plazas with irregular number of planted trees.	0.24	2,8 (1,58 km from the drainage canal)

---

[5] Normalized Difference Vegetation Index (NDVI) calculated by using LANDSAT 8 (17th December 2017).
[6] DL: data loggers

To evaluate the impact of the shade on the temperature variations, we used the Shadow generator plugin in QGIS, which creates pixel wise shadow estimates based on both ground and building/vegetation digital surface models (DSM). The methodology is based on the work of Ratti and Richens (1990) and is further developed and described in Lindberg and Grimmond (2011). In this experiment, daily shadow pattern was determined for all LCZs (CETESB and CMR are the same due to proximity) using integrated building+vegetation DSM. To create the shadow pattern, 23rd January was used to represent the summer period and 30th August 2018 was used for winter.

Shadows were produced for a specific day, during 08:00 – 17:00 on each season (summer and winter) to analyze and quantify the interference of building and vegetation (as a function of Sun position) on its pattern for LCZs and CETESB. Table 2 illustrates the shadow fraction of each area given in percentage. Figures 7 to 14 exhibit daily shadow pattern for summer and winter: figures 7 – 8 show daily shadows pattern to HRB; Figures 9 – 10 represent CETESB and CMR's shadows; figures 11 – 12 display CLR1; and 13 – 14 represent CLR2. A significant variation is observed within the day and for each season. HRB is one of the regions with the higher variation, and CLR2 shows the smaller variation with the higher insolation over the year.

Table 2. Amount of shadow (in percentage) extracted for each LCZ and CETESB files (hourly) for each season studied.

SEASONS and LCZ(s)	HOURS									
	8	9	10	11	12	13	14	15	16	17
SUMMER										
HRB	46	45	38	30	19	9	21	32	44	47
CTB	43	31	22	15	8	3	11	17	26	36
CLR1	30	20	13	9	5	2	6	10	17	26
CLR2	33	23	15	10	4	1	6	12	18	27
WINTER										
HRB	30	38	46	44	37	41	46	47	49	42
CTB	42	42	32	24	22	22	23	27	36	49
CLR1	49	38	29	23	18	18	21	26	34	46
CLR2	45	30	21	15	13	13	14	18	26	39
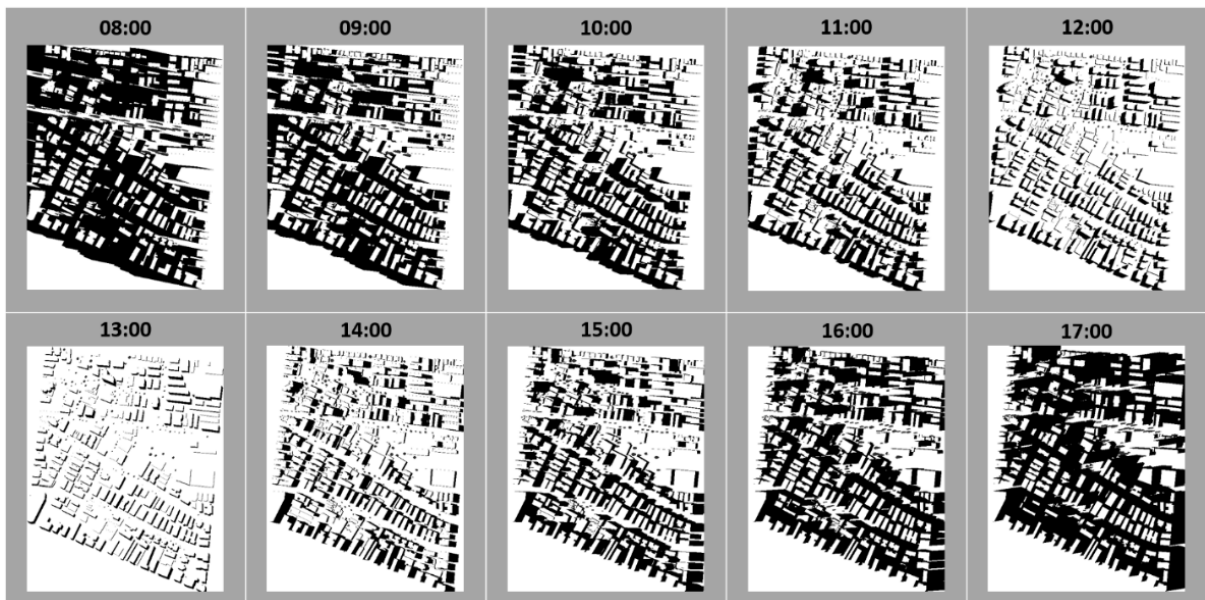
Figure 6. HRB daily shadow pattern from 08:00 – 17:00 on 23rd January 2018 (Summer).
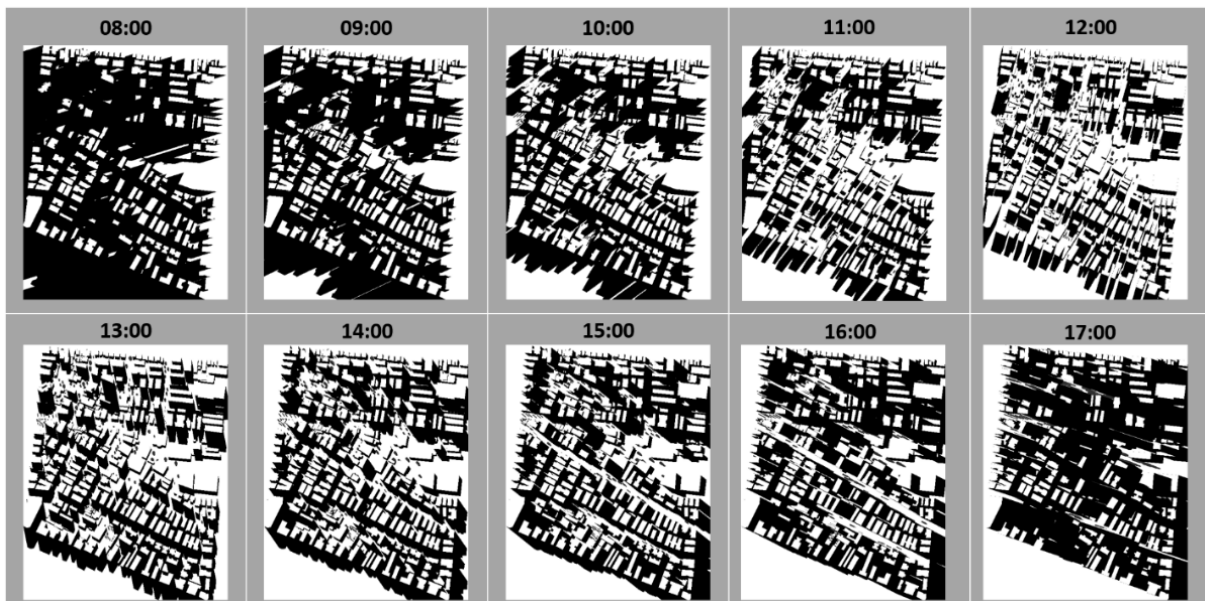
Figure 7. HRB daily shadow pattern from 08:00 – 17:00 on 30th August 2018 (Winter).
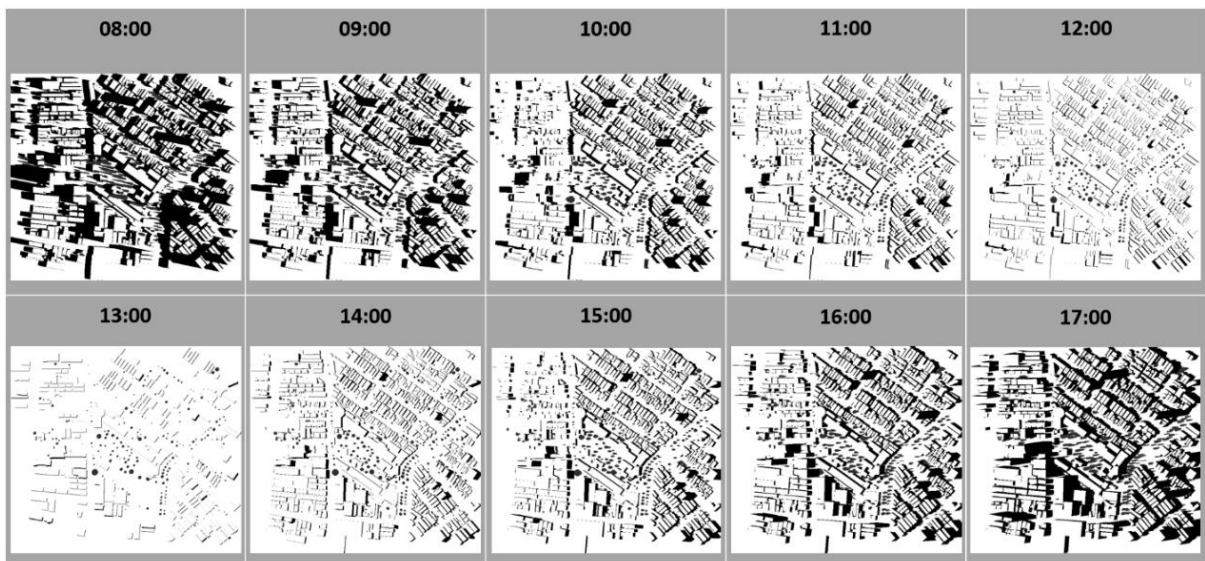
Figure 8. CETESB (and CMR) daily shadow pattern from 08:00 – 17:00 on 23rd January 2018 (Summer).
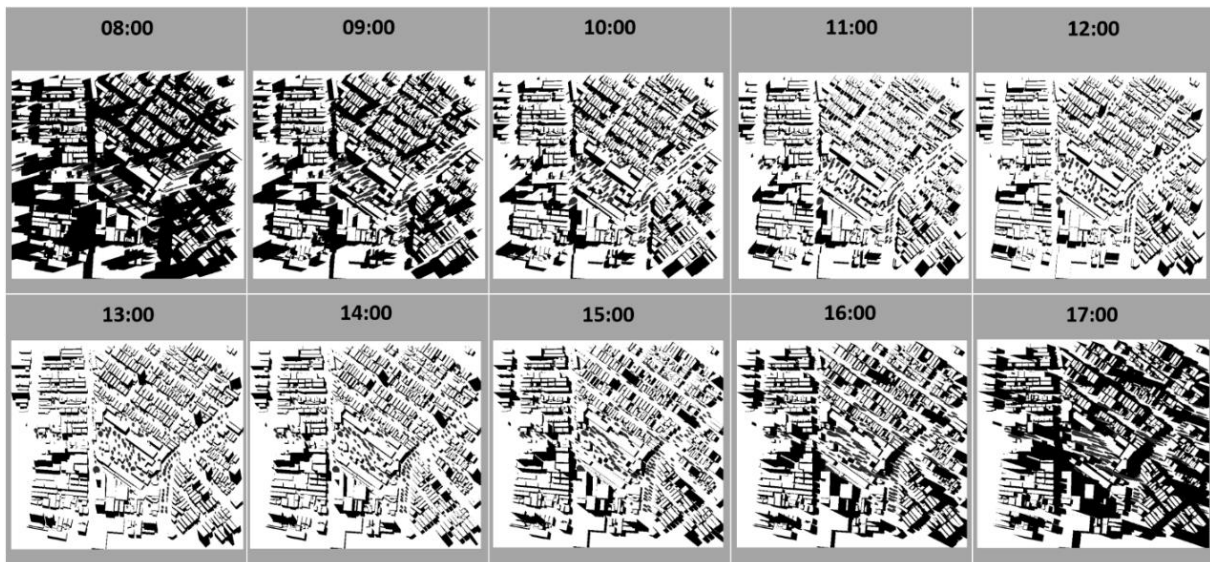
Figure 9. CETESB (and CMR) daily shadow pattern from 08:00 – 17:00 on 30th August 2018 (Winter).
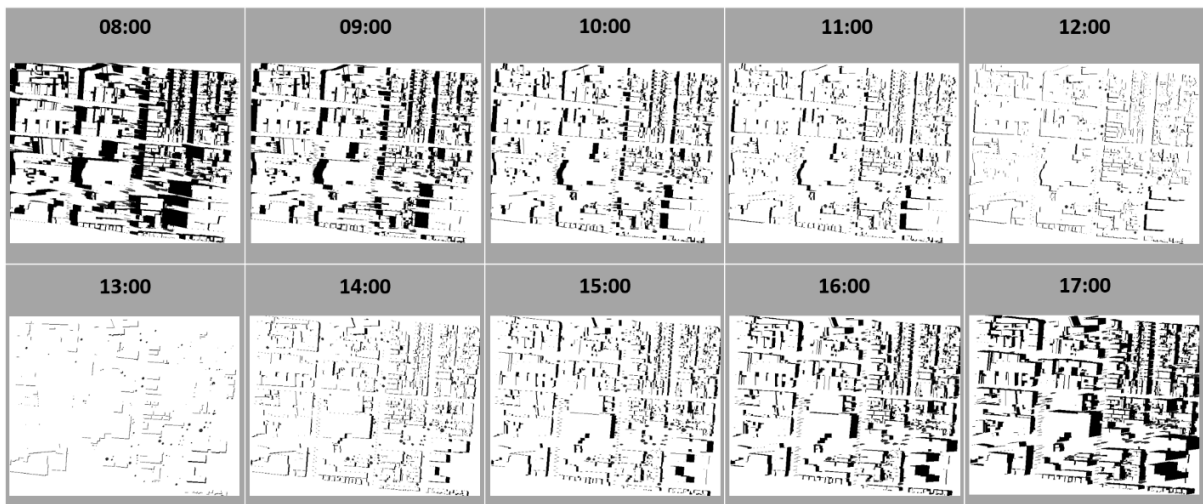
Figure 10. CLR1 daily shadow pattern from 08:00 to 17:00 on 23rd January 2018 (Summer).
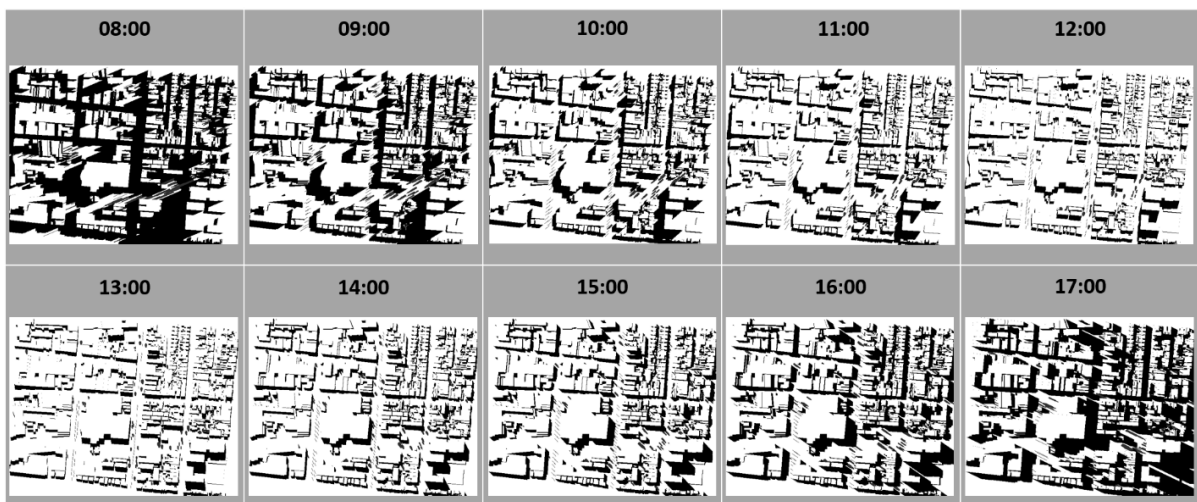
Figure 11. CLR1 daily shadow pattern from 08:00 to 17:00 on 30th August 2018 (Winter).
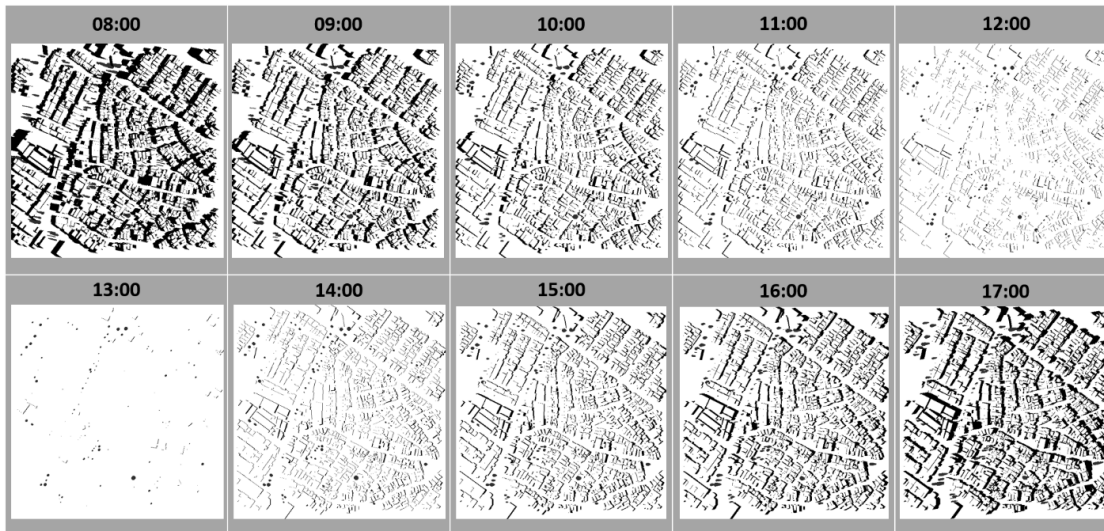
Figure 12. CLR2 daily shadow pattern from 08:00 to 17:00 on 23rd January 2018 (Summer).
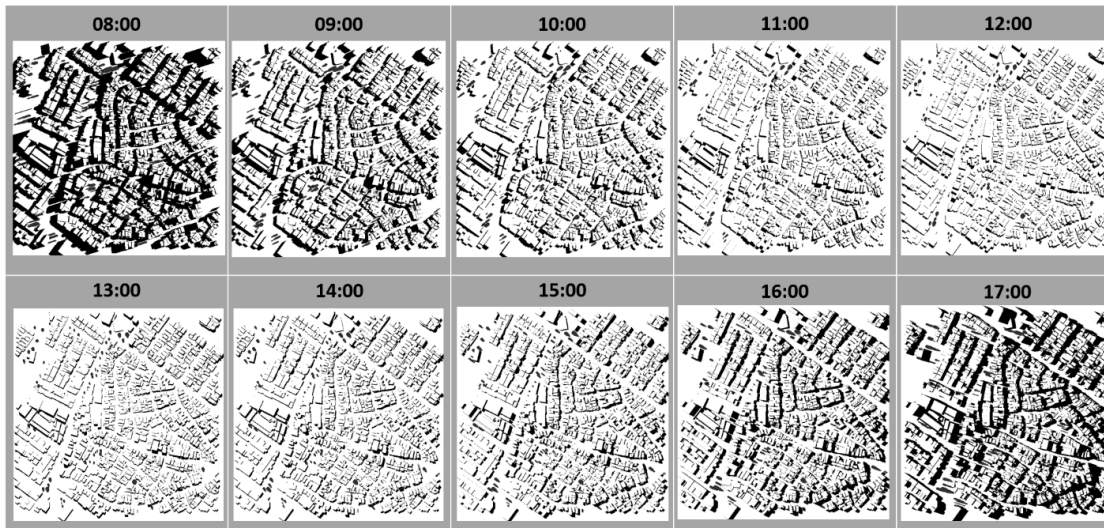
Figure 13. CLR2 daily shadow pattern from 08:00 to 17:00 on 30th August 2018 (Winter).

2.4 Seasonal variation of the canopy layer heat island (UHI$_{UCL}$)

The present analysis is based on data logger campaign conducted from 15th November 2017 to 11th October 2018. The resulting dataset has passed through different filtering levels to select the days where all the controls that regulate the canopy-level UHI were ideal, i.e. calm, clear days when the radiation cooling is strong and turbulent mixing is weak (Oke et al., 2017). In summary, data was organized in two seasons: summer, from 1st December 2017 to 31st January 2018; and winter, from 1st August to 30st September. Within the seasons, the main goal of the present research is to examine the diurnal thermal behavior of the UHI$_{UCL}$ based on seasons to illustrate changes in development and magnitude. The UHI magnitude for each LCZ was defined as the difference between the maximum LCZ temperature and a temperature of the reference station (INMET – LCZ$_9$) over a specified period, i.e. UHI$_{UCL, max}$ = LCZ$_X$ – LCZ$_9$.

3.   RESULTS

3.1 Seasonal variation of the UHI_{UCL}

During the period considered in the analysis, weather conditions varied significantly, with a considerable number of days with rainfall, especially during the summer. As expected, the cloud cover was extensive during the whole considered period and only a few clear days could be selected according to standard definitions (less than 3 octas of cloud cover, see e.g. Jonsson, 2005). For this study, 'clear' days have ≤3 octas, 'partly cloudy' present 5 to 7 octas and 'overcast' > 7 octas. To evaluate both scales for all LCZs and CETESB, only clear days with light wind (<2,5 m/s) and without precipitation were chosen. Therefore, for summer, only 2 days in December and 7 days in January matched this ideal meteorological condition. During winter, only 2 days in August and 3 days in September could be used. Nevertheless, for this selection, based on radiation data from CETESB and INMET, it was possible to observe the influence of cloud cover variation on air temperature between them.

Therefore, in order to avoid erroneous discussions, we chose the days when the daytime radiation exposure at both official stations was more homogeneous. Figure 15 and 16 summarizes the seasonal UHI_{UCL} magnitudes for summer and winter based on the last classification. Figures are organized to give emphasis on the nocturnal UHI. Sunset and sunrise are considered to happen at 20:00 and 6:30 during summer, and 18:00 and 06:00 during winter. The UHI magnitude is determined by the maximum difference of the air temperature at each area (LCZ_X) against the results from the reference station (INMET – LCZ_9), as described in the section 2.4.   Considering both seasons, an average difference of around 1°C is observed between summer and winter.
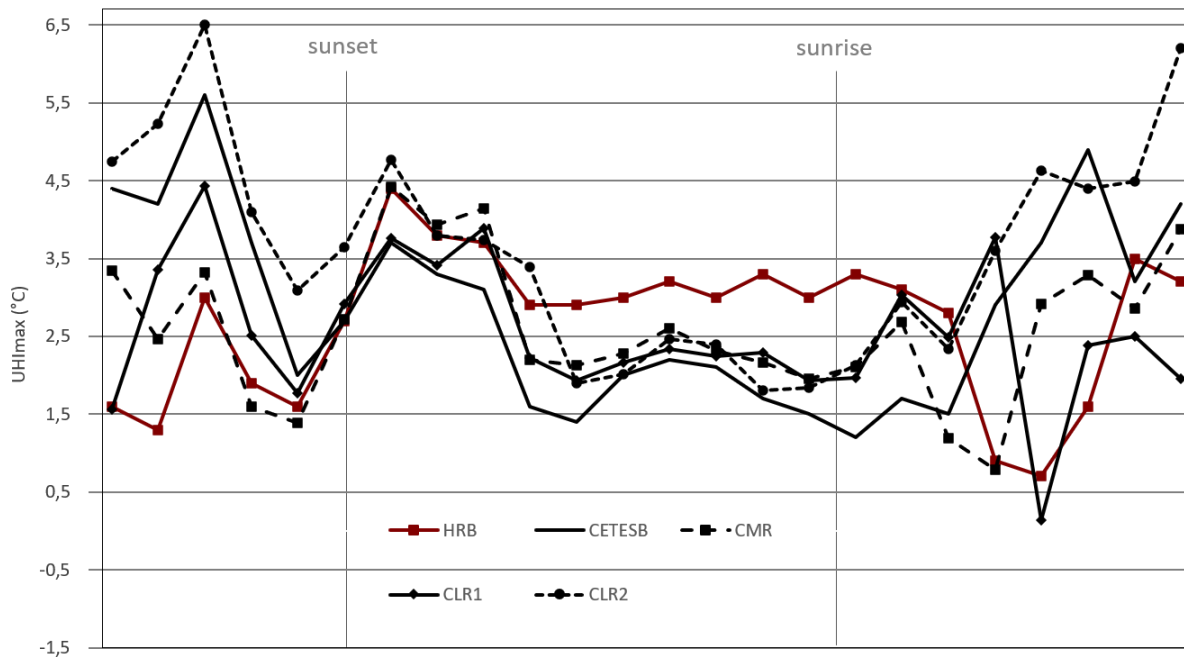
Figure 14. Summer UHIUCL, max diurnal variation among LCZs.
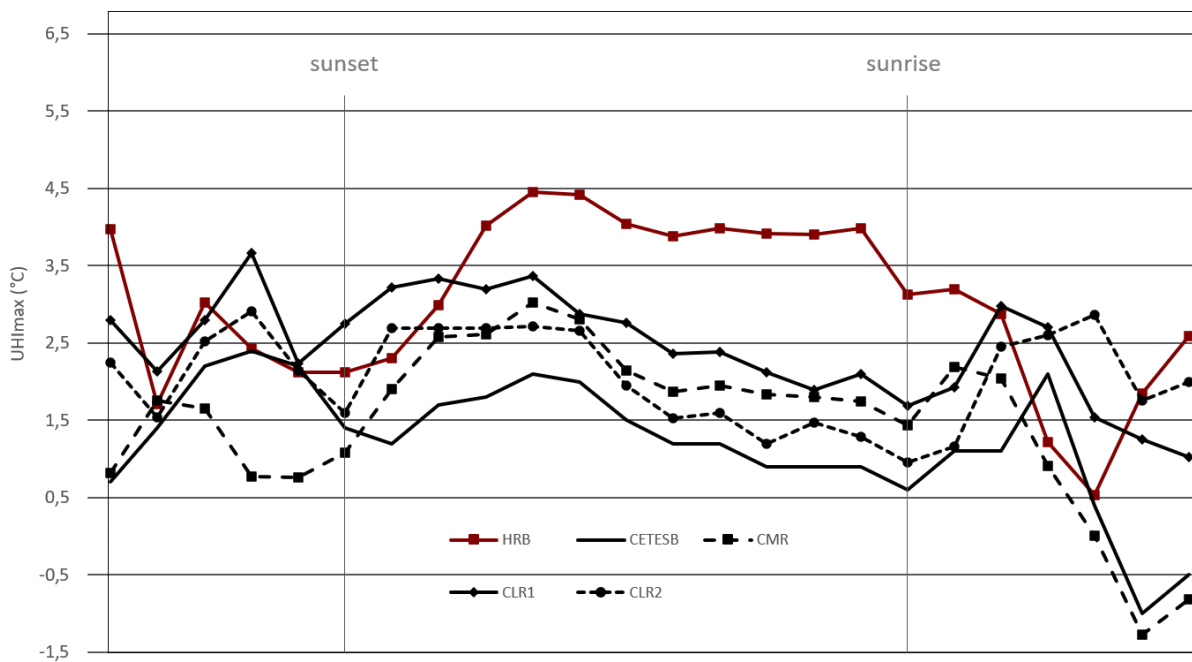
Figure 15. Winter UHIUCL, max diurnal variation among LCZs.

To assist the discussion of the intra-urban UHI differences, wind flow taken at INMET and CETESB stations were summarized in Fig. 17 and 18 for summer and winter, respectively. In general, INMET showed a greater variance of direction and higher speed in both seasons compared with CETESB. During the dawn (00:00 – 05:00), the main wind directions come from the southwest (SW) and west (W) for both seasons, while the northwest (NW) is common only in summer. For summer, the mean wind speed (m/s) was higher than winter, varying between 0,5 to 3,6. In the morning (06:00 – 11:00), the most frequent wind directions are west

(W), southwest (SW), south (S), and southeast (SSE). At the afternoon (12:00 - 17:00), the sea breeze that comes from the southeast (SSE) is prevalent with wind speeds varying between 2.1 to 4.0. At night (18:00 - 23:00), while during the summer the main direction is from the east (E), for winter it comes from the west (W) and east (E). For both seasons, the eastward winds are greater than 2.1, while in other directions, the mean speed is ≤2.1. In contrast, CETESB is dominated mainly by two breeze patterns at mesoscale. The sea breeze blowing toward the mainland begins in the late morning and remains acting until the middle of the night when the land breeze starts to dominate until the early morning. Wind speed for both breezes varies from 0.5 – 2.6 m/s. While the sea breeze comes from south and southeast (S - SSE), the land breeze comes from northwest (NW) direction.
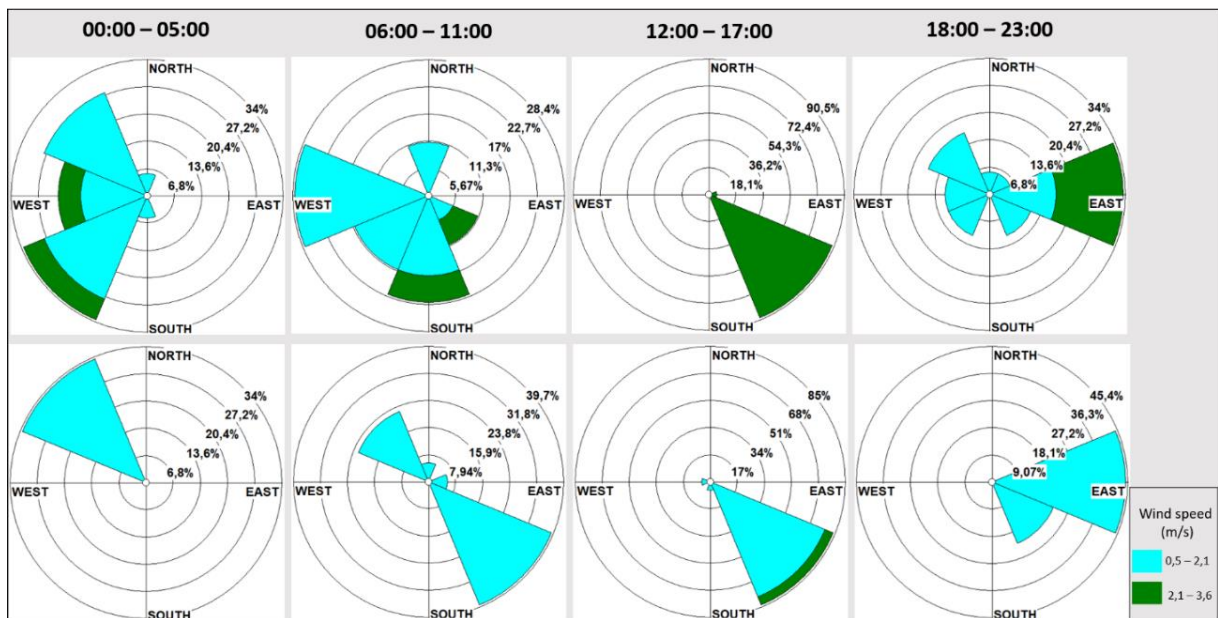
Figure 16. Summer. Hourly wind flow from INMET (up) and CETESB (down).
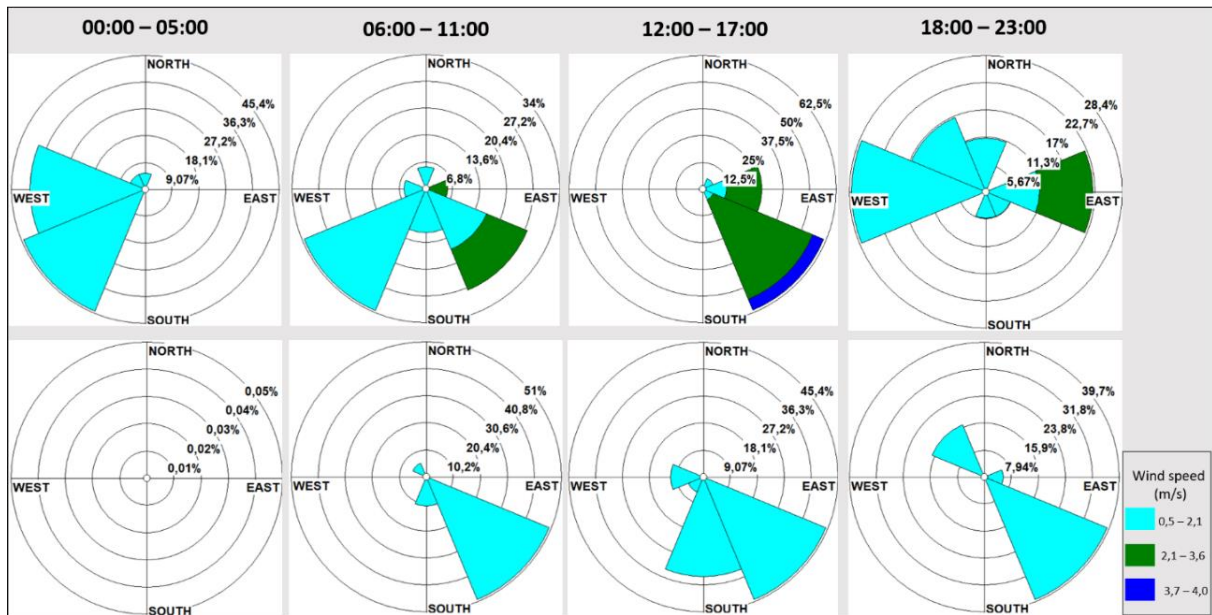
Figure 17. Winter. Hourly wind flow from INMET (up) and CETESB (down).

4. DISCUSSION

To explain the seasonal variability of the observed nocturnal UHI values, i.e. ~1°C (summer < winter), it is essential to consider (1) the thermal admittance and (2) the weather. Higher soil moisture, higher heat storage capacity and thermal admittance make the rural surroundings thermally more homogenous than urban surfaces (Oke et al., 2017), which may explain the lower UHIs magnitude found here and in many tropical cities (Singapore, Colombo, Hong Kong, Kuala Lumpur and Johor Bahru). Since summer represented the wettest period, i.e. 632,2mm (compared to 144,4mm in winter), those results may be related to moisture on the soil in the reference area (LCZ$_9$). Soils located in areas with more trees and grass are expected to present larger thermal admittance. Thus, the weaker cooling rates tend to reduce the magnitude of the UHI (Oke et al., 2017). Those results agree with other studies at tropical cities, where the highest UHI magnitudes were found during the drier season, e.g. for Singapore, the maximum UHI is observed during June and the minimum during the wet period in January (Chow and Roth, 2006). In Seoul, Korea, the maximum magnitude of the heat island happened during autumn and winter, while during the humid summer it takes its minimum (Kim and Baik, 2005).

Although other several weather elements are related to UHI, the main ones are wind and cloud (Oke et al., 2017). Through atmospheric transport and mixing, the wind is the main driver of advection and turbulent exchange that limit horizontal and vertical temperature differences (Oke et al., 2017). Thus, the wind influences the UHI by altering the different cooling rates between urban and rural landscapes. This movement of air between these environments can

result in a weakening of the urban-rural air temperature difference (Morris & Simmonds, 2001). Cloud cover is an important modulating control of the UHI_{UCL}, since it affects the shortwave and longwave radiation, the main drivers of heating and cooling rates, respectively (Morris & Simmonds, 2001; Oke et al., 2017). At night, cloud cover provides natural insolation that absorbs and reemits infrared radiation downward, which is available for absorption by the surface and partially offsets the surface radiative loss. Through this process, the nocturnal radiative cooling may be slowed, hence decreases the differences in the observed temperatures between urban and non-urban areas (Morris & Simmonds, 2001). In this context, the seasonal UHI difference between the warm and cool season could be also explained due to thermal admittance and static stability, i.e. clearly, calm and clear sky conditions, especially taking to account the UHI development in HRB (see Fig. 16).

Moreover, UHI exhibited a strong relationship between canyon geometry (e.g. H/W and SVF), often perceived in temperate cities (Oke, 1981). A comparison of nocturnal UHIs and urban geometry showed that UHI intensity increases with increasing height to width (H/W) ratios of street canyons (see e.g. Oke 1981, 1988). Canyons with higher H/W generally absorb and store a significant amount of incoming shortwave radiation and lose less longwave radiation at night. SVF is related to the amount of visible sky at a given point, i.e. the sky available for a thermal energy dispersion. Clear relationship of it can be observed in the present study, as the location with the lowest value of SVF (HRB - 0.133) is associated with the highest nocturnal (specially at late night) value for both seasons during the nighttime.

The seasonal intra-urban differences during the daytime may be explained by solar exposure, shading, and vegetation. During the summer, higher solar radiation (~900W/m2) increases urban heat storage and consequently, the air temperature. As shown in Fig. 15, CLR2 promotes the highest UHIUCL magnitudes (~6°C). This can be explained by both the heights of buildings and the devoid of vegetation. Low buildings receive much more shortwave radiation, which warms up the air at spaces between buildings more than in other LCZs. This result is illustrated by comparing SVF and the percentage of shading among LCZs (see Table 2). For example, at 17h, CLR2 that has the highest SVF (0.691) and the lowest percentage of shadow (27) showed the highest UHI magnitude (6,5°). In the other hand, HRB, which represents the lowest SVF and the highest percentage of shadow (47), exhibited the lowest UHI (3°C) at the same time. The reason is that less solar radiation is absorbed at street level for lowest SVF, which provides shading during the daytime. Related to vegetation, most studies argue that the lack of greenery in the city tends to result in higher daytime air temperatures. The presence of vegetation in urban areas tends to reduce the maximum temperatures during the day, reducing the radiative changes at surface level. The effect of vegetation on urban warming

phenomena not only manifests itself indirectly in the form of a reduction in the sensible heat flux from colder surfaces but also directly through evaporative cooling.

The existence of cool islands in cities has been already reported in numerous urban climatological studies. Lower urban temperatures may occur because of the less positive thermal balance in the specific urban zones than that of the reference station. For the present study, a persistent shadow occurs at the CETESB station (and CMR), which is probably the reason for the decrease in temperature in winter (Fig. 16). This may be observed in Fig. 19, which illustrates the hourly/monthly radiation from 2011 to 2019 based on CETESB data. This persistent shading in August (at 9) and September (at 10) result in a drop in the radiation, and consequently, in the air temperature. Since this could erroneously point toward the existence of a cool island (and related to the largest amount of vegetation, for example), the present study aim to reinforce that sometimes a more comprehensive evaluation of the meteorological conditions at both urban and reference stations should be done to guarantee the consistency of the analysis.
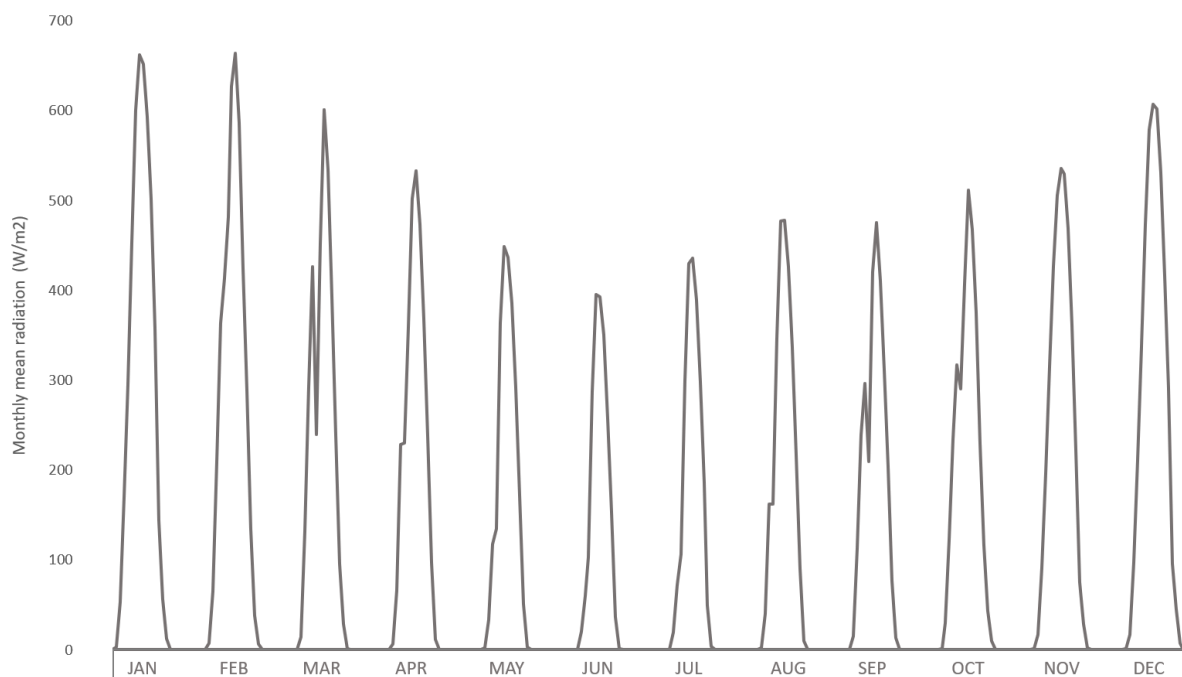
Figure 18. CETESB monthly mean radiation (2011 – 2019).

Moreover, due to the sea breeze, the cool island has been reported in coastal cities, like in Bilbao (Acero et al., 2012), Singapore (Chow & Roth), Sri Lanka (Emmanuel & Johansson, 2006), and Tel Aviv (Mousavi-Baygi et al., 2010). However, as presented by Prata (2005) and how was observed in CETESB's air quality report (2014), the buildings on the edge of Santos form a barrier that hinders the penetration of the sea breeze. Prata (2005), at the time when the largest buildings had 26 floors, observed through measurements *in loco* that, at the seafront, the

wind velocities were higher than those in different points behind the building's barrier. The CETESB report shows that its station located in a region with reduced roughness and closer to the coast ("*Ponta da Praia*") has a greater variation in wind direction and sea breeze intensity compared to the station further into the urban area (the station used in this study). It is noteworthy that nowadays, the buildings beside the coast have more than 30 floors, with heights up to 120 m. A similar result was exhibited when comparing wind flow from INMET and CETESB (Fig 17 and 18), as discussed previously.

5.   CONCLUSION

As discussed, the different urban environments considered in the definition of LCZs show two distinct thermal responses that must be rethought in order to understand the role of buildings in the city's climate strategy, especially in tropical coastal areas. Firstly, HRB enhances the mutual shading of buildings, which is beneficial during the daytime and can be contributed to the thermal comfort of dwellers. On the other hand, it can cause negative impacts, such as the highest nocturnal UHI and the obstruction of the penetration of the sea breeze to the other areas of the city. Secondly, since CLR is a common building pattern in tropical cities, this kind of construction contributes to the dispersion of thermal energy and longwave radiation during the night, they imply in higher temperatures during the day due to the absence of shading devices. This is further intensified by the lack of green areas, such as parks, or even trees on the sidewalks. On this way, the main findings from this study are:

(1)   There is distinct seasonal variability in the UHI for all sites. Generally, higher UHI_{UCL} magnitudes were observed during the drier season (winter) and lower intensities during the wet season (summer). These results may be explained by the variability of moisture content at the reference station in summer and the static stability weather during the winter.

(2)   Since HRB present the highest UHI at night for all season, the relationship between urban canyon geometry and UHI intensity is stronger.

(3)   Shading and urban landscape features such as street trees could help to reduce the assimilated radiation and consequently the temperature. In this respect, the lack of shading devices and trees make CLR2 hotter than other LCZs during morning and afternoon.

(4)   Analyses related to radiation should be more explored in studies related to UHI in coastal cities since those regions represent areas with cloudiness varying throughout the day.

REFERENCES

Amorim, M. C. C. T. Características do Clima Urbano de Presidente Prudente/SP. In: João Lima Sant'Anna Neto. (Org.). Os climas das cidades brasileiras. Presidente Prudente: UNESP/FCT/Programa de Pós-graduação em Geografia, p. 165-196. 2002.

Assis, E. S.; Frota, A. B. Urban bioclimatic design strategies for a tropical city. Atmospheric Environment, Great Britain, v. 33, n.24, p. 4135-4142. 1999.

Bejaran, R. A, Camilloni I. A. Objective method for classifying air masses: an application to the analysis of Buenos Aires' (Argentina) urban heat island intensity'. Theoretical and Applied Climatology 74: 93–103. 2003.

B. Bechtel, P.J. Alexander, J. Böhner, J. Ching, O. Conrad, J. Feddema, G. Mills, L. See, I. Stewart. Mapping Local Climate Zones for a Worldwide Database of the Form and Function of Cities. ISPRS Int. J. Geo-Inf., 4 (2015), pp. 199-219, 10.3390/ijgi4010199. 2015.

Bechtel, B., Demuzere, M., Sismanidis, P., Fenner, D., Brousse, O., Beck, C., Van Coillie, F., Conrad, O., Keramitsoglou, I., Middel, A., Mills, G., Niyogi, D., Otto, M., See, L., Verdonck, M.-L. Quality of Crowdsourced Data on Urban Morphology—the Human Influence Experiment (HUMINEX). Urban Sci. 1, 15. https://doi. org/10.3390/urbansci1020015. 2017.

Bechtel, B., Alexander, P. J., Beck, C., Böhner, J., Brousse, O., Ching, J., et al. Generating WUDAPT level 0 data - current status of production and evaluation. Urban Climate, 27, 24–45. https://doi.org/10.1016/j.uclim.2018.10.001. 2019.

Brazilian Institute of Geography and Statistics (IBGE). Cidades: Santos-SP. Disponível em: <http://cod.ibge.gov.br/3ZR>. 2018

Cammiloni, I; Barruncand, M. Temporal variability of the Buenos Aires, Argentina, urban heat island. Theor Appl Climatol 107:47–58. 2012.

Chow, W., Roth, M. Temporal dynamics of the urban heat island of Singapore. International Journal of Climatology 26: 2243–2260 (DOI 10.1002/joc.1364). 2006.

Crawford, B; Krayenhoff, E. S; Cordy, P. The urban energy balance of a lightweight low-rise neighborhood in Andallo, Chile. Ther. Appl. Climatol 131:55-68. 2018.

Duarte, D. Variáveis urbanísticas e microclimas urbanos - modelo empírico e proposta de um indicador. Fórum Patrimônio: Ambiente Construído e Patrimônio Sustentável (UFMG. Online), v. 3, p. 1-36, 2010.

Duarte, D. O impacto da vegetação no microclima em cidades adensadas e seu papel na adaptação aos fenômenos de aquecimento urbano. Contribuições a uma abordagem interdisciplinar. São Paulo: FAUUSP, 2015 (Tese de Livre-docência).

Duarte, D. Vegetation and climate-sensitive public places. In: Rohinton Emmanuel. (Org.). Urban climate challenges in the Tropics: rethinking planning and design opportunities. 1ed.London: Imperial College Press, p. 111-162. 2016.

Emmanuel R. Assessment of impact of land cover changes on urban bioclimate: the case of Colombo, Sri Lanka. Architectural Science Review 46: 151–158. 2003.

Emmanuel R. An Urban Approach to Climate-Sensitive Design: Strategies for the Tropics. Spoon Press: London. 2005a.

Emmanuel R. Thermal comfort implications of urbanisation in a warm-humid city: the Colombo Metropolitan Region (CMR), Sri Lanka. Building and Environment 40: 1591–1601. 2005b.

Emmanuel, R., Johansson, E. Influence of urban morphology and sea breeze on hot humid microclimate: the case of Colombo, Sri Lanka. Climate Research 30: 189–200. 2006.

Erell, E.,Williamson, T. Intra-urban differences in canopy layer air temperature at a mid-latitude city. Int. J. Climatol. 27, 1243–1255. 2007.

Fenner, D.; Meier, F.; Scherer, D.; Polze, A. Spatial and temporal air temperature variability in Berlin, Germany, during the years 2001–2010. Urban Climate. 10 (Part 2), 308–331. 2014

Ferreira, L. S.; Duarte, D. H. S. Exploring the relationship between urban form, land surface temperature and vegetation indices in a subtropical megacity. Urban Climate, v. 27, p. 105-123. 2019.

Georgeson, L.; Maslin, M.; Poessinouw, M.; Howard, S. Adaptation responses to climate change differ between global megacities. Nature Climate Change, v. 6, n. 6, p. 584-588, 2016.

Giannopoulou, K., Santamouris, M., Livada, I., Georgakis, C., Caouris, Y. The impact of canyon geometry on intra urban and urban: suburban night temperature differences under warm weather conditions. Pure Appl. Geophys. V167 (11), 1433–1449. 2010.

Giridharan, R., Ganesan, S., Lau, S. S. Y. Daytime urban heat island effect in high-rise and high-density residential developments in Hong Kong. Energy and Buildings 36: 525–534. 2004.

Giridharan R, Lau SSY, Ganesan S. Nocturnal heat island effect in urban residential developments of Hong Kong. Energy and Buildings 37: 964–971. 2005.

Grimmond, C.S.B. Roth, M. Oke, T.R. Au, Y.C. Best, M. Betts, R. Carmichaelf, H. Cleugh. W. Dabberdt, W. Emmanuel, R. Freitas, E. Fortuniak, K. Hanna, S. Klein, P. Kalkstein, L.S. Liu, C.H. Nickson, A. Pearlmutter D. Sailor, D. and Voogt, J. 2010. Climate and More Sustainable Cities: Climate Information for Improved Planning and Management of Cities (Producers/Capabilities Perspective). Procedia Environmental Sciences. 247–274 pp.

Jauregui, E. Tropical urban climate: review and assessment. Proceedings, Technical Conference in Mexico City: Urban Climatology and its Applications with Special Regard to Tropical Areas, WMO-No 652. 26 – 45 pp. 1984.

Jauregui, E., Godinez, L., Cruz, F. Aspects of heat-island development in Guadalajara, Mexico. Atmos. Environ. 26, 391–396. 1992.

Kawashima, R. S.; Almeida, C. M.; Giannotti, M. A.; Quintanilha, J. A. Análise das mudanças temporais de cobertura da terra na região portuária da Baixada Santista-SP e a proposição de modelos de dinâmica espacial. In: Simpósio Brasileiro de Sensoriamento Remoto (SBSR), 17., 2015, João Pessoa. Anais... São José dos Campos: INPE, 2015. Artigos, p. 1082-1089. DVD,

On-line. ISBN 978-85-17-00076-8. Available in <http://www.dsr.inpe.br/sbsr2015/files/p0199.pdf>.

Kim, Y., Baik, Jong-Jin. Spatial and temporal structure of the urban heat island in Seoul. J. Appl. Meteorol. 44, 591. 2005.

Kotharkar, R; Bagade, A. Evaluating urban heat island in the critical local climate zones of an Indian city. Landscape and Urban Planning. 169: 92–104. 2018.

Kubota, T; Ossen, D. R. Spatial Characteristics of Urban Heat Island in Johor Bahru City, Malaysia. Available in: Proceedings of the 3rd Symposium of South East Asian Technical University Consortium (SEATUC). 2014.

Lombardo, M. A. Ilha de Calor na Metrópole Paulistana. Tese (Doutorado em Geografia). Universidade de São Paulo. 1984.

Matzarakis, A. Rayman 1.2. Disponível em: freiburg.de/rayman/intro.htm 2009.

Matzarakis, A.; Rutz, F.; Mayer, H. Modelling radiation fluxes in simple and complex environments: Basics of the RayMan model. International Journal of Biometeorology, v. 54, n. 2, p. 131–139. 2010.

Monteiro C. A de F. Teoria e clima urbano. Série Teses e Monografias, São Paulo:USP/Igeog, n 25. 1976.

Morris, K. I; Salleh, S. A; Chan, A; Ooi, M. C. G; Abakr, Y. A; Oozeer, M. Y; Duda, M. Computational study of urban heat island of Putrajaya, Malaysia. Sustainable Cities and Society, 19,359–372. 2015.

Mousavi-Baygi, M., Ashraf, Batool, Miyanabady, Ameneh. The investigation of Tehran's heat island by using the surface ozone and temperature data. Int. J. Appl. Environ. Sci. (ISSN: 0973-6077) 5 (2), 189–200. 2010.

Nicol, J. E. High-resolution surface temperature patterns related to urban morphology in a tropical city: a satellite-based study. Journal of Applied Meteorology 35: 135–146. 1996.

Nicol, J. E., Wong, M. S. Modeling urban environmental quality in a tropical city. Landscape and Urban Planning 73: 49–58. 2005.

Oke, T.R. The energetic basis of the urban heat island. Q. J. R. Meteorol. Soc. 108 (455), 1–24. 1982.

Oke, T.R. Urban climatology and the tropical city. In: Proceedings, Technical Conference in Mexico City: Urban Climatology and its Applications with Special Regard to Tropical Areas, WMO-No 652. 1-25 pp. 1984.

Oke, T. R; Johnson, G.T; Steyn, D. G; Watson, I. D. Simulation of surface urban heat islands under "ideal" conditions at night, part 2: diagnosis of causation. Boundary-Layer Meteorology 56: 339–358. 1991.

Oke, T.R. Mills, G. Christen, A. Voogt,J. A. Urban Climate. Cambridge. 525p. 2017.

Palme, M; Lobato, A; Claudio, C. Quantitative Analysis of Factors Contributing to Urban Heat Island Effect in Cities of Latin-American Pacific Coast. In: 4th International Conference on Countermeasures to Urban Heat Island (UHI) 2016. Procedia Engineering. 99 – 206 pp. 2016.

Padmanabhamurty B. Some aspects of the urban climates of India. Urban Climatology and its Applications with Special Regard to Tropical Areas, World Climate Programme, WMO Publication No. 652. World Meteorological Organization: Geneva; 136–165. 1986.

Perera, N. G. R., & Emmanuel, R. A "Local Climate Zone" based approach to urban planning in Colombo, Sri Lanka. Urban Climate. http://dx.doi.org/10.1016/j.uclim.2016.11.006 Advance online publication. (2016).

Prata, A. R. Impacto da altura de edifícios nas condições de ventilação natural do meio urbano. Tese de Doutorado. São Paulo. Universidade de São Paulo. 2005.

Ratti CF, Richens P. Urban texture analysis with image processing techniques. In: Proceedings of the CAADFutures99, Atalanta, GA. 1999.

Ribeiro, H. Heat island in Sao Paolo, Brazil: effects on health. Critical Public Health 15: 147–156. 2005.

Roth, M. Review of urban climate research in (sub) tropical regions. International Journal of Climatology. 27, 1859–1873 pp. 2007.

Roth, M; Chow, W. T. A historical review and assessment of urban heat island research in Singapore. Singapore Journal of Tropical Geography, 33(3), 381–397. 2012.

Runnalls, K., Oke, T.R., Dynamics and controls of the near-surface heat island of Vancouver, British Columbia. Phys. Geogr. 21 (4), 283–304. 2000.

Sailor, D. J., Dietsch, N. The urban heat island mitigation impact-screening tool (MIST). Environmental Modelling & Software, 22(10), 1529–1541. 2007.

Sharma, R., Hooyberghs, H., Lauwaet, D., & De Ridder, K. Application of Urban Climate for an Asian tropical city—The case of Delhi. Living planet symposium, Vol. 740, 210 August. 2016.

Secretary for Planning and Sustainable Development. Caracterização Socioeconômica de São Paulo Região Metropolitana da Baixada Santista, 2011. Governo do Estado de São Paulo. Available in:http://www.planejamento.sp.gov.br/noti_anexo/files/uam/trabalhos/RMBS.pdf.

Siu, L. W; Hart, M. A. Quantifying urban heat island intensity in Hong Kong SAR, China. Environmental Monitoring and Assessment, 185(5), 4383–4398. 2013.

Souza, L. C. L. Thermal environment as a parameter for urban planning. Energy Sustainable Development, v. XI n.4, p. 44-53. 2007.

Steward, I. D; Oke, T. R. Local climate zones for urban temperature studies Bull. Am. Meteorol. Soc., 93, pp. 1879-1900, 2012, 10.1175/bams-d-11-00019.1. 2012.

Stewart, I.; Global Cities Institute, University of Toronto, Toronto, Canada, LCZ metric. Personal communication, 2016.

Stewart, I.D.; Oke, T.R.; Krayenhoff, E.S. Evaluation of the "local climate zone" scheme using temperature observations and model simulations. Int. J. Climatol. 2014, 34, 1062–1080.

Tan, Z; Lau, K. K; Ng, E. Urban tree design approaches for mitigating daytime urban heat island effects in a high-density urban environment. Energy and Buildings 114: 265–274. 2016.

Thomas, G., Sherin, A. P., Ansar, S., & Zachariah, E. J. Analysis of urban heat island in Kochi, India, using a modified local climate zone classification. Procedia Environmental Sciences, 21, 3–13. 2014.

Tso, C. P. A survey of urban heat island studies in two tropical cities. Atmospheric Environment 30: 507–519. 1996.

United Nations. Desa/Population Division. World population/urbanization prospects. Available in: https://population.un.org/wup/Maps/. 2018.

Wong, N.H., Yu, C. Study of green areas and urban heat island in a tropical city. Habitat International 29: 547–558. 2005.

Wong, N. H., Tan, Y. P., Loh, L. F. Historical analysis of long-term climatic data to study urban heat islands in Singapore. Architectural Science Review 48: 25–40. 2005.

Xiaoshan Yanga, Lingye Yaoa, Tao Jina, Lilliana L.H. Penga, Zhidian Jianga, Zhenyu Hua, Yanhua Yec. Assessing the thermal behavior of different local climate zones in the Nanjing metropolis, China. Building and Environmental. 137: 171 – 184. 2018.

Young, A. F. Adaptation actions for integrated climate risk management into urban planning: a new framework from urban typologies to build resilience capacity in Santos (SP). City Territ Archit, 3:12 DOI 10.1186/s40410-016-0042-0. 2016.

Analysis of Local Climate Zones and vegetation cover using land surface temperature and mean radiant temperature in a coastal city with a tropical climate

Abstract

The tropical and subtropical regions have been changing the land surface and consequently the micro-urban climate through a rapid process of urbanization and demographic growth. One way to understand this alteration is to assess the thermal behaviour of different urban environments. In this study, the Solar and Long Wave Environmental Irradiance Geometry model (SOLWEIG) and LANDSAT were employed to investigate the influence of distinct Local Climate Zones (LCZ) on the land surface temperature (LST) and the mean radiant temperature (Tmrt). A warm summer day in 2017 was selected to explore: (1) the LST as estimated from Landsat 8 and from the outgoing longwave radiation (Lup), (2) the spatial Tmrt variations in each LCZ; and (3) the effectiveness of urban forest structure on Tmrt reduction. For the analyzed period (10 LT), thermal radiant environments could be considered quite harmful. Results showed a good agreement between the LST approaches, which showed a similar thermal pattern. As expected, the higher building environments presented the lower LST. Nevertheless, there was an average decrease of around 10°C in surface temperature based on Lup. For Tmrt, the spatial variations (34° - 60°) were largely influenced by building density and height, street orientation, as well as by greenery. Regarding vegetation cover, canopy elevation was a much more significant explanatory variable for Tmrt than the number of trees. Considering the necessity to improve the urban planning and design practice, the study demonstrated that LST and Tmrt variation can be used to identify LCZs more high-thermally exposed. Besides, the results also instigate to rethink the strategies of implementation of trees to enhance the thermal comfort, especially in compact low-rise environments, by optimizing the tree canopy instead of the number of individuals.

Keywords: Mean radiant temperature; land surface temperature; urban canopy; SOLWEIG.

1. INTRODUCTION

Since the eighties, discussions about urban climate in tropical regions became not only an academic issue but also an emergent discussion in urban planning. The improvements in data acquisition and the advance in urban climate studies are essential to understand its impact on developing countries, which have high population growth rates and are mostly in tropical and subtropical climates (Oke, 1984; Roth, 2007).

Studies regarding the effects of urbanization on human health and thermal comfort in tropical and sub-tropical cities have gained increasing attention (Masmoudi & Mazouz, 2004; Duarte, 2015; Chen et al., 2016; Hirashima, Assis and Nikolopoulou, 2016; Lau et al., 2016; Sun et al., 2017; Shinzato & Duarte, 2018). In densely built-up and inhabited cities, the accumulation of heat leads to a heat island, which can be persistent and exceed tolerable values, especially in tropical climates. The mitigation of heat stress and air pollution adverse effects have been addressed in different ways, especially using ventilation, vegetation and appropriate choice of building materials (Jauregui, 1984; Weihi, 1984; Emmanuel, 2005; Grimmond et al., 2010; Mills, 2011; Emmanuel, 2016).

Thermal discomfort in tropical regions is closely related to radiation; Radiation control in buildings is the most efficient way to minimize heat gains from the covering. Therefore, heat resulting from urban surfaces and buildings should be minimized (Emmanuel, 2005). In urban design, the control mechanisms for heat storage are mainly related to the design of the roads, the built density, the height (variation) of the buildings and their typologies as well as greenery.

One way to understand how changes in the urban environment influence the quality of health of dwellers is to assess microclimate and its influence on thermal comfort in different open spaces, such as streets, canyons, parks, etc. (Oke et al., 2017). In this perspective, land surface temperature (LST) and mean radiant temperature (Tmrt) are considered two important parameters for urban climate studies. LST is directly related to land surface characteristics (Voogt & Oke, 2003). The replacement of natural land cover by artificial materials modifies the physical properties of the surfaces and the radiation balance (Givoni, 1998; Voogt and Oke, 2003; Weng, 2009). Tmrt is one of the most important meteorological variables governing the human energy balance and thermal comfort outdoors, especially during clear and calm summer days (Mayer & Hoppe, 1987). Tmrt is the net product of all short and longwave radiation fluxes from the surroundings to which a human body is exposed. When compared to other variables influencing thermal comfort, such as air temperature (Ta) and humidity, Tmrt displays larger spatial variation over short distances (Ali-Toudert & Mayer, 2007; Lindberg et al., 2013). In urban outdoor spaces, Tmrt is determined mainly by building geometry, street layout, ground and facade albedo, and vegetation cover (Lindberg et al., 2016). These elements can be effectively altered by design interventions. Therefore, understanding how the spatial variation of Tmrt is affected by different urban features is significant and may lead to a better understanding of climate-responsive urban design and planning. Solar and LongWave Environmental Irradiance Geometry (SOLWEIG) is one of the most common ways to determine Tmrt. The model follows the same methodology commonly adopted to observe Tmrt (as used, for example, by Höppe 1992), with shortwave and longwave radiation fluxes from six

directions being individually calculated to derive Tmrt (Lindberg, Onomura and Grimmond, 2016). SOLWEIG has been evaluated extensively and applied at urban locations worldwide, such as Gothenburg (Thorsson et al., 2010), London (Lindberg e Grimmond, 2011), Stockholm (Thorsson et al., 2014), Porto (Lau et al., 2015), Shanghai (Chen et al., 2016) and Adelaide (Thom et al, 2016).

Thus, the objective of the present study is to investigate both the spatial variation of LST and Tmrt on a clear hot summer day as affected by different urban geometry and vegetation cover conditions in a high-density tropical coastal city using Local Climate Zones classification (LCZ) (Stewart & Oke, 2012). Here, different urban settings in terms of LCZs are compared and their implications on the LST and Tmrt are discussed. SOLWEIG is used to simulate Tmrt within the study area and to determine LST based on Lup (which is further compared with the LST from Landsat 8). With the results, we evaluate the intraurban thermal response and discuss the influence of vegetation to enhance the microclimate, especially in spaces with greater vulnerability for the urban population.

2. MATERIALS AND METHODS

a.   Study area

Santos (23° 56′ 13.16″ S, 46° 19′ 30.34″ W), located on the central coast of the State of São Paulo (Brazil), configures an isolated compartment in the form of a lowland, with separate hills between the *Serra do Mar* and the Atlantic Ocean. The city has a typical Tropical Atlantic climate influenced by the proximity of the ocean and its influences on atmospheric circulation patterns, which play an essential role in climate elements such as temperature, humidity, precipitation, and wind direction. The median annual temperature in Santos is around 21.9° C, with a difference of 5° C between summer and winter seasons (Miller et al., 2012). On average, Santos receives about 2500 mm of total annual precipitation concentrated from October to April (75%) and an average monthly total of 317 mm (Miller et al., 2012). Regarding ventilation pattern, the alternation of the sea and land breeze establishes a permanent thermal exchange. Urban activities, such as summer tourism, petrochemical complex, regional construction activity, exploration of oil and gas from the Santos Basin, as well as infrastructure linked to the Port of Santos have been promoting changes in the micro-urban climate of Santos city (Kawashima et al., 2015).

b.	Methodological framework

The methodological framework of the current study is shown in Fig. 20. Four LCZs that represent distinct urban environments within Santos were chosen. Field survey was conducted to obtain data of the landcover of each LCZ (i.e. height/weight (H/W), sky view factor (SVF), trees, waterbody, street axis, and buildings). On-site measurements were carried out on December 17th, 2017. This day was chosen as representative since it was relatively the most desirable for summer (calm, warm, and clear) among the days that the field measurement carried out in Santos (15th November 2017 to 11th October 2018). Air temperature (Ta) and relative humidity (RH) were collected by data loggers (HOBO Pro v2) from 00:00 to 23:00 h with a time interval of 5 min. For Ta, the accuracy is 0.2°C for the range between 0° to 50°C with 0.02°C of the resolution, and for RH, the resolution is 0.03% with an accuracy of +/- 2.5% between 10% and 90% RH (typical), to a maximum of +/- 3.5% out of this range. Each equipment was covered by a radiation shield and lifted up to 2.5 m from the ground. The output data from SOLWEIG, Lup and Tmrt, were analyzed in three different approaches. First, Lup and LANDSAT 8 images were investigated to obtain surface temperature. Second, spatial Tmrt, at the same interval of the satellite (10 LT), was analyzed to complementary the thermal environments promoted by different urban design. Third, the influence of vegetation on Tmrt was analyzed into distinct time window. Finally, the conclusions of the current research are given, which emphasizes the thermal behaviors as well as urban devices for each LCZs. The following sections provide detailed information on each procedure.
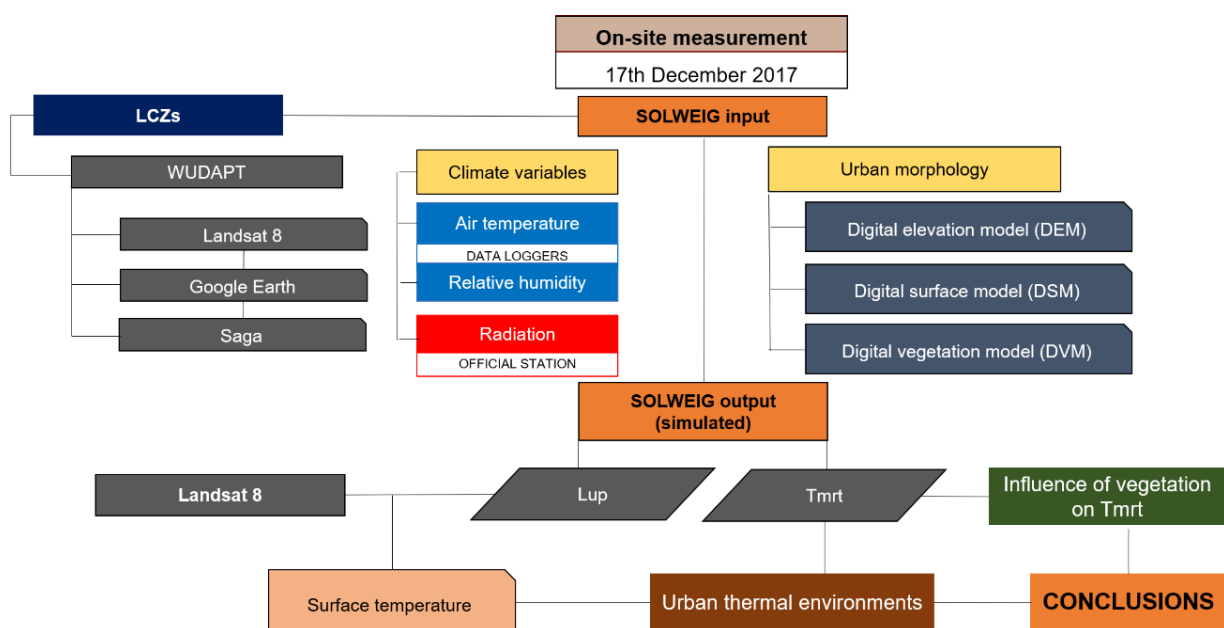
Figure 19. Methodological framework of the current study.

Local Climate Zones map

The LCZ map was produced in agreement with World Urban Database and Access Portal Tools (WUDAPT) methodology workflow (Bechtel et al., 2015). It is based on three daytime LANDSAT 8 scenes (July 26th and November 15th, 2017 and August 30th, 2018), on training areas selected in Google Earth, and on the algorithm for Local Climate Zone classification within the System for Automated Geoscientific Analyses (SAGA) version 6.4. The classification algorithm is the so-called Random Forest classifier, which consists of integrated decision trees that classify each image pixel into one LCZ type. The LCZ map spatial resolution is 100m. Based on the LCZ classification, our study sites include compact high-rise (LCZ1– HRB), mid-rise (LCZ2 – CMR) and low-rise buildings (LCZ3 - CLR1 and CLR2). Figure 21 shows both the LCZ classification of Santos's island city and study places as well as localization of Santos. The accuracy of the LCZ map was produced by Benjamin Bechtel[7] (Bechtel et al., 2019), which showed Overall Accuracy (OA) of 0.78 and the Kappa coefficient was 0.75.
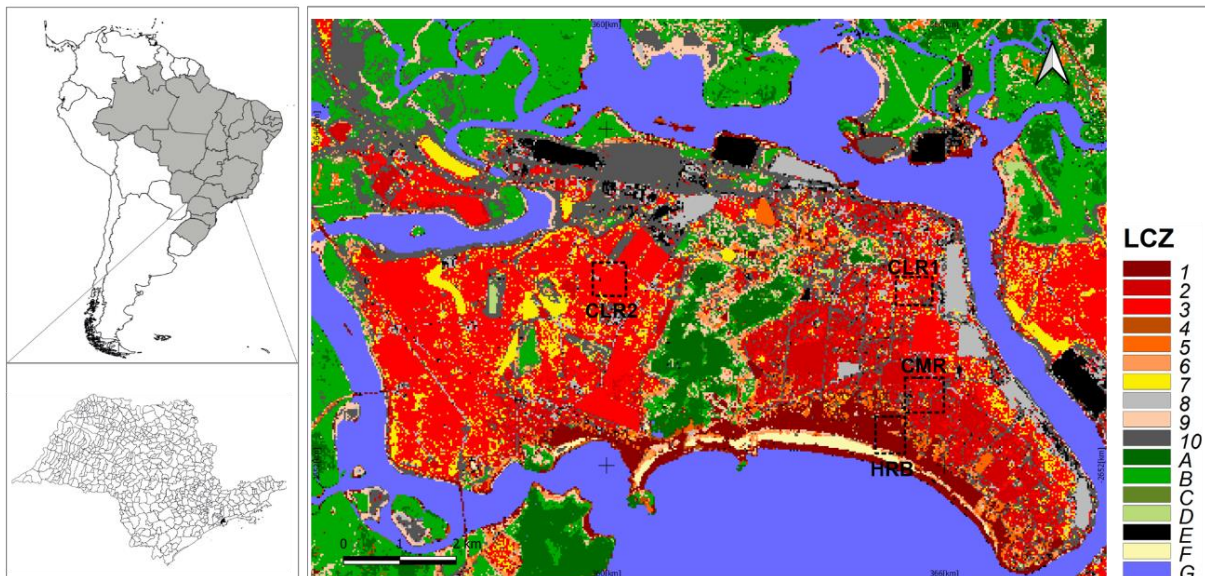
Figure 20. Santos - Local Climate Zone classification. The highlighted rectangles represent the LCZs analyzed in this article.

SOLWEIG

SOLWEIG estimates spatial (2-D) variations of 3-D radiation fluxes and the Tmrt in complex urban settings. Both 3D vegetation (trees and bushes) and ground cover variations are considered in the model. In this study, 2019a version of SOLWEIG is used (Lindberg & Grimmond, 2019), which requires meteorological data consisting of time-series of air

---

[7] See Bechtel et al., 2019 to assess more information about LCZ workflow and WUDAPT.

temperature (Ta), relative humidity (RH), global (G), diffuse (D) and direct (I) solar radiation as well as DSMs of building and vegetation. As diffuse and/or direct solar radiation are not commonly available, the model also permits calculation of D from G in conjunction with Ta and RH, according to the Reindl et al., (1990) approach. Direct shortwave radiation on a surface perpendicular to the Sun is then estimated:

$$I = (G - D)/ sin(\eta)$$

where η is the Sun's altitude angle above the horizon (Lindberg, Onomura and Grimmond, 2016).

For this work, both outgoing longwave radiation (Lup) and Tmrt in four LCZs in Santos were simulated using SOLWEIG model. Figures 22 through 26 show screenshots from Google Earth® (GE) of all LCZs along with a Digital Surface Model (DSM) and SVF for each LCZ. The DSMs were created using GE tools and Structure from Motion (SfM) technology and a better description of the procedures may be found in Bourscheidt & Breunig (2019). The resulting DSM has a spatial resolution of 1 meter and does not include the vegetation (it is based only in the buildings inside the urban area). Additionally, 3D model from GE may differ from the imagery in some areas due the difference in the acquisition date of each product (satellite views are more recent). The SVF rasters are based on this DSM and were processed within the Urban Multi-scale Environmental Predictor - UMEP[8] (pre-processor steps).
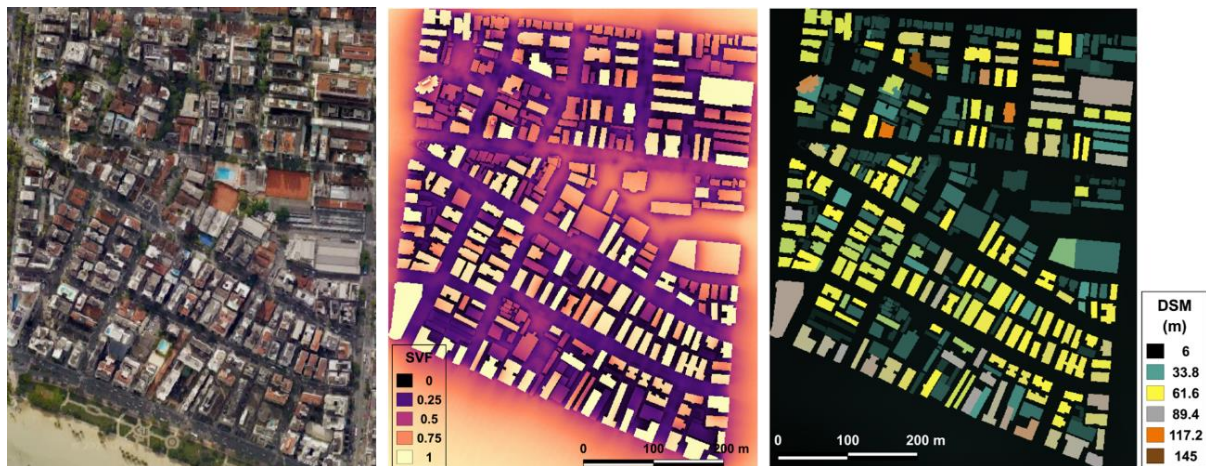
Figure 21. Screenshots from Google Earth (left), SVF (middle) and digital surface model (right) of the compact high-rise building (HRB). Differences between the image and the models are related to the date of acquisition of each product (satellite images are more recent).

---

[8] UMEP is a free climate service tool, designed for researchers and service providers. This tool can be used for a variety of applications related to outdoor thermal comfort, urban energy consumption, climate change mitigation etc. Since SOLWEIG is a tool within UMEP, we used the first steps available in UMEP to create both meteorological and spatial data as well as urban geometry, called in plugin as pre-processor. For more information see https://umep-docs.readthedocs.io/en/latest/pre-processor/Pre-Processor.html.
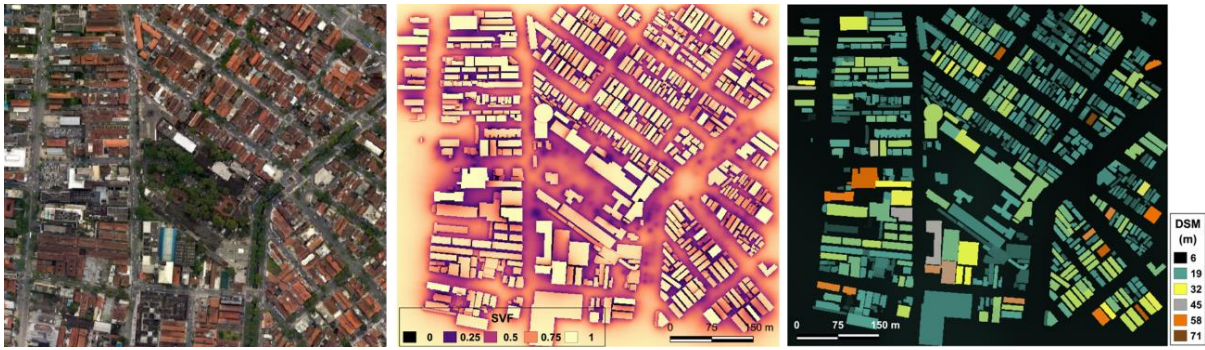
Figure 22. Screenshots from Google Earth (left), SVF (middle) and digital surface model (right) of the compact mid-rise building (CMR). Differences between the image and the models are related to the date of acquisition of each product (satellite images are more recent).
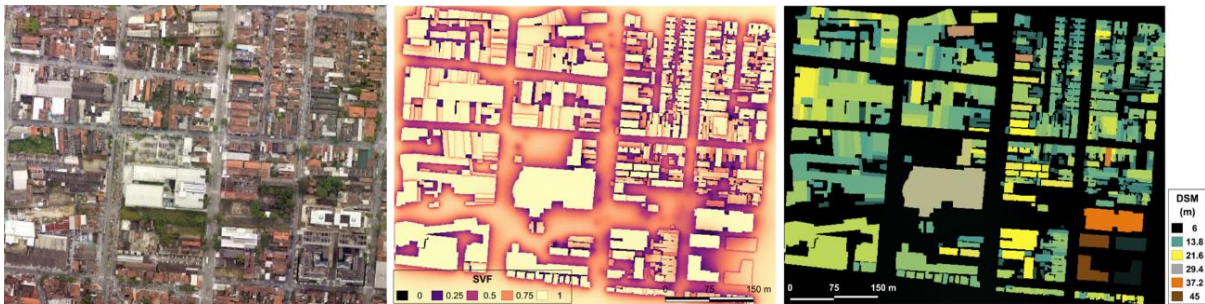
Figure 23. Screenshots from Google Earth (left), SVF (middle) and digital surface model (right) of the compact low-rise building (CLR1). Differences between the image and the models are related to the date of acquisition of each product (satellite images are more recent).

Figure 24. Screenshots from Google Earth (left), SVF (middle) and digital surface model (right) of the compact low-rise building (CLR2). Differences between the image and the models are related to the date of acquisition of each product (satellite images are more recent).

A clear and hot summer day on December 17th, 2017 (Table 3) was selected for investigation. To run the model, the following meteorological variables were obtained from São Paulo State Environmental Company (CTB) station, represented by CMR: barometric pressure (Pa), wind speed (Ws), incoming shortwave radiation (Radg). Besides, additional air temperature (°C) and relative humidity (RH) for HRB, CLR1 and CLR2 were obtained from data loggers placed within each LCZ.

Table 3. Meteorological data from CTB (official station) and LCZs.

Hour	HRB (°C)	HRB (RH)	CTB (°C)	CTB (RH)	CLR1 (°C)	CLR1 (RH)	CLR2 (°C)	CLR2 (RH)	Ws (m/s)	Press (Pa)	Radg (W/m2)
0	25,7	80,8	24,6	89	25,1	83,7	25,1	83,8	0.1	101	0
1	25,6	81,0	24,1	91	24,6	86,2	24,4	88,2	0.1	101	0
2	25,4	82,4	23,8	93	24,2	88,0	24,4	88,2	0.1	101	0
3	24,9	84,1	23,4	95	23,7	89,8	23,9	87,0	0.1	100	0
4	24,8	85,0	23,2	96	23,6	90,1	23,7	89,8	0.1	100	0
5	24,8	85,0	23,0	97	23,8	89,9	23,2	90,1	0.1	100	0
6	24,6	84,8	22,8	97	23,2	90,3	23,1	90,7	0.1	100	0
7	24,9	84,0	22,6	98	23,8	89,1	23,9	88,9	0.1	100	9
8	25,7	83,2	24,6	92	27,2	77,9	27,1	77,5	0.7	101	171
9	27,5	77,7	28,7	75	29,7	70,2	29,5	69,1	0.9	101	435
10	28,0	77,5	31,3	66	32,2	60,7	32,0	60,6	1	101	661
11	29,6	72,2	32,8	62	28,4	71,5	33,7	59,1	1.3	101	838
12	30,7	65,9	34,0	54	31,5	59,5	33,5	56,5	1.5	101	975
13	32,8	58,5	33,6	56	32,8	57,0	34,9	52,7	1.6	101	1045
14	33,2	59,2	34,5	53	32,3	56,2	36,5	46,7	1.6	101	1047
15	31,8	57,6	34,6	52	31,8	58,5	34,9	49,7	2	101	976
16	31,6	58,7	34,5	52	33,7	51,8	35,5	48,3	1.9	101	840
17	31,6	56,3	34,2	51	33,0	53,3	35,1	48,7	1.6	101	650
18	31,0	56,7	33,0	53	31,8	53,9	33,4	54,1	1.4	100	72
19	30,5	57,0	30,9	57	30,7	56,2	31,9	55,7	1.3	100	39
20	29,9	56,8	29,9	58	30,1	55,4	30,8	55,2	1.2	100	8
21	29,8	54,6	29,1	59	29,2	60,0	30,2	57,9	0.9	101	0
22	29,1	63,5	28,6	61	28,7	67,8	29,1	67,7	0.1	101	0
23	28,6	66,0	28,0	71	28,8	69,4	28,6	72,3	0.1	101	0

Standard absorption coefficients for shortwave and longwave radiation were used to run SOLWEIG, i.e. 0.7 and 0.95, respectively. The surface albedo for building and ground surfaces was set to 0.2 and 0.15, respectively. The emissivity of building walls was set to 0.9, representing a combination of concrete and glass, and the emissivity of ground surfaces was set to 0.95 for rough concrete.

Based on the input DSM, meteorological data, surface characteristics, and Santos's geographical location, Tmrt values were calculated for a standing person, using the surface projection factors of 0.22 for the east, west, north and south directions, and 0.06 for the upward and downward directions. The simulations were conducted for each hour from 00:00 to 23:00.

To include the vegetation in the analysis, a new "vegetation DSM" was generated manually for all sites through 3D GE by using information from a point layer that specifies both the positions and the attributes of each tree. 3D Vegetation is described by two different grids. First, a canopy DSM (CDSM) which represents the top of the vegetation and second, a trunk zone DSM (TDSM) that describes the bottom of the vegetation.

Comparison with Landsat

A great number of studies were conducted in the recent years to validate Tmrt obtained with SOLWEIG (Lindberg & Grimmond, 2011; Chen et al, 2016; Lau et al., 2016; Thom et al., 2016), most of them are made only in specific locations. Thus, to understand the thermal behavior in terms of radiative energy from the roofs, walls, and ground and its influence on Tmrt among the different areas, LCZs were further evaluated in terms of land surface temperature (LST), which was calculated from LANDSAT imagery and by using outgoing longwave radiation (Lup) from SOLWEIG model. Those variables are expected to be comparable when land cover scheme in SOLWEIG is used to better represent the different ground cover materials (F. Lindberg, personal communication, 2020).

Since Lup is a measure of the amount of energy emitted to space by earth's surface, oceans, and atmosphere, it might be converted to LST by using Stefan–Boltzmann law. According to the Stefan-Boltzmann law, the amount of long-wave radiation is proportional to the fourth power of the surface temperature of the emitting material. As a result, the surface temperature of the surroundings, such as pavement and building walls, can be used as an indication of the level of long-wave radiation (Lau et al., 2015). In this way, the following formula was used to estimate LST for each LCZ layer at the same time (10:00 Local Time) and date, chosen to agree with the LANDSAT overpass:

$$LST = \left(\frac{L_{up}}{5.67 * 10^{-8}}\right)^{1/4} - 273.158$$

Where LST is the land surface temperature and L_{up} is the outgoing longwave radiation obtained from the model for each LCZ at 10:00 (LT). This approximation ignores the additional components usually used in satellite LST estimation.

LANDSAT 8 image (path-row 219/77) from December 17th, 2017 at 13:04 GMT was used. Simple Atmospheric Correction (DOS1) was applied on bands 2-7 by using the Semi-Automatic Classification Plugin (Congedo, 2016) and surface temperature was estimated with the Land Surface Temperature Plugin (Isaya Ndossi & Avdan, 2016) in QGIS 2.16 software. Within the plugin, the user needs to follow some steps: calculate the radiance from digital number (DN); obtain the NDVI as a reference for the emissivity; calculate the brightness temperature including the emissivity; and finally, to determine the surface temperature removing the effects from the atmosphere. A Radiative Transfer Equation (RTE) was used in this last step in an attempt to remove the effect of the atmosphere, which requires the insertion of atmospheric transmittance, upwelling and downwelling parameters.

Those values were estimated for the study area using the Atmospheric Correction Parameter Calculator (ACPC) (Barsi et al., 2003). ACPC simulates atmospheric parameters for specific dates, times, and locations, according to the profile modeled by the National Centers for Environmental Prediction (NCEP) on a 1 ° x 1 ° grid (Barsi et al., 2003; Isaya Ndossi & Avdan, 2016; Yu et al., 2014). Based on Isaya Ndossi and Avdan (2016), weather data can be used in conjunction with NCEP information to model the accuracy of surface temperature estimation. In this sense, meteorological data obtained from the automatic surface station of the CTB and the estimated ACPC parameters are presented in Table 4.

Table 4. Parameters for the application in the surface temperature.

Date	Atmospheric Transmission	Upwelling Radiance (W/m²/sr/um)	Downwelling Radiance (W/m²/sr/um)
17-12-2017	0.48	4.59	6.77

The influence of vegetation on Tmrt

Based on this new model, Tmrt values were calculated a second time through SOLWEIG. The new outputs were used to obtain the difference between estimates with and without vegetation was obtained for all LCZs in the same interval:

$$\Delta Tmrt = Tmrt \text{ (with vegetation) - Tmrt (without vegetation)}$$

The resulting Tmrt variation (ΔTmrt) was then evaluated for all LCZs against the number of trees and the mean canopy elevation (obtained from the CDSM). The values of both variables were extracted using a grid (net fish) with 50m resolution in QGIS software. Grid cells without any trees (i.e., canopy = 0) were dropped from the analyses. Three time periods were considered: the hottest time of the day (14:00), the daytime average (6:00 to 19:00), and the full day average (24 hours period). The results from these analyses are presented in the section 3.3.

3. RESULTS AND DISCUSSION

3.1 Land surface temperature comparison

Fig. 26 shows the LST obtained from Landsat and Lup. The spatial pattern of the Tmrt is presented in Fig. 27 and 28. All analyses were conducted in the same day and time, 17th December 2017 at 10:00. The summary statistics of the LST for the different areas is presented in Table 5, which also shows the results for Lup and Tmrt.
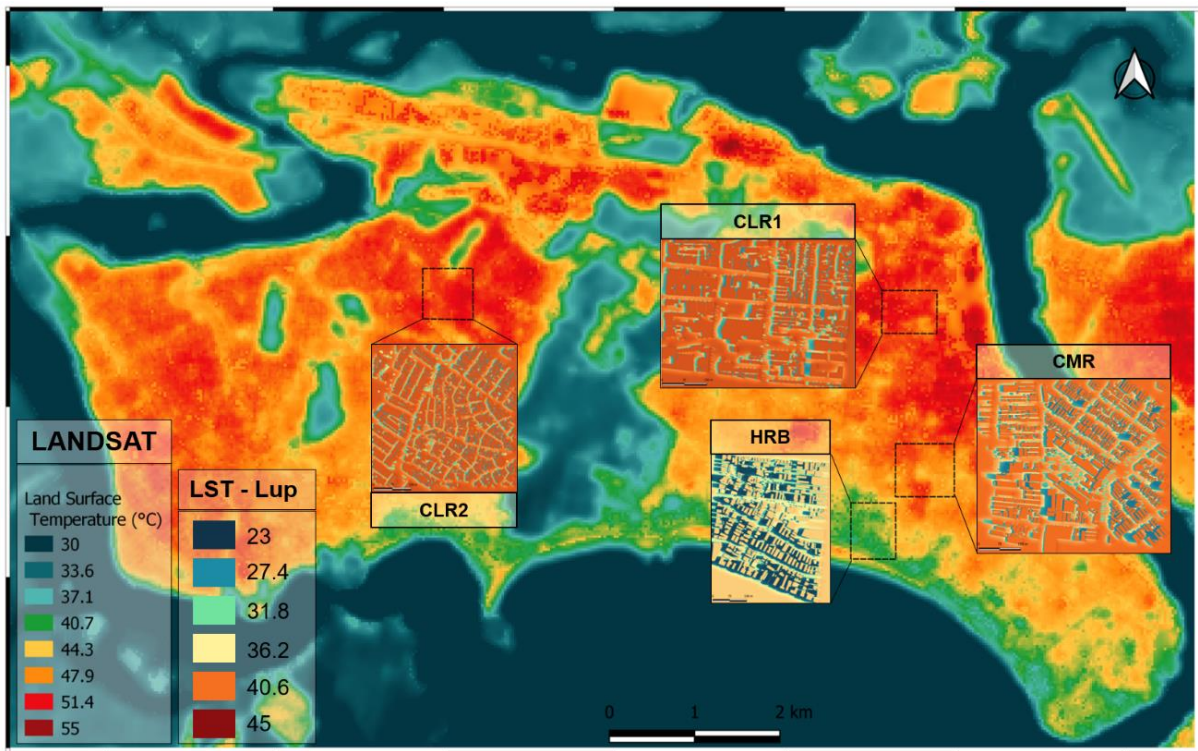
Figure 25. LST obtained from LANDSAT 8 and Lup in the study area. The highlighted images of the LCZs correspond to the LST using Lup.

The thermal difference between the LCZs is clear from the Landsat image in Fig. 26. While HRB has LST values between 40 - 47°C, CMR presented temperatures between 44 - 51°C. On the other hand, CLRs showed values over 50°C distributed throughout the area. For LST calculated using Lup (Fig. 26), the thermal pattern was like the observed with Landsat for all LCZs, with the lowest values in HRB and the highest in CLRs. Areas of tightly-packed tall buildings (HRB) appeared slightly cooler because of mutual shade, while the opposite occurred in LST obtained in the CLRs (higher temperatures) since the height of the houses (less than 3 and 2 floors in CLR1 and CLR2, respectively) limits the extent of shaded areas. On the other hand, the LST at CMR may be related to both the shading of buildings between 3 - 6 floors and the trees, whereas more heavily vegetated areas, especially with tree canopies, have a lower daytime surface temperature (Oke et al., 2017).

Nevertheless, there is an average decrease of around 10°C in surface temperature based on Lup. For example, CMR showed mean values of 47.8°C with Landsat, while the mean value is 37.7° C for Lup LST. Further, the standard deviation (STD) is larger for all areas (over 4°C). HRB shows the highest STD (4.77) and CLR1 the lowest (4.02). Another observation from Landsat LST is the lower STD for all areas, representing a homogenous temperature in each one. These results could be explained mainly by (1) the different resolutions of Landsat (30m) and SOLWEIG (1m), considering that better resolution implies in larger spatial variations, (2) by the impact of the atmosphere in the calculation of the LST from Landsat that could have not

been completely addressed by the RTE model, resulting in an unrealistic higher temperature at the ground, (3) by the built environments energy balance. While LANDSAT 8 considers the energy balance of facets, in this case, roofs and walls, SOLWEIG uses only the emissivity values of the ground surface and walls to calculate Lup (Lindberg, Holmer and Thorsson, 2008). Thus, since roofs and walls are more exposed to the sun and formed mostly of low albedo and high emissivity materials, they absorb more radiation and consequently show higher surface temperature. At the ground level, LST tends to be smaller because it will depend on orientation, exposure, and access to radiation through SVF and H/W (Oke et al., 2017).

3.2   Spatial Tmrt at 10:00

Considering the Tmrt (Fig. 27 – 28), in each LCZ the temperature had an increase of ~20°C when compared to the LST - Lup. These results were expected since Tmrt is calculated by using both longwave and shortwave radiation. The STD also increased for all LCZs, which means largely spatial variation on Tmrt in each area. HRB displayed, once again, the highest STD. In such condition, with a radiation ~ 650 W/m² and a clear sky, while the ΔTa among LCZs was ~3°C, the ΔTmrt variation between HRB and CMR was ~5°C, and between HRB and CLRs was ~10°. Thus, the spatial Tmrt is clearly higher in CLRs, and it can be explained by the fact that due to the low building heights, and consequently higher SVF (≥ 0.5), those areas receive much more short wave radiation, which warms up the air at spaces between buildings more than in other LCZs, like CMR and HRB. In addition, while CLRs showed lower Tmrt only in the west side (~ 44°) due to opposite sun's position, at the same time window, deep canyons on HRB further a greater cooling by obstructing direct radiation and promoting shadow. As a consequence, in those areas within HRB, the Tmrt was lower than 40° (~34°).
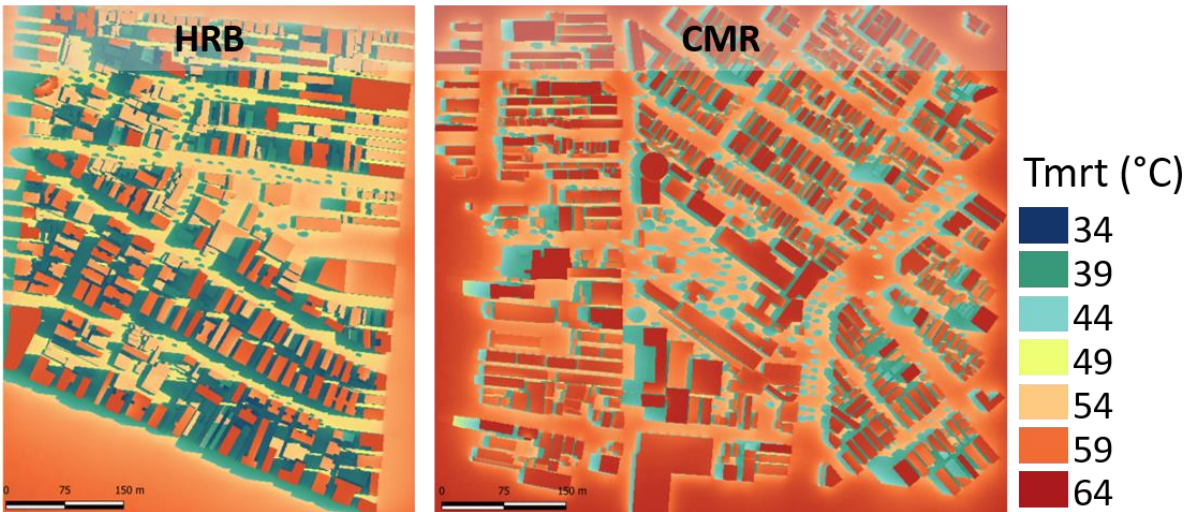
Figure 26. Tmrt for HRB and CMR at 10:00.

Figure 27. Tmrt for CLR1 and CLR2 at 10:00.

Table 5. Descriptive statistics for LST (Landsat), LST (Lup) and Tmrt at 10:00 am.

	Landsat 8				Lup				Tmrt			
	HRB	CMR	CLR1	CLR2	HRB	CMR	CLR1	CLR2	HRB	CMR	CLR1	CLR2
Max	46.8	51.0	52.6	52.5	39.6	43.5	44.1	44.3	60.9	63.0	66.3	63.4
Mean	42.1	47.8	50.2	50.3	32.7	37.7	39.8	39.5	49.9	55.4	58.5	58.2
Min	38.7	44.5	46.4	43.5	23.9	26.5	27.4	27.3	34.7	37.4	38.5	38.4
STD	1.59	1.44	1.23	1.28	5.66	4.77	4.02	4.18	9.05	7.55	6.49	6.72

3.3   The influence of vegetation on Tmrt

Influence during the warmest period

Figures 29 and 30 show the influence of the vegetation on the spatial distribution of Tmrt at 14:00 for all LCZs (HRB and CMR in Figure 29; CLR1 and CLR2 in Figure 30) in conformity with tree canopy (ΔTmrt x CDSM). Although HRB has a considerable number of trees (213 individuals) and they are homogeneously distributed throughout the area, most of them (> 80%) have a crown diameter of up to 5 meters. This fact reduces the radius of influence of the vegetation on Tmrt both under the tree and at its shaded area throughout the day. For CMR, the largest number of trees (260 individuals), 56% of them have 1-5m of crown diameter, and 41% are up to 10m, which increases the radius of influence on Tmrt throughout the day due to increased shading.
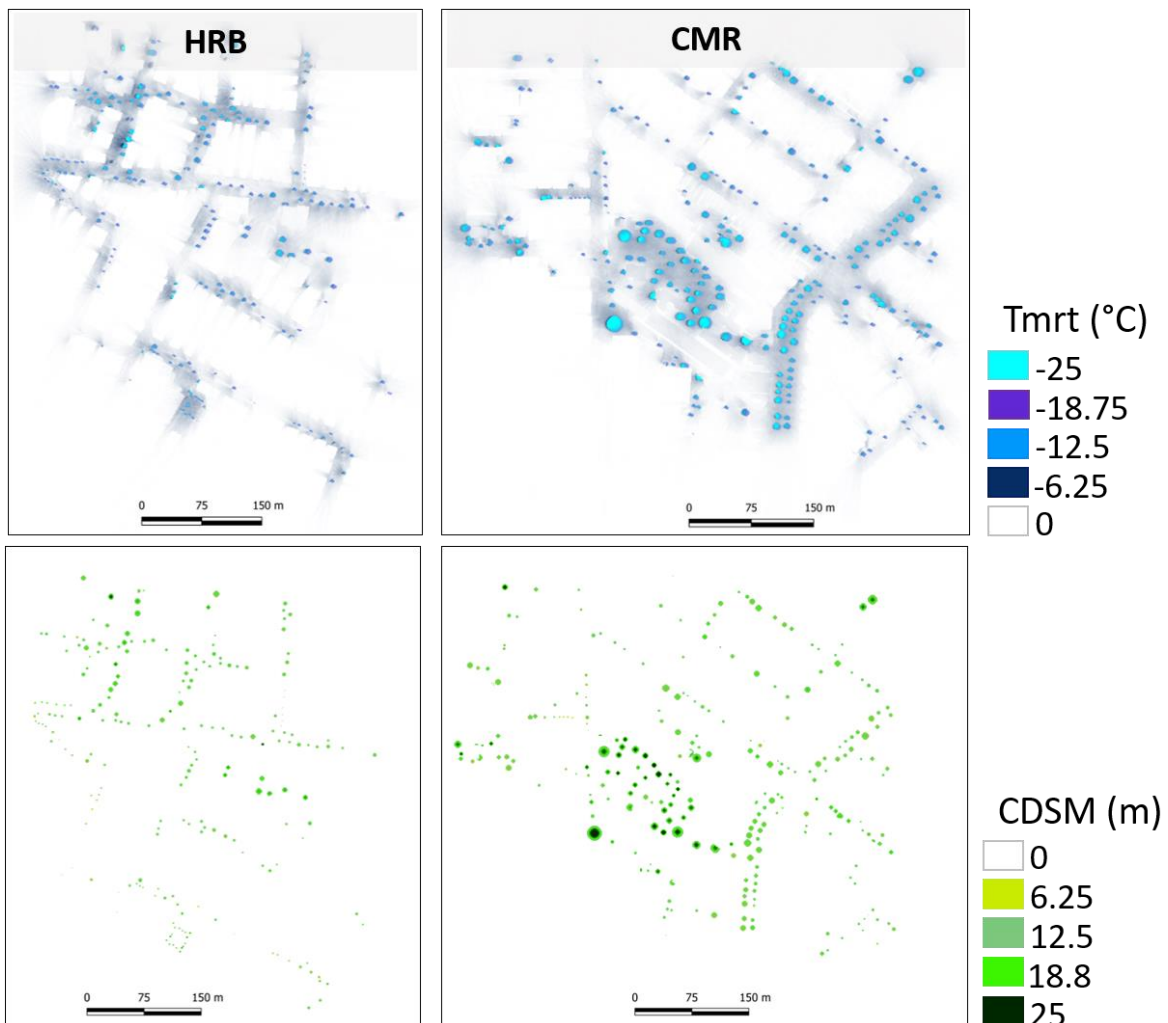
Figure 28. ΔTmrt (top side) and Canopy DSM (bottom side) for HRB and CMR.

CLR1 (223 trees) showed a high concentration of trees on the east side; the west side has fewer trees with lower canopy diameter (<5 m). Another peculiarity of this area is the existence of palm trees with the lowest canopy (1m) beside the avenue flowerbed, which have a reduced impact on the Tmrt. CLR2 has the smallest number of trees (104 individuals), concentrated in the west side of the area. Most of the trees are in public spaces and few are found on the sidewalks. On sidewalks, the canopies have around 1-5m (59%) and in the public squares, 6-10m (35%). Only a few trees have more than 11m (6%).

For all areas, Tmrt is reduced mainly around the area underneath the vegetation (> -20°C), including the shadowed area, with some impact in the surroundings (< -4°C). In this way, the shadows at 14:00 were projected from W-E, and its radius of influence depends on canopy diameter.
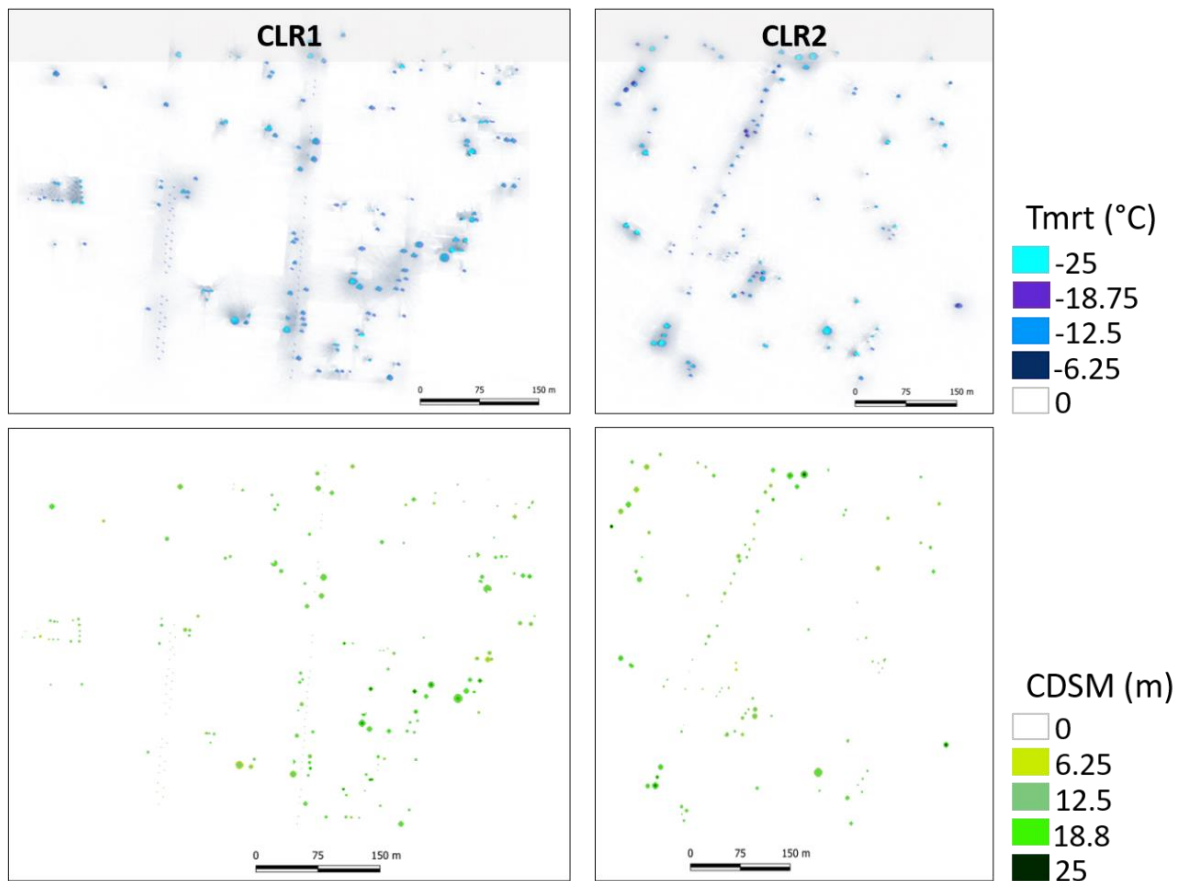
Figure 29. ΔTmrt (top side) and Canopy DSM (bottom side) for CLR1 and CLR2.

To reinforce the spatial analysis presented above, the role of vegetation canopy on Tmrt variation is further investigated for all LCZs by comparing ΔTmrt against the number of trees and the mean canopy elevation (see figure 31) using a grid analysis, as described in the methodology. The determination coefficient analyses show that the canopy elevation is a much more significant explanatory variable for Tmrt than the number of trees (R^2 values of 0.9 and 0.37, respectively). Thus, an average variation of 1m in the canopy implies a difference of approximately 3°C in the Tmrt. In contrast, the number of trees is uncertain, since almost 10 trees could impact in just 1°C on Tmrt.
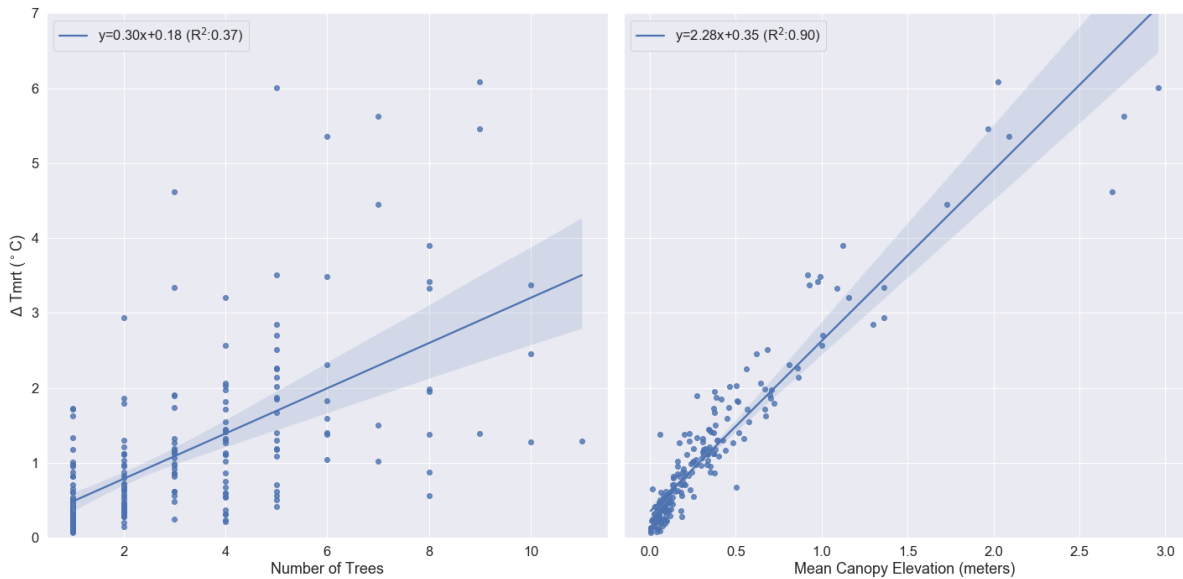
Figure 30. Influence of vegetation on Tmrt. Number of trees (left side) and mean canopy elevation (right side).

Temporal influence of vegetation on Tmrt

Since the previous section was focused on the hottest part of the day, a broad analysis was carried to examine the temporal influence of vegetation on Tmrt in each LCZ. For this, two additional intervals were considered, daytime (6h - 19h) and full-day (0h - 23h). Both mean canopy elevation and the number of trees were evaluated using the grid (net fish) approach already described. The results for this analysis are shown in Fig. 32. Regardless the general lower R^2 values for the number of trees (top panel) among LCZs compared to the average canopy (as already observed for the hottest period of the day), some other aspects/features may be highlighted.

Firstly, there is a significant reduction on the impact of the vegetation when moving from the hottest period (14:00) to the daily average (7° to 2°C of variation), which implies that vegetation tends to compensate the difference during nighttime. This is reinforced by the general lower explanatory power of the linear regression during the full day period, suggesting that the influence of vegetation is greater at daytime for all LCZs. As already known, tree shading lowers Tmrt during the day, at nighttime, restriction of longwave radiation emission beneath dense tree canopies can result in slightly elevated Tmrt relative to open areas (Sun et al., 2017).

Secondly, an interesting variation is observed mainly in the HRB considering the average canopy (bottom plots) when moving from full-day to the daytime period: while the R^2 values are quite similar at the 24 hour period, there is a consistent discrepancy in the values for the daytime period, with the highest R^2 value at CLR2 (0.87) and the lower at HRB (0.65). Moreover, it is noteworthy that in the four plots CMR, CLR1, and CLR2 show a similar slope

while, in contrast, HRB exhibited significant changes in the behavior of the curves relative to the analyzed intervals. This observation is probably related with shading variations by high buildings, which decrease the direct shortwave radiation and minimize the importance of the vegetation during daytime at HRB. At night, on the other hand, canyons with lower sky view factor reduce longwave cooling, resulting in greater radiative contribution from urban surfaces on Tmrt.
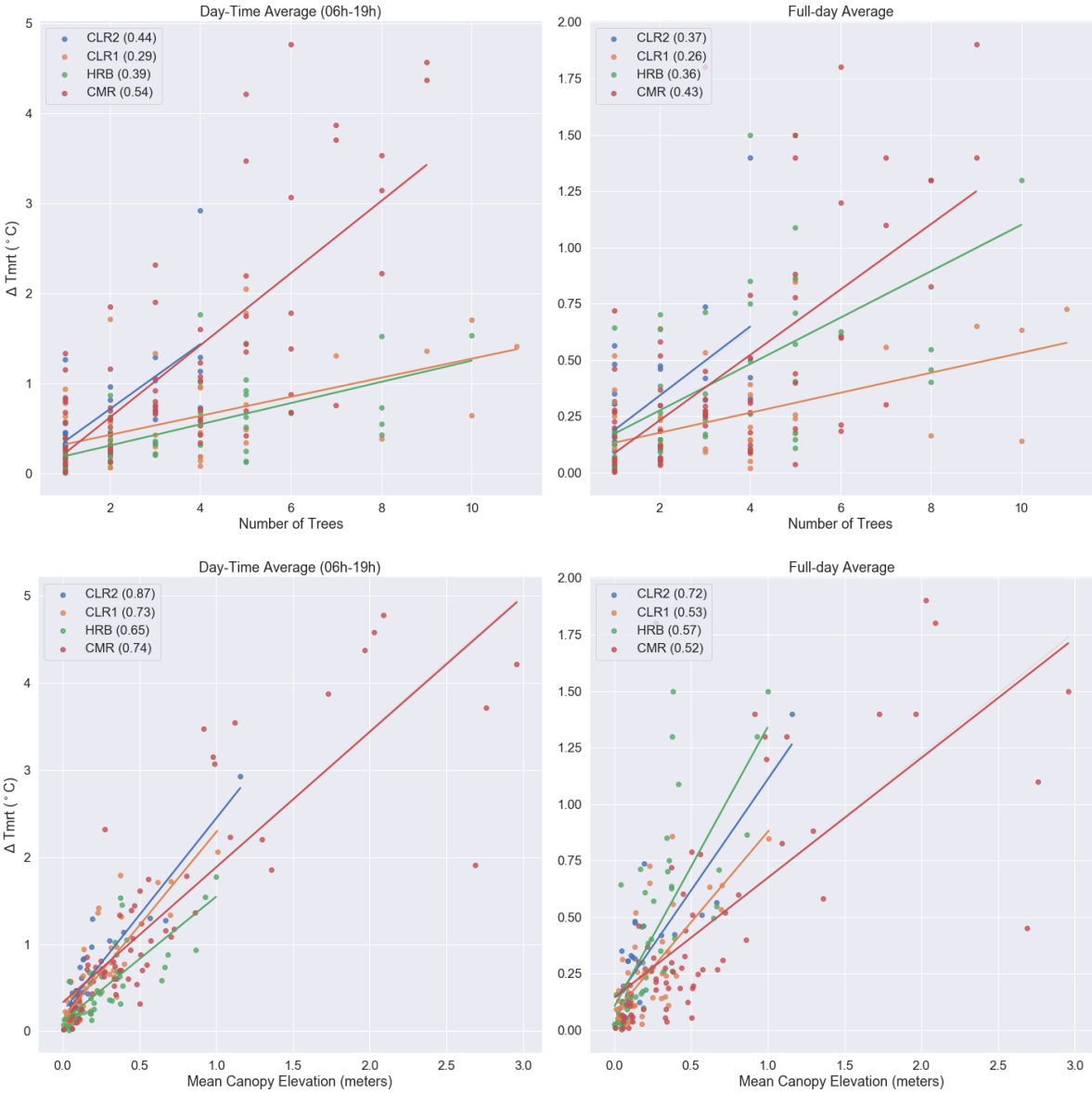
Figure 31. Temporal influence of the number of trees (top) and average canopy (bottom) on Tmrt in each LCZ (legend in the plots). Daytime period is shown in the left side and full day in the right. R^2 values are showed within the parenthesis for each LCZ.

The most effective way to reduce Tmrt in urban areas is by providing shadow to decrease incoming shortwave radiation, as described in other studies (Ketterer & Matzarakis, 2014; Lee, Mayer, and Chen, 2016; Thorsson et al., 2014) and is being reinforced by the

results from this work. Shading in urban areas comes from both buildings and trees. As shown in Fig. 29 - 30 the reduction of Tmrt is higher around each vegetation unit, i.e., where shadows from vegetation are found, which is also in agreement with previous studies (Lindberg et al., 2013; Sun et al., 2017; Thom et al., 2016; Thorsson et al., 2014).

Although the reduction in Tmrt from each vegetation unit is determined mostly by the canopy of the trees (Fig. 31), Fig. 32 shows that the reduction in the average Tmrt over the LCZs from increasing the greenery cover will also depend on the built environment density and height of the buildings, especially at daytime period. This indicates that introducing vegetation in areas with low building density (higher SVF), such as CLR2, could reduce Tmrt more effectively than introducing vegetation into a dense and lofty urban setting, like HRB. Thus, properly altering the urban geometry and cover vegetation might be an effective and relatively simple way to mitigate heat stress during periods with higher temperatures (Lindberg & Grimmond, 2011; Shashua-Bar et al., 2012; Mayer et al., 2008). Thus, in order to maximize the cooling effect type, arrangements and location of vegetation need to be considered. In terms of vegetation type, trees with canopy larger than 5m of diameter are preferred over lower vegetation (bushes, ground vegetation) due to their ability to provide shade (Lindberg & Grimmond, 2011). During the day, the cooling effect of trees is mainly due to shading (Mayer et al., 2008; Lindberg & Grimmond 2011), which implies that vegetation should be placed near surfaces that tend to heat up, i.e. trees near sunlit facades in the afternoon or even green walls. This means that in compact low-rise buildings the effectiveness of vegetation is clearer than in medium or high-rise buildings, which have more influence of buildings geometry and associated shadows. Nevertheless, planting trees cannot be negligible in high built-up areas, since vegetation lowers Tmrt through not only by shading but also by evapotranspiration (Chen et al., 2016).

4. CONCLUSION

This paper presents a pilot study using SOLWEIG model to examine the spatiotemporal variation of Tmrt and LST (estimated from both Lup and Landsat 8), as well as the influence of vegetation on Tmrt during a hot day in a high-density coastal city.

A general offset between LANDSAT and Lup LST was observed, which is probably associated with the radiative balance conditions intrinsic to each method. On the other hand, both approaches showed a similar spatial thermal pattern in each LCZ, following the behavior of Tmrt. Spatial variation of Tmrt is found to be higher in compact low-rise than high and

mid-rise buildings due to the exposure to direct short-wave radiation. Although, areas along sunlit high building walls are also found to be hot spots.

Regarding the influence of vegetation on Tmrt, average canopy showed a general better explanatory power than the number of trees (R^2 of 0.9 and 0.37, respectively) considering the Tmrt variation, with a general variation of 2.3°C for each canopy unit. Besides, the importance of greenery in areas without mutual building shading, normally represented by LCZ3, is greater than in a complex built environment like HRB.

In conclusion, two main approaches should be considered to reduce Tmrt in coastal tropical cities: increase the urban greenery and rethink the design of tall buildings so that they promote comfort at pedestrian levels throughout the day, such as overhanging facades and extended canopies. Additional recommendations are:

- Trees with canopy > 5m are preferred over lower vegetation such as bushes and grass, considering that large trees can produce more extensive areas of shadow.
- In high and mid-rise building, trees should be used on the sunlit facades at daytime and besides the sidewalk to protecting pedestrian from direct sun exposure, especially when the sun is at the highest altitude.
- Evergreen trees should be used instead of deciduous trees because they give shade in all seasons.

REFERENCES

Ali-Toudert, F; Mayer, F. H. (2007). Effects of asymmetry galleries, overhanging facades and vegetation on thermal comfort in urban street canyons. *Sol. Energy* 81:742–754.

Barsi, J. A.; Barker, J. L.; Schott J. R. (2003). An atmospheric correction parameter calculator for a single thermal band earth-sensing instrument. In: *Geoscience and Remote Sensing Symposium*, 2003, Tolouse. Proceedings...2003. IEEE, 2003. p. 3014-3016. Available in: <http://ieeexplore.ieee.org/document/1294665/>.

Bechtel, B., Alexander, P. J., Beck, C., Böhner, J., Brousse, O., Ching, J. (2019). Generating WUDAPT level 0 data - current status of production and evaluation. *Urban Climate*, 2019, 27, 24–45. https://doi.org/10.1016/j.uclim.2018.10.001.

Bechtel, B; Alexander, P; Böhner, J; Ching, J; Conrad, O; Feddema, J; Mills, G; See, L; Stewart, I. (2015). Mapping local climate zones for a worldwide database of form and function of cities. *International Journal of Geographic Information*, 4(1), 199-219. doi:10.3390/ijgi4010199.

Bourscheidt, V; Breunig, Fabio Marcelo. (2019). Lightning attractiveness index for urban areas based on digital surface model. In: *XIX Simpósio Brasileiro De Sensoriamento Remoto*. Santos. Anais Do XIX Simpósio Brasileiro De Sensoriamento Remoto. Campinas: GALOÁ, 2019. v. 17.

Chen, L; Yu, B; Yang, F; Mayer, H. (2016). Intra-urban differences of mean radiant temperature in different urban settings in Shanghai and implications for heat stress under heat waves: A GIS-based approach. *Energy and buildings*. http://dx.doi.org/10.1016/j.enbuild.2016.09.014.

Congedo, L. Semi-Automatic Classification Plugin Documentation: Release 5.0.2.1. Available in :<http://dx.doi.org/10.13140/RG.2.2.29474.02242/1>.

Duarte, D. H. S. (2015). O impacto da vegetação no microclima em cidades adensadas e seu papel na adaptação aos fenômenos de aquecimento urbano. Contribuições a uma abordagem interdisciplinar - São Paulo, 2015. 167. *Tese* (Livre Docência - Departamento de Tecnologia da Arquitetura) – FAUUSP.

Emmanuel, R. (2005). An Urban Approach to Climate-Sensitive Design. Strategies for the Tropics. New York*: Spon Press*.

Emmanuel, R. (2016). Urban Climate Challenges in the Tropics: Rethinking Planning and Design Opportunities, London: *Imperial College Press*, ISBN: 9781783268405, 366 pp.

Givoni, B. (1998). Climate considerations in building and urban design. *Van Nostrand Reinhold*: New York.

Grimmond, C.S.B. Roth, M. Oke, T.R. Au, Y.C. Best, M. Betts, R. Carmichaelf, H. Cleugh. W. Dabberdt, W. Emmanuel, R. Freitas, E. Fortuniak, K. Hanna, S. Klein, P. Kalkstein, L.S. Liu, C.H. Nickson, A. Pearlmutter D. Sailor, D. and Voogt, J. (2010). Climate and More Sustainable Cities: Climate Information for Improved Planning and Management of Cities (Producers/Capabilities Perspective). *Procedia Environmental Sciences*. 247–274 pp.

Hirashima, S. Q. S; Assis, E. S; Nikolopoulou, M. (2016). Daytime thermal comfort in urban spaces: A field study in Brazil. *Building and Environment*.

Höppe, P. (1992). A new procedure to determine the mean radiant temperature outdoors. *Wetter Leben* 44:147–151.

Isaya Ndossi, M.; Avdan, U. (2016). Application of Open Source Coding Technologies in the Production of Land Surface Temperature (LST) Maps from Landsat: A PyQGIS Plugin. *Remote Sensing*, v. 8, n.5, p. 413.

Jauregui, E. (1984). Tropical urban climate: review and assessment. Proceedings, Technical Conference in Mexico City: Urban Climatology and its Applications with Special Regard to Tropical Areas, *WMO*-No 652. 26 – 45 pp.

Kawashima, R. S.; Almeida, C. M.; Giannotti, M. A.; Quintanilha, J. A. (2015). Análise das mudanças temporais de cobertura da terra na região portuária da Baixada Santista-SP e a proposição de modelos de dinâmica espacial. In: *Simpósio Brasileiro de Sensoriamento Remoto* (SBSR), 17. João Pessoa. Anais... São José dos Campos: INPE, 2015. Artigos, p. 1082-1089. DVD, On-line. ISBN 978-85-17-00076-8. Available in: http://www.dsr.inpe.br/sbsr2015/files/p0199.pdf.

Ketterer, C; Matzarakis, A. (2014). Human-biometeorological assessment of heat stress reduction by replanning measures in Stuttgart, Germany, *Landsc. Urban Plan* 122: 78–88.

Lau, K.K.-L; Lindberg, F; Rayner, D; Thorsson, S. (2015). The effect of urban geometry on mean radiant temperature under future climate change: a study of three European cities. *Int. J. Biometeorol*. 59: 799–81.

Lau, K.K.-L; Ren, C; Ho, J; Ng, E. (2016). Numerical modelling of mean radiant temperature in high-density sub-tropical urban environment. *Energy Build*. 114: 80–86.

Lee, H; Mayer, H; Chen, H. L. (2016). Contribution of trees and grasslands to the mitigation of human heat stress in a residential district of Freiburg, Southwest Germany. *Landsc. Urban Plan*. 148: 37–50.

Lindberg, F; Grimmond, C. S. B. (2019). SOLWEIG_v2018a Department of Earth Sciences, University of Gothenburg, Sweden, University of Reading, UK. Available in: https://umepdocs.readthedocs.io/en/latest/OtherManuals/SOLWEIG.html.

Lindberg, F; Grimmond, C.S.B. (2011). The influence of vegetation and building morphology on shadow patterns and mean radiant temperatures in urban areas: model development and evaluation. *Theor. Appl. Climatol*. 105: 311–323.

Lindberg, F; Holmer, B; Thorsson, S. (2008). SOLWEIG 1.0 - modelling spatial variations of 3D radiant fluxes and mean radiant temperature in complex urban settings. *Int J Biometeorol* 52:697–713

Lindberg, F; Holmer, B; Thorsson, S; Rayner, D. (2013). Characteristics of the mean radiant temperature in high latitude cities—implications for sensitive climate planning applications. *Int J Biometeorol* 58: 613–627.

Lindberg, F; Onomura, S; Grimmond, C.S.B. (2016). Influence of ground surface characteristics on the mean radiant temperature in urban areas. *Int. J. Biometeorol*. 60: 1439–1452. DOI 10.1007/s00484-016-1135-x.

Lindberg, F; Thorsson, S; Rayner, D; Lau, K. (2016). The impact of urban planning strategies on heat stress in a climate-change perspective, *Sustain. Cities Soc*. 25: 1–12.

Masmoudi, S; Mazouz, S. (2004). Relation of geometry, vegetation and thermal comfort around buildings in urban settings, the case of hot arid regions. *Energy and Buildings*.

Mayer, H; Holst, J; Dostal, P; Imbery, F; Schindler, D. (2008). Human thermal comfort in summer within an urban street canyon in Central Europe. *Meteorol* Z 17:241–250

Mayer, H; Höppe, P. (1987). Thermal comfort of man in different urban environments. *Theor. Appl. Climatol*. 38: 43–49.

Miller R, Lacambra C, Ariza C, Bloch R, Papachristodoulou N, Monroy J, Zaidi Z, Pelling M, PhungT. (2012). Climate change adaptation planning in Latin American and Caribbean Cities.

A report submitted by *ICF GHK* in association with King's College London and Grupo Laera, p 112.

Mills, G. (2011). Cubes and canyons: Different perspectives on the urban climate. In: Hebbert, M; Jankovic, V; Webb, B. (ed.). City Weathers. Meteorology and urban design 1950-2010. *Proceedings… Manchester*. p.21-24.

Oke, T.R. (1984). Urban climatology and the tropical city. In: Proceedings, Technical Conference in Mexico City: Urban Climatology and its Applications with Special Regard to Tropical Areas, *WMO*-No 652. 1-25 pp.

Oke, T.R; Mills, G; Christen, A; Voogt, J. A. (2017). Urban Climate. *Cambridge*. 525p.

Reindl, D. T; Beckman, W.A; Duffie, J.A. (1990) Diffuse fraction correlation. *Sol Energy* 45:1– 7.

Roth, M. (2007). Review of urban climate research in (sub) tropical regions. *International Journal of Climatology*. 27, 1859–1873 pp.

Shashua-Bar, L; Tsiros, I. X; Hoffman, M. (2012). Passive cooling design options to ameliorate thermal comfort in urban streets of a Mediterranean climate (Athens) under hot summer conditions, *Build. Environ*. 57: 110–119.

Shinzato, P.; Duarte, D. H. S. (2018). Impacto da vegetação nos microclimas urbanos e no conforto térmico em espaços abertos em função das interações solo-vegetação-atmosfera. *Ambiente Construído*, Porto Alegre, v. 18, n. 2, p. 197- 215.

Steward, I. D; Oke, T. R. (2012). Local climate zones for urban temperature studies Bull. Am. *Meteorol. Soc.*, 93, pp. 1879-1900, 2012, 10.1175/bams-d-11-00019.1.

Sun, S; Xu, X; Lao, Z; Lu, W; Li, Z; García, E. H; He, L; Zhu, J. (2017). Evaluating the impact of urban green space and landscape design parameters on thermal comfort in hot summer by numerical simulation. *Building and Environmental*. 123: 277-288

Thom, J. K; Coutts, A. M; Broadbent, A. M; Tappera, N. J. (2016). The influence of increasing tree cover on mean radiant temperature across a mixed development suburb in Adelaide, Australia. *Urban Forestry & Urban Greening.* 20:233 – 242.

Thorsson, S; Lindberg, F; Björklund, J; Holmer, B; Rayner, D.P. (2011). Potential changes in outdoor thermal comfort conditions in Gothenburg, Sweden due to climate change: the influence of urban geometry. *Int. J. Climatol*. 31, 324–335. https://doi.org/10.1002/joc.2231.

Thorsson, S; Rocklöv, J; Konarska, J; Lindberg, F; Holmer, B; Dousset, B; Rayne, D. (2014). Mean radiant temperature — A predictor of heat related mortality, *Urban Clim*. 10:332–345.

Voogt, J.A., Oke, T.R. (2003). Thermal remote sensing of urban climates. *Remote Sens. Environ*. 86, 370–384. https://doi.org/10.1016/s0034-4257(03)00079-8.

Weihe, W.H. (1984). Life expectancy in tropical climate and urbanization. Proceedings, Technical Conference in Mexico City: Urban Climatology and its Applications with Special Regard to Tropical Areas, *WMO*-No 652. 313 – 353 pp.

Weng, Q. (2009). Thermal infrared remote sensing for urban climate and environmental studies: methods, applications, and trends. ISPRS J. Photogram. *Remote Sens*. 64, 335–344. https://doi.org/10.1016/j.isprsjprs.2009.03.007.

Young, A. F. (2016). Adaptation actions for integrated climate risk management into urban planning: a new framework from urban typologies to build resilience capacity in Santos (SP). *City Territ Archit*.

Yu, X.; Guo, X.; Wu, Z. (2014). Land surface temperature retrieval from Landsat 8 TIRS - comparison between radiative transfer equation-based method, split window algorithm and single channel method. *Remote Sensing*, v. 6, n. 10, p. 9829-9852.

Socio-spatial inequality and its relationship to thermal (dis)comfort in two major Local Climate Zones in a tropical coastal city

Abstract

Brazil is the country with the highest social inequality in South America and it is in the ranking of the 10 countries with the highest inequality in the world. This socioeconomic disparity reflects not only on the families' income but also on the precariousness and/or lack of essential services for the human being's quality of life. This reality can also be observed in the configuration and formation of urban spaces, which have different features within the same city. Urban designs, such as building heights and orientations, streets axis, type of buildings, sky view factor, presence of green areas, as well as water bodies alter the microclimate. Therefore, these changes interfere with the thermal comfort of dwellers, especially in open spaces. In this context, this research investigates the relationship between socio-spatial inequalities and the thermal comfort of two distinct Local Climate Zones in Santos using a combination of measurement and modelling. Mean radiant temperature (Tmrt) and the physiologically equivalent temperature (PET) were simulated by using SOlar and LongWave Environmental Irradiance Geometry model (SOLWEIG) to highlight the seasonal micro-urban climate of high-rise building (HRB) and compact low-rise (CLR). The results indicate that HRB, which have the high-income average, happens to be a less stressful area in the cool and warm seasons, with a difference of Tmrt over 10°C related to CLR. On the other hand, CLR, that had the lowest income average, is the most stressful urban space, with extremely high Tmrt values scattered throughout the area. Thus, the observed precariousness of the urban environment found in the CLR seems to have a negative impact on the thermal comfort of residents throughout the year. This fact demonstrates that public and private actions tend to favor spaces with a higher concentration of income and land valuation, and consequently improve the urban design in these areas, like seafront in Santos.

Keywords: Local climate zones. Social inequality. PET. Mean radiant temperature. Thermal comfort

1. INTRODUCTION

It is well known that cities are growing rapidly, particularly in developing countries. Projections show that the proportion of global population living in urban areas will increase to 70% by 2050 (UN, 2018). The increasing urban population and quickly rising on global temperatures will put additional pressure on cities, resulting in unhealthy living conditions

(WMO, 2013; Verdonck et al., 2018). Therefore, large populations will be in developing countries, most of them located in the tropics. This projection is alarming since in these regions, in addition to the high exposure of solar radiation throughout the day, dwellers are suffering by economic inequality that is reflected in the growing precariousness of housing, in the formation of informal settlements and, consequently, in the degradation of quality and health of the inhabitants. In this context, based on World inequality report (2018), inequality is extreme in Brazil, in the Middle East, and in South Africa, the world's most unequal regions. In these three large emerging regions, inequality currently reaches extreme levels: the top 10% earners capture 55% to 65% of national income. Moreover, since urban systems are complex and uneven, and the urban atmosphere is the product of the interaction between climate variables and socioeconomic interventions, then the various social groups do not experience or relate to the urban climate in the same way. In this perspective, the urban climate may be interpreted as a social construction (Sant'Anna Neto, 2011).

One way to understand how changes in the urban environment influence the quality of health of dwellers is to assess the microclimate and its influence on the thermal comfort in different open spaces, such as streets, canyons, parks, etc. (Oke et al., 2017). Therefore, mean radiant temperature (Tmrt) is one of the four environmental parameters (followed by the air temperature, relative humidity and wind speed) that govern the human energy balance, and consequently, play an important role in human thermal comfort (Gál & Kántor, 2020). Tmrt is the net product of all short and longwave radiation fluxes from the surroundings to which a human body is exposed. When compared to other variables influencing thermal comfort, such as air temperature (Ta) and humidity, Tmrt displays larger spatial variation over short distances (Ali-Toudert & Mayer, 2007; Lindberg et al., 2013).

Thermal comfort is described as the condition of mind that expresses satisfaction with the thermal environment and it is assessed by subjective evaluation (ANSI/ASHRAE, 2005). In this way, many studies relating to outdoor thermal comfort have increased over the years (Johansson et al., 2014), especially in tropical regions (Emmanuel et al., 2007; Johansson & Emmanuel, 2006; Johansson et al., 2013; Johansson et al., 2018; Yahia et al., 2018). Many indices were developed to define and to assess thermal perception, e.g. The Standard Effective Temperature (SET) (Gagge, Fobelets, and Berglund, 1986), the Physiologically Equivalent Temperature (PET) (Höppe, 1999), and The Universal Thermal Climate Index (UTCI). Although the UTCI has recently become quite common, the most applied index is PET. Based on the Munich Energy Model for Individuals (MEMI), PET was introduced by Höppe and Mayer (1987). According to Höppe (1999), it is equivalent to the air temperature at which, in a typical indoor setting, the heat balance of the human body (work metabolism 80 W of light

activity, added to basic metabolism; heat resistance of clothing of 0.9 clo) is maintained with core and skin temperatures equal to those under the conditions being assessed. PET has been tested in different climate zones around the world (Cohen, Potchter, and Matzarakis, 2013; Hirashima et al., 2018; Hwang, Lin, and Matzarakis, 2011; Johansson & Emmanuel, 2006; Johansson & Yahia, 2011; Johansson et al., 2018; Matzarakis & Mayer, 1996; Monteiro & Alucci, 2006; Thorsson et al., 2007; Yang, Lau, and Qian, 2011).

Several studies comparing the influence of urban design on microclimate variations and their impact on Tmrt and PET have been done in the last decades, most of them using simulations through computational models to assess those impacts, e.g. Envi-met, SOLWEIG, and Rayman (Johansson & Emmanuel, 2006; Emmanuel et al., 2007; Lin et al., 2010; Yang & Lin, 2016; Anjos, 2017; Sun et al., 2017; Tan et al., 2017; Yahia et al., 2018). In this context, the city of Santos (Sao Paulo) has already been the subject of important studies in climatology and parameterization in the context of climate change (Alfredini et al., 2013; Alfredini et al., 2014; Alfredini, Arasaki, and Pezzoli, 2015; Young, 2016). However, up to the present time, there are no studies that relate and analyze the socio-spatial inequality and its influence (and negative self-feedback) on microclimate alteration in the current urban scenario or the perspective of its expansion. Thus, the aim of this research is to assess the influence of socio-spatial inequality and its underlying relationship with the urban design and fabric materials on thermal comfort in outdoor spaces at distinct Local Climate Zones in Santos, i.e. compact high-rise (HRB) and compact low-rise building (CLR). As the present study focuses on the thermal impact of built environments, Tmrt and PET seem to be the ideal approaches.

2. MATERIALS AND METHODS

2.1 Study area

The study was conducted in Santos, located in Baixada Santista Metropolitan Area (BSMA), which comprises nine municipalities (i.e. Santos, São Vicente, Cubatão, Guarujá, Praia Grande, Mongaguá, Itanhaém, Peruíbe, and Bertioga), with a population of ~1 900 000 (IBGE, 2018). Santos is separated into two distinct areas: the insular area that is the base of this study, with $39.4 \, km^2$, where 99% of the population (~ 433.000 hab.) is essentially urban (density of $10,636.7 \, hab/km^2$); and a continental area that is an environmental protected.

Climate conditions

Santos has a typical Tropical Atlantic climate influenced by the proximity of the ocean and its influences on atmospheric circulation patterns, which play an essential role in climate elements such as temperature, humidity, precipitation, and wind direction. Santos's climate is warm and wet throughout the year. Miller et al., (2012) defined October through April as the "wetter/warmer" and May through September as the "wet/warm" season. The annual temperature is about 21.9°C with a 5°C difference between summer and winter seasons. On average, Santos receives about 2.500 mm of total annual rainfall with 75 percent of the total rainfall occurring during the months from October through April (Miller et al., 2012). Regarding ventilation, sea and land breeze establish a permanent thermal exchange. In addition, winds from the south and southeast, accompanied by the polar masses, are predominant from April to September, being responsible for carrying moisture to the region and increasing cloud cover (Prata, 2005). In contrast, wind from northwest is characterized by the arrival of cold fronts, which causes changes in weather, blowing more intensely from May to August. In January, intense Northwest winds bring summer storms (Afonso, 2001).

Urban context

Several historical factors contributed to the process of Santos's urbanization. The Port complex, installed in the early 19th century, and the Anchieta highway, constructed in the middle of 20th, were the two main triggers of greater economic subsidies that contributed to the urban organization and configuration. Due to the port, the expansion of the urban area of Santos took place from its historical center, where urban equipment, public buildings, and the real estate valuation of the entire area were erected (Santos, 2012). In 1947, Anchieta highway promoted tourism to the municipality. Simultaneously, the region also went through a strong phase of industrial development, giving rise to an integrated petrochemical complex in the city of Cubatão. Thus, tourism and industry imposed a complete shift in the socio-spatial and urban configuration of the city of Santos. Demographic pressures in the insular part of the city drove real estate prices upwards. This process, associated with land shortages, had two simultaneous and direct consequences in the physical expansion of the city (Miller et al 2012; Santos, 2012; Young, 2008). The process of verticalization and valorization of land around the coast and the consequent occupation of this location by the class with the highest income. On the other hand, the accentuation of social inequalities occurred, that contributed to the migration of low-income population to the northwest side of the city and to other municipalities. These locations are marked by both difficult access and complete lack of infrastructure as well as environmentally fragile, i.e. along mangroves, rivers, and hills.

These factors have so far contributed to the development of three main areas in Santos city: (i) the southeastern region, located near the beach, where most investment and economic dynamism are concentrated; (ii) the northern area, which coincides with the old historical nucleus; and (iii) the northwest region, which concentrates residential compact low-rise buildings and a large number of informal settlements with mostly low-income residents (Miller et al, 2012).

On-site measurement

In this research, two Local Climate Zones (Fig. 33) that represent the socio-spatial inequality in the city of Santos will be analyzed. The first, compact high-rise building (HRB), located at the seafront, has the prevalence of vertical commercial and residential buildings, characterized by flats ranging from 50 to 120 m. In relation to green areas, trees, and grass patches are present, both in the horizontal beachfront park and along the drainage channels, as well as in the walkways. It is worth mentioning, that HRB has a large flux of people and vehicles over the entire year, with a significant increase in summer holidays. Moreover, based on the last Demographic census (Brazilian Institute of Geography and Statistics – IBGE, 2010), this area showed the highest nominal income, greater than R$5108 (Fig. 34)[9]. The second area, compact low-rise (CLR), situated in the northwest side, is dominated by residential compact low-rise buildings (z = 10 - 14 m). A relevant feature of this area is the occupation (starting in the 1950s) without a clear legal urban growth and sprawl regulation, resulting not only in tortuous but also narrow streets. According to the same census (IBGE, 2010), the northwest side exhibited both the lowest nominal income (Fig. 34) and a concentrated number of informal settlements. CLR is scarce of both trees and grass as well as parks. Thus, this area is densely built upon impermeable soils.

---

[9] It is worth mentioning that in 2010 the minimum wage in Brazil was R$510.
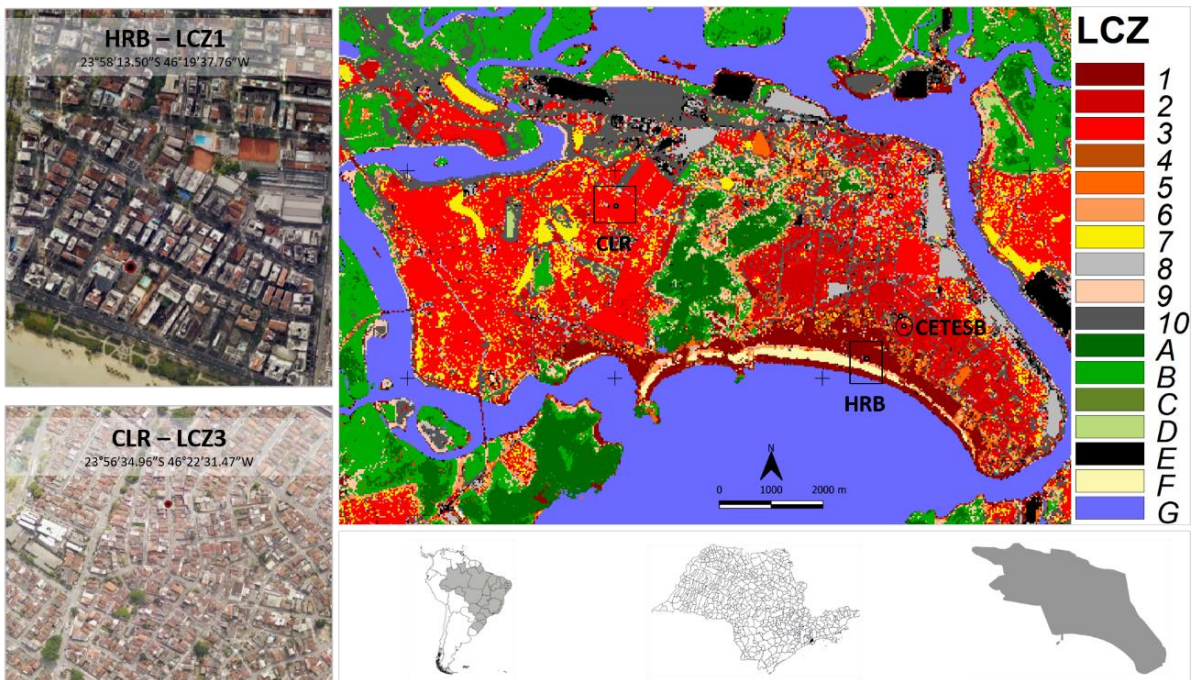
Figure 32. This figure shows the location of Santos, as well as HRB and CLR. In the images we can see the geographic coordinate of data loggers within each LCZ. In addition, the official climate station. (Environmental Company of the State of São Paulo - CETESB).
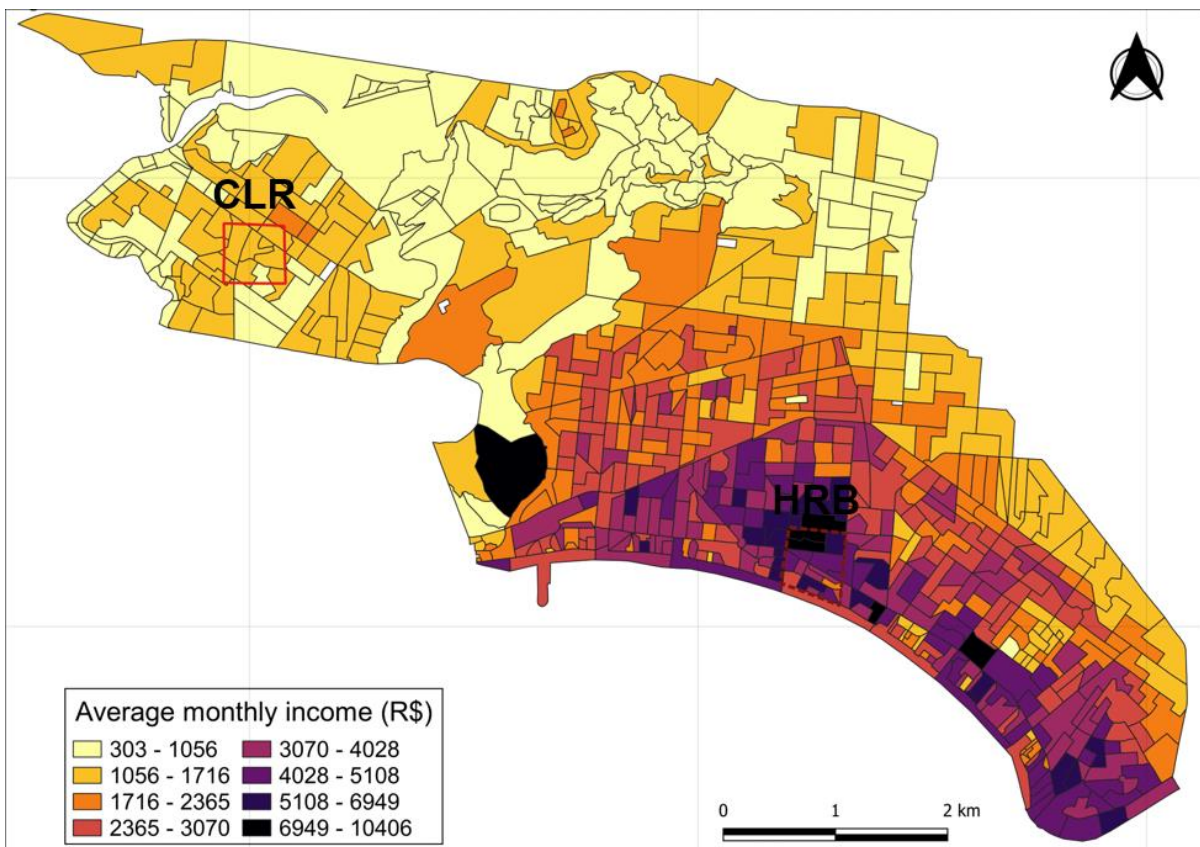
Figure 33. Value of the average monthly nominal income of persons responsible for permanent private households (IBGE census, 2010). The highlighted rectangles represent the two LCZs considered in this research, HRB and CLR.

2.2 SOLWEIG

Seasonal mean radiant temperature (Tmrt) and PET (Höppe, 1999) were calculated by using SOlar and LongWave Environmental Irradiance Geometry model (SOLWEIG). Field measurements were carried out at HRB (Fig. 35) and CLR (Fig. 36) on December 17th 2017 (summer) and August 30st 2018 (winter). These days were chosen as representative since they were relatively the most suitable for both season (calm and sunny) among the days the field measurement was carried out in Santos (15th November 2017 to 11th October 2018).

Figure 34. Urban morphology featured in HRB. Highlight for building digital surface model (DSM) (left), SVF (right), trees, and points of interest (used PET calculations).

Figure 35. Urban morphology featured in CLR. Highlight for building digital surface model (DSM) (left), SVF (right), trees, and points of interest (used for PET calculations).

Air temperature (Ta) and relative humidity (RH) were collected by data loggers (HOBO Pro v2) with a time interval of 5 min. For Ta, the accuracy is 0.2°C for the range between 0° to 50°C with 0.02°C of the resolution , and for RH, the resolution is 0.03% with an accuracy of +/- 2.5% between 10% and 90% RH (typical), to a maximum of +/- 3.5% out of this range. Each equipment was covered by a radiation shield and installed at 2.5 m from the ground. Wind speed (WS), Press (P), and Radiation (Radg), as the initial condition for SOLWEIG simulation, were provided by CETESB, located in Santos (see Fig. 33). Tables 6 and 7 summarizes the hourly meteorological data from each season for the days used in the simulations.

Table 6. Meteorological data in Summer (December 17th 2017).

Hour	HRB (°C)	HRB (RH)	CLR (°C)	CLR (RH)	WS (m/s)	Press Pa	Radg (W/m2)
10	28.0	77.4	32.0	60.5	1.0	101	661
11	29.6	72.2	33.7	59.0	1.3	101	838
12	30.7	65.9	33.5	56.4	1.5	101	975
13	32.8	58.4	34.8	52.6	1.6	101	1045
14	33.2	59.1	36.5	46.6	1.6	101	1047
15	31.8	57.61	34.94	49.72	2.0	101	976

Table 7. Meteorological data in Winter (August 30st 2018).

Hour	HRB (°C)	HRB (RH)	CLR (°C)	CLR (RH)	WS (m/s)	Press Pa	Radg (W/m2)
10	22.1	83.7	24.4	77.1	1.3	101	209
11	24.7	75.1	25.3	72.1	1.0	101	415
12	25.9	71.1	25.7	72.6	1.0	101	820
13	26.8	67.9	25.4	72.7	1.1	101	830
14	23.7	78.0	24.9	74.7	1.1	101	706
15	23.5	78.7	25.0	73.7	1.2	101	561

a) Tmrt

The SOLWEIG model estimates spatial (2-D) variations of 3-D radiation fluxes and the Tmrt in complex urban settings. Both 3D vegetation (trees and bushes) and ground cover variations are considered. In this study, SOLWEIG 2019a is used (Lindberg & Grimmond, 2019), which requires meteorological time series consisting of air temperature (Ta), relative humidity (RH), global (G), diffuse (D), and direct (I) solar radiation. Table 8 summarizes the input values of the parameters used. As diffuse and/or direct solar radiation are not commonly available, the model also permits calculation of D from G in conjunction with Ta and RH,

according to the approach described in Reindl et al. (1990). Direct shortwave radiation on a surface perpendicular to the Sun is then estimated as:

$$I = (G - D)/ sin(\eta)$$

where η is the Sun's altitude angle above the horizon (Lindberg, Onomura, and Grimmond, 2016).

Table 8 Input data and parameter settings for SOLWEIG simulation.

	Required input	**Data / Value**
Meta data	Building data	Building DEM, 1m resolution
	Vegetation data	Vegetation DSM, 1m resolution
	Weather	1hour time series of Ta, RH, Pa, RAGD and Wind Speed
Urban parameters	Emissivity of buildings walls	0.90
	Emissivity of ground surface	0.95
	Building surface albedo	0.20
	Ground surface albedo	0.15
	Transmissivity of shortwave radiation through trees	0.70
	Transmissivity of longwave radiation through trees	0.95
Personal parameters	Absorption coefficients for shortwave radiation	0.70
	Absorption coefficients for longwave radiation	0.95
	Posture	Standing

b) PET

According to the model, the calculation of thermal sensation required adjustment of the following constants: body surface has been standardized to 1.9 m^2, which represents a human with a height of 1.75 m and a bodyweight of 75 kg (Mayer & Höppe, 1987); the rate of metabolic energy transformation (work metabolism) based on 80 W for a standing person and the insulation factor of clothing (clo) has been standardized to 0.5. Age was standardized as 35 for a man. To assess the seasonality of the thermal comfort in Santos, five points of interest within both HRB and CLR were chosen (Figures 37 and 38; the spatial location of each point may be seen on Figures 35 and 36).
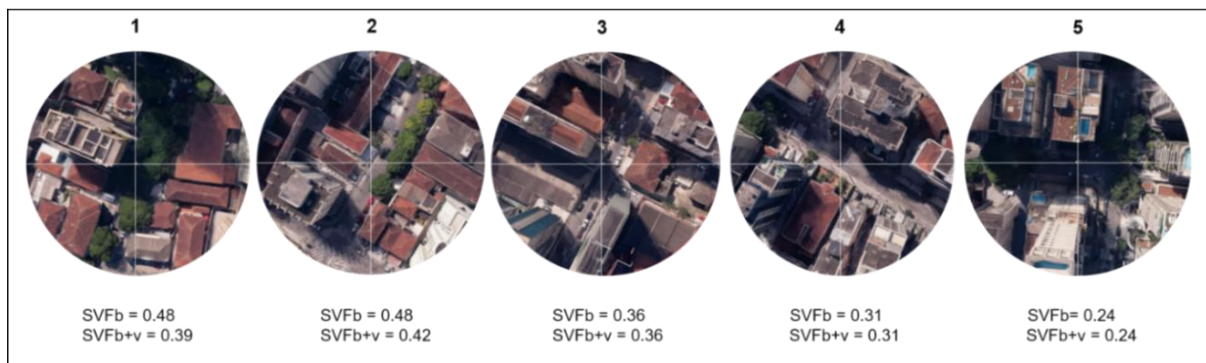
Figure 36. Points of interest from HRB. In the figure, a 50 m radius was plotted considering the point used to calculate PET in SOLWEIG. Thus, the intersection of the lines presents the analyzed point. For each Point (1 - 5) there are two SVF: the first contemplating only buildings (SVF_b), the second, buildings and vegetation (SVF_{b+v}). Source of the image: Google Earth.
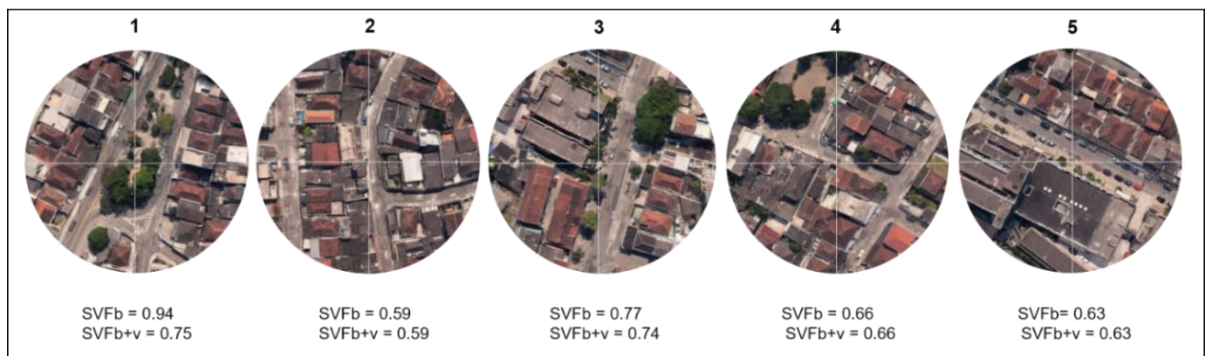
Figure 37. Points of interest from CLR. In the figure, a 50 m radius was plotted considering the point used to calculate PET in SOLWEIG. For each Point (1 - 5) there are two SVF: the first contemplating only buildings (SVF_b), the second, buildings and vegetation (SVF_{b+v}). Source of the image: Google Earth.

To better relate (and validate) PET against the actual human heat sensation, many field surveys based on questionnaires have been undertaken in different climatic zones, (Becker et al., 2003; Cohen, Potchter, and Matzarakis, 2013; Nikolopoulou, Bakera, and Steemers, 2001; Nikolopoulou & Lykoudis, 2007; Shashua-Bar, Tsiros, and Hoffman, 2012). In Brazil, studies carried out by Hirashima, Assis, and Nikolopoulou (2016) in Belo Horizonte (MG), Monteiro (2008) in São Paulo (SP) and Souza (2010) in Salvador (BA) may be highlight. For this study, PET calibrated by Monteiro (2008) (Table 9) was chosen due to the proximity of cities (~ 65 km).

Table 9 PET indices developed by Monteiro (2008).

PET (°C)	HUMAN SENSATION
4 – 12	Cool
12 – 18	Slightly cool
16 – 26	Neutral
26 – 31	Slightly warm
31 – 43	Hot
> 43	Very hot

3. RESULTS AND DISCUSSION

3.1. Seasonal variations of Tmrt

Figures 39 and 40 display the hourly seasonal variations of Tmrt for the two LCZs in Santos, from 10:00 to 15:00. During summer (Fig. 39) and for the considered time window, CLR showed a more continuous temporal pattern of Tmrt: at 11:00, the solar radiation is already very high (~800 W/m²), and because of the high Ta (above 32°C), Tmrt can exceed 65°C in sunlit areas; 41°C in green areas; and 55°C in shaded areas. Between 14:00 – 15:00, the highest values of Tmrt (over 75 °C) are scattered throughout all areas due to the higher amount of shortwave radiation reaching the surface and due to the reflection from both the ground and walls. Considering the HRB, because of the tall buildings and lower SVF, the lower values (<45°C) were found at the deep shadow cast by canyons, even at the hottest time (14 - 15h). It is noticeable that HRB shows a much more diverse spatial distribution of Tmrt compared to CLR, with standard deviation variating between 2 – 16°C during the study period. In contrast, CLR has deviations of Tmrt between 2 – 10 °C. Those values were higher between 14 - 15h for both LCZ, which highlight the importance of shades on decreasing Tmrt during the warmest period.
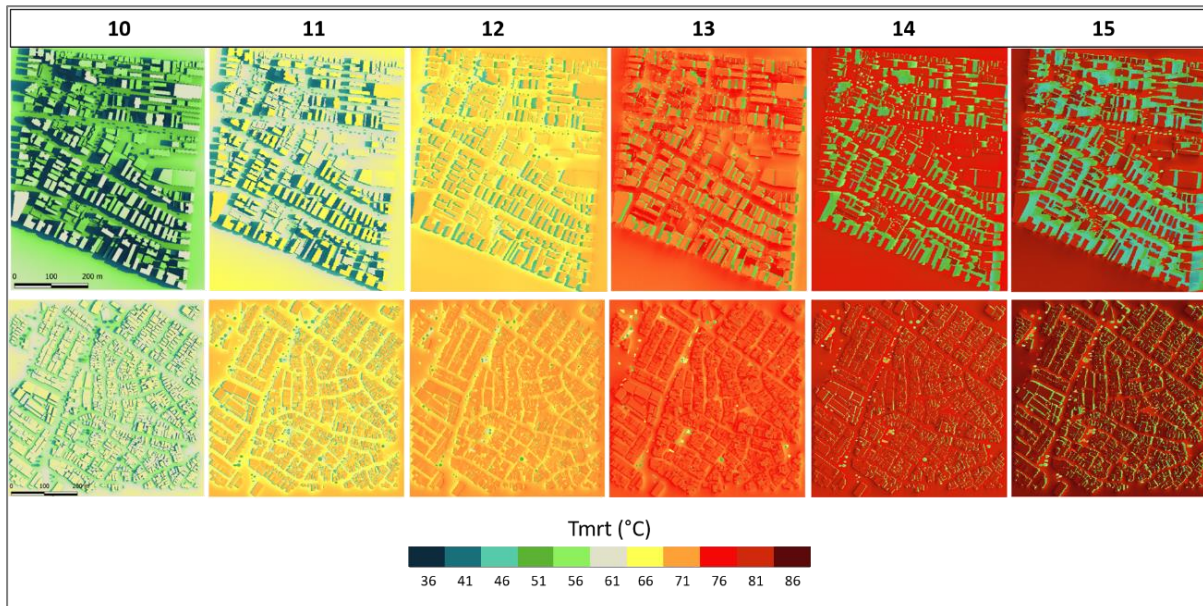
Figure 38. Hourly Tmrt maps from 10:00 to 15:00 for HRB (top) and CLR (bottom).

The difference is also reflected in the local scale. For instance, at 11:00 in HRB, for a tall building with a large open paved space in the north, the Tmrt values on this facing wall could be 25 °C higher than the Tmrt values on the shaded side. In comparison, at the same time, in CLR, Tmrt values in shaded street canyons are around 10 °C lower than the nearby open

ground space and Tmrt values in the sunlit side of E-W streets are normally 15 °C higher than in the western shaded side of nearby N-S street canyons. Nevertheless, the difference in the values of Tmrt between different locations across the site can be above 30°C (40°C at 14:00 – 15h) during the day for both LCZs.

For winter (Fig. 40), the spatial pattern of Tmrt is similar to the summer for both LCZs, but with lower Tmrt values. Thus, the maximum Tmrt for HRB and CLR was 64°C (14 – 15h). In the same way, the difference in the values of Tmrt between different locations across the same LCZ does not exceed 30°C. These results can be explained by the lower radiation (≤830 W/m^2), which promoted a decreased of ~8°C between seasons.
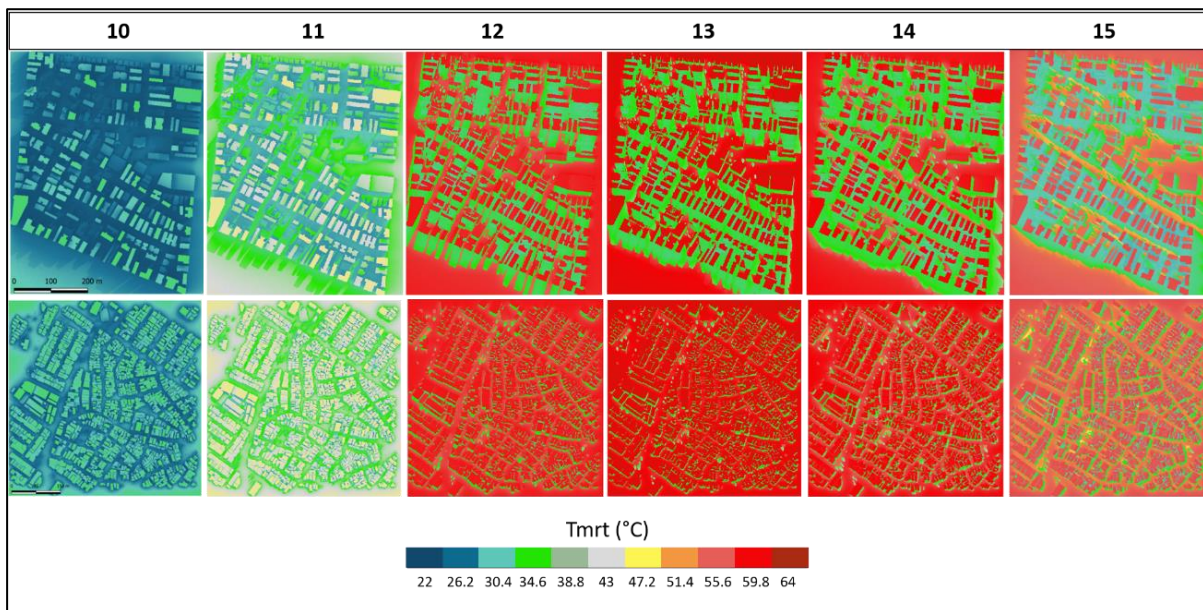
Figure 39. Hourly Tmrt maps from 10:00 to 15:00 for HRB (top) and CLR (bottom).

Considering the spatiotemporal variations of Tmrt, there are large spatial variations in daytime Tmrt within the LCZs, which are controlled mainly by urban geometry, i.e., street orientations, building height and spacing of individual street canyons (Ali-Toudert & Mayer, 20017; Lee, Mayer, and Chen, 2016; Lindberg & Grimmond, 2011; Lau et al., 2015). As observed from other studies using SOLWEIG in different latitudes (Chen et al., 2016; Lau et al., 2015; Lau et al., 2016), during clear summer days with high solar irradiance, the highest Tmrt is usually found in sunlit areas at noon or early afternoon, in most cases at 14:00. These locations experience high levels of both direct and reflected shortwave radiation, as well as longwave radiation from wall surfaces exposed to the sun (Lindberg et al., 2013; Oke et al., 2017). Nevertheless, Tmrt can reach values around 65-90°C in sub-tropical and tropical cities, such as Santos in Brazil (this study), Shanghai (Chen et al., 2016) and Hong Kong (Lau et al.,

2016) in China, while in cities at higher latitudes, like Porto, Portugal (Lau et al., 2015), the values may not exceed 65°C.

3.2 Seasonal variations of PET

The variations of thermal sensation, considering all points of interest throughout the hours (10 – 15h, in a total of 30 samples) and for the specific seasons, is indicated in Fig. 41. It can be observed that the PET values of CLR for summer are completely within the category of "very hot", which well reflects the real thermal comfort situation. Moreover, although HRB is covered by high-buildings and lower SVF, those features were not enough to promote notably better thermal comfort level in the summer, ranging mainly within "hot" and "very hot". Considering the hottest period and the sun's positions, this result can be associated to lack of shading, especially around noon time. Thus, PET values of both LCZs can even exceed 60 °C, suggesting a health concern for the citizens exposed to the direct solar radiation in hot summer days in Santos.

For the cool season, both LCZs varied among "neutral", "slightly warm", and "hot" classification. However, while HRB mainly exhibited the "neutral" category, CLR has a considerably portion of the values (over 25%) on "hot". The same occurred in studies carried out in Dar es Salaam (Yahia et al., 2018), where the lowest SVF (0.4 at City Center) displayed the lowest PET (40°C). This may be explained by the fact that compact high-rise urban morphologies can reduce the amount of direct solar radiation, which reaches the ground surface. Thus, solar exposure and SVF are two key factors that determine the daily heat balance in the urban structure (Mills, 1997).
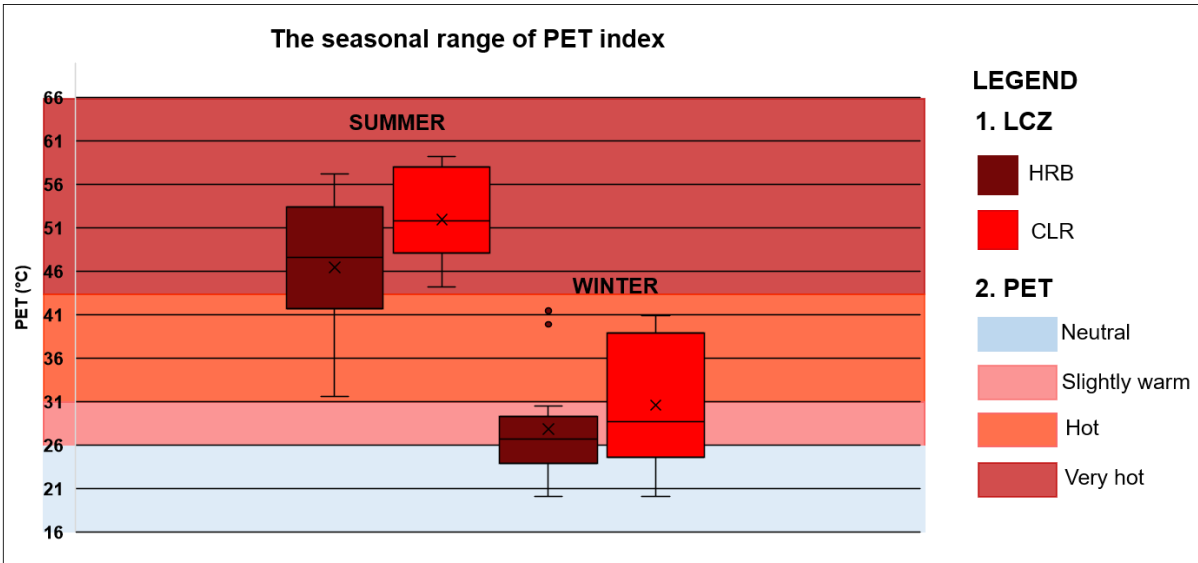

Figure 40. Seasonal range of PET between HRB and CLR.

Relating to CLR, since it represents a compact area with small variations in both SVF (Fig. 34) and height of buildings (Fig. 36) and with scarce vegetation, dwellers are more exposed to the thermal discomfort. Thus, for all points of interest, especially during summer, it is evident that the built environment had a negative impact on thermal comfort since throughout the day all points stayed in the "very hot" category with only small variations in PET ($\leq 15°C$).

From the observed results and already stated by other authors, shade seems to be crucial to maintain comfortable thermal conditions in cities located in tropics (Emmanuel, Rosenlund, and Johansson, 2007). CLR, which consists of mainly one-story buildings, displays higher PET than HRB. The results corroborated with previous studies, e.g., Emmanuel et al., 2007; Yahia, 2014, and Yahia et al., 2018. Moreover, while ΔTa (HRB - CLR) was ~4° for the warm season, $\Delta Tmrt$ (HRB – CLR) was ~10°. However, at noon, high-rise buildings cannot create shade due to the high solar elevations. It implies that additional measures, such as vegetation or shading devices, must be taken to reduce the radiant heat load at noon in tropics (Yahia et al., 2018).

Moreover, according to the Complementary Law No. 1.005, one goal of the Santos Master Plan is to increase the population density by vertical social housing in the northwest area, where CLR is localized. It may improve the thermal comfort of the dwellers in this area, since the results confirmed that CLR is under the most stressful conditions, especially in summer, compared to the HRB. It is worth mentioning that, according to the collected data, sometimes only the verticalization (e.g. low SVF) is not enough to promote thermal comfort. In this way, in addition to the shading devices, the increment in trees coverage become evident, especially in pedestrian circulation paths (Emmanuel, 2005). However, new residential projects in Santos are showing the same patterns latter years, with more launched high standard buildings in waterfront than social housing (Tables 10 and 11). Thus, this kind of constructions are serving the interests of a minority of the population that has high income, following the same trend evidenced throughout decades of urbanization.

Table 10. Projects launched in Santos in the current period.

Enterprise	Type	Standard	Neighborhood	Distance from seafront (m)
Vianna Home[10]	Residential	High	Boqueirão	1200
Times Square[1]	Residential	High	Embaré	600
Terrazas[1]	Residential	High	Ponta da Praia	600
Ville de France[1]	Residential	High	Ponta da Praia	450
Praiamar[1]	Residential	High	Aparecida	700
Praiamar [1]	Business	High	Aparecida	700

---

[10] Grupo Mendes – www.grupomendes.com.br. Acess on 21 January 2020.

Green Garden[11]	Residential	High	Embaré	800
Golden Palace[2]	Residential	High	Ponta da Praia	300
Tarumã[12]	Residencial	High	Vila Rica	200
Braúna[3]	Residencial	High	Gonzaga	400
Guanandi[3]	Residencial	High	Gonzaga	700
Barú[3]	Residencial	High	Gonzaga	1000
Tribuna Square[3]	Business	High	Town	4000
Acqua Play[13]	Residencial	High	Marapé	1200
Bossa Nova[4]	Residencial	High	Marapé	1200

Table 11. COHAB SANTISTA.

Name	Localization	Units
Caneleira IV	Morro da Caneleira	200
Santos T	Encruzilhada	133
Santos O	São Manoel	205
Santos R	Morro Nova Cintra	326

Thus, in view of the low income of large portion of population in Santos (Fig. 33), the occupation of irregular places for housing is noted in significant quantities[14], especially in the northwest area (Fig.42), specially by the informal settlements known as *Palafitas* (Fig. 42a. social housing unit in Santos (Santos O – Table 11).

---

[11] Aliança Construtora – www.aliancaconstrtutora.com.br. Acess on 21 January 2020.
[12] Vertice – www.verticesantos.com.br. Acess on 21 January 2020.
[13] Tecnisa – www.tecnisa.com.br/imoveis/sp/santos/apartamentos. Acess on 21 January 2020.
[14] It is important to highlight that 20 % of city population was living in slums according to IBGE (2010).
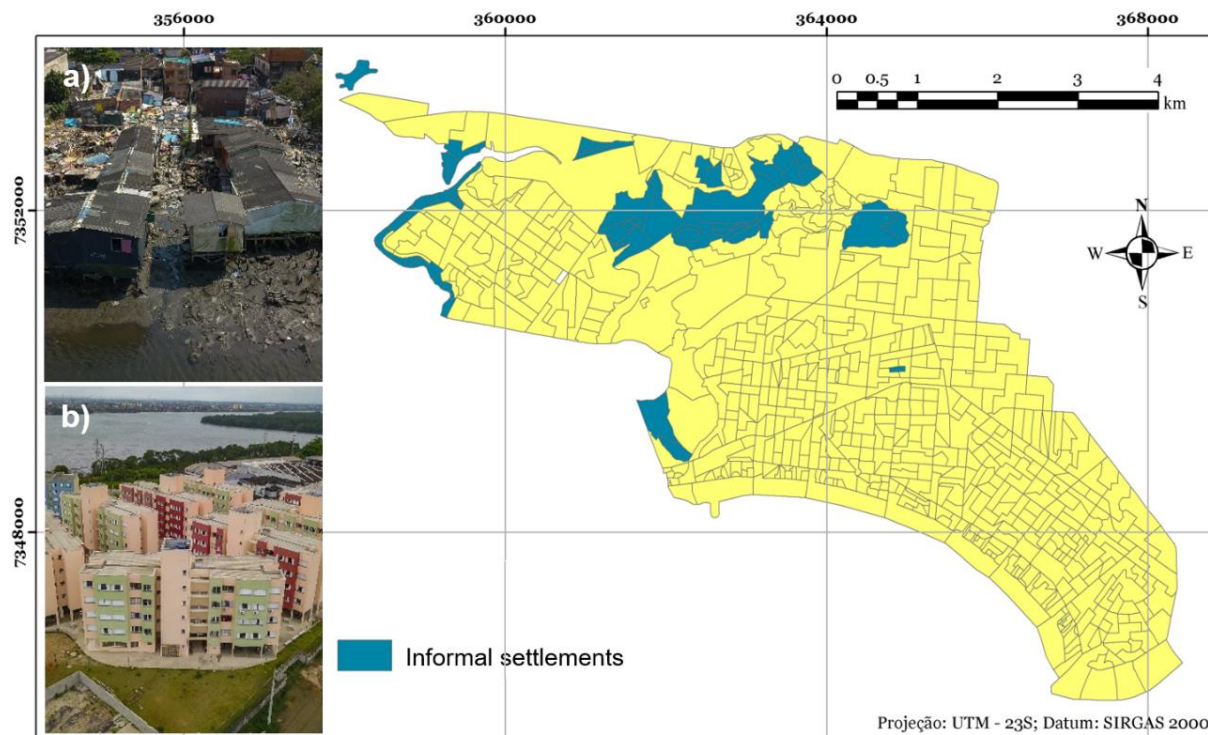
Figure 41. Informal settlements in Santos based on the last census (IBGE, 2010). A (top – left): Palafitas. B (down – left): Social housing. Source: *Portal do Governo de São Paulo*.

4. CONCLUSION

This study investigated the relationship between urban design and socio-spatial inequalities and their influence on urban microclimate and outdoor comfort in two distinct Local Climate Zones. The historical context of urbanization in Santos shows that throughout its formation, until nowadays, both public and private companies plan and define better urban environments and design in areas with greater land value, and consequently, where the high-income population is concentrated.

And this arrangement impacts in the micro-urban climate, so that spatial variation of Tmrt is found to be higher in compact low-rise than high-rise buildings due to the exposure to direct short-wave radiation. Although, areas along sunlit high building walls are also found to be hot spots, especially at 14:00 – 15:00 (Tmrt > 65°C). Thus, spatiotemporal Tmrt differences are largely influenced by both building density and height, as well as by vegetation.

Regarding the thermal sensation, in the warm season, the maximum PET was estimated to be above 60 °C in both LCZs. In matter of fact, during summer, PET was clearly above the comfort range suggested by Monteiro (2008). However, for some areas in HRB, the values stayed in the "hot" range, probably due to the increased shade and tree coverage. Thus, planting trees is obviously a useful strategy for creating shade and enhancing thermal comfort in outdoor

urban spaces. It should be an option to be considered in both LCZs, but with more urgency in CLR, due to absence of shading.

Finally, not only the location of LCZs determines the urban microclimate and the thermal comfort of residents but also the process of urbanization. This linked to the action of state and private agents, which promote spaces of overvaluation with different infrastructures, especially because of the tourism and business industry. Using other strategies on this matter could, thus, improve the life quality of all citizens.

REFERENCES

Alfredini, P; Arasaki, E; Pezzoli, A; Fournier, CP. Impact of climate changes on the Santos Harbor, São Paulo State (Brazil). Int J Mar Navig Saf Sea, 2013. p. 609-617.

Alfredini, P; Arasaki, E; Pezzoli, A; Arcorace, M; Cristofori, E. Exposure of Santos Harbor metropolitan area (Brazil) to wave and storm surge climate changes. Water Qual Expo Health. 2014.

Alfredini, P; Arasaki, E; Pezzoli, A. The impacts of sea-level rise in Santos Harbour (Brazil) for the next decades. E-proceedings of the 36th IAHR World Congress the Hague, the Netherlands, 2015, p 12.

Anjos, M. W. B. (2017). Orientações climáticas para o planejamento urbano numa cidade costeira do nordeste do Brasil: Aracaju-SE. *Tese de Doutoramento*. Universidade de Lisboa. Instituto de Geografia e Ordenamento do Território.

Becker, S., Potchter, O., Yaakov, Y. (2003). Calculated and observed human thermal sensation in an extremely hot and dry climate. *Energy and Buildings*, 35(8), 747 - 756.

Cohen, P., Potchter, O., Matzarakis, A. (2013). Human thermal perception of Coastal Mediterranean outdoor urban environments. *Applied Geography*. 1 – 10.

Hirashima, S. Q. S., Assis, E. S., Nikolopoulou, M. (2016). Daytime thermal comfort in urban spaces: A field study in Brazil. *Building and Environment*. 245 – 253.

Emmanuel R, Rosenlund H, Johansson E. (2007) Urban shading façade design option for the tropics? A study in Colombo, Sri Lanka. *Int J Climatol* 27:1995–2004.

Emmanuel R. (2005). Thermal comfort implications of urbanisation in a warm-humid city: the Colombo Metropolitan Region (CMR), Sri Lanka. *Building and Environment* 40: 1591–1601

Gagge AP, Fobelets A, Berglund LG. (1986). A standard predictive index of human response to the thermal environment. *ASHRAE Trans* 92: 709–731.

Johansson E, Emmanuel R. (2006). The influence of urban design on outdoor thermal comfort in the hot, humid city of Colombo, Sri Lanka. *Int J Biometeorol* 51:119–133.

Johansson E, Yahia MW. (2011). Subjective thermal comfort in urban spaces in the warm-humid city of Guayaquil, Ecuador. In: *Architecture and Sustainable Development* – 27th PLEA Conference, Louvain-la- Neuve, July 13–15, vol I, pp 577–582.

Johansson E, Yahia MW, Arroyo I, Bengs C. (2018). Outdoor thermal comfort in public space in warm-humid Guayaquil, Ecuador. *Int J Biometeorol* 62:387–399.

Mayer, H., Höppe, P. (1987). Thermal comfort of man in different urban environments. *Theoretical and Applied Climatology*, 38, 43 – 49.

Miller R, Lacambra C, Ariza C, Bloch R, Papachristodoulou N, Monroy J, Zaidi Z, Pelling M, PhungT. (2012). *Climate change adaptation planning in Latin American and Caribbean Cities*. A report submitted by ICF GHK in association with King's College London and Grupo Laera, p 112.

Mills, G. (1997). An urban canopy-layer climate model. *Theor Appl Climatol* 57:229–244.

Monteiro, L. M., Alucci, M. P. (2006). Calibration of outdoors thermal comfort models. In. *Passive and low energy architecture*. Proceedings of the 23rd conference, Vol. I (515 - 522), Geneva, Switzerland, 6 e 8 September.

Monteiro, L. M. (2008). Modelos preditivos de conforto térmico: quantificações de relações entre variáveis microclimáticas e de sensação térmica para avaliação e projeto de espaços abertos. *TESE*. Faculdade de arquitetura e urbanismo da Universidade de São Paulo. 378p.

Nikolopoulou, M., Lykoudis, S. (2007). Use of outdoor spaces and microclimate in a Mediterranean urban area. *Building and Environment*, 42(10), 3691e3707.

Sant'anna, Neto, J. L. (2011). O clima urbano como construção social: da vulnerabilidade polissêmica das cidades enfermas ao sofisma utópico das cidades saudáveis. *Revista Brasileira de Climatologia.*

Shashua-Bar, L., Tsiros, I. X., Hoffman, M. (2012). Passive cooling design options to ameliorate thermal comfort in urban streets of a Mediterranean climate (Athens) under hot summer conditions. *Building and Environment*, 57, 110 - 119.

Souza, S.H.M. (2010). Avaliação do desempenho térmico nos microclimas das praças: Piedade e Visconde de Cayrú, Salvador/BA. *Dissertação* (Mestrado), Programa de Pós-graduação em Engenharia Ambiental Urbana da Escola Politécnica da Universidade Federal da Bahia, Salvador.

Tan, Z; Lau, KK-L; Ng, E. (2017). Planning strategies for roadside tree planting and outdoor comfort enhancement in subtropical high- density urban areas. *Build Environ* 120:93–109.

Thorsson, S; T. Honjo, F. Lindberg, I. Eliasson, E.M. Lim. (2007). Thermal comfort and outdoor activity in Japanese urban public places. *Environmental Behavior* 39 660–684.

United Nations. 2018. Desa/Population Division. *World population/urbanization prospects*. Available in: https://population.un.org/wup/Maps

Verdonck, M; Demuzere, M; Hooyberghs, H; Beck, C; Cyrys, J; Schneider, A; Dewulf, R; Coillie, F. V. (2018). *Landscape and Urban Planning*. 178:183-197.

World Meteorological Organization. (2013). *The global climate 2001–2010*: A decade of climate extremes summary report.

Yahia, MW; Johansson, E. (2014). Landscape interventions in improving thermal comfort in the hot dry city of Damascus, Syria—the example of residential spaces with detached buildings. Landsc Urban Plan 125:1–16.

Yahia MW; Johansson E; Thorsson S; Lindberg F; Rasmussen, MI. (2018). Effect of urban design on microclimate and thermal comfort outdoors in warm-humid Dar es Salaam, Tanzania. Int J Biometeorol 62(3):373–385.

Yang F; Lau SSY; Qian F. (2011). Thermal comfort effects of urban design strategies in high-rise urban environments in a sub-tropical climate. Archit Sci Rev 54:285–304.

Yang, S-R; Lin, T-P. (2016) An integrated outdoor spaces design procedure to relieve heat stress in hot and humid regions. Build Environ 99: 149–160.

Young, A. F. Adaptation actions for integrated climate risk management into urban planning: a new framework from urban typologies to build resilience capacity in Santos (SP). *City Territ Archit*. 2016.

CONSIDERAÇÕES FINAIS

O objetivo principal da tese foi examinar a dinâmica e o comportamento térmico de diferentes Local Climate Zones em Santos (São Paulo - Brasil), usando uma combinação de medição e modelagem. Dessa maneira, dados de temperatura do ar e umidade relativa foram coletados em distintas LCZs, cada uma delas selecionadas para representar a espacialidade morfológica urbana e socioeconômica da cidade de Santos. As LCZs foram projetadas para descrever a paisagem urbana em termos das variáveis que regulam a temperatura do ar próximo à superfície, como a altura dos edifícios, o fator de visão do céu, a largura das ruas, a cobertura da superfície vegetativa, entre outros. Por meio do mapeamento das LCZs, classificamos os recortes analisados em *compact high-rise* (HRB), *compact mid-rise* (CMR), e *compact low-rise* (CLR1 e CLR2)*.* No decorrer da tese utilizamos os dados de campo e demais ferramentas, como as imagens termais do LANDSAT 8 e o modelo de simulação SOLWEIG para averiguar a dinâmica termal de cada LCZ, como a sazonalidade da Ilha de Calor Urbano (ICU), a temperatura radiante média (TRM), a temperatura de superfície (TS), e o conforto térmico (PET).

No primeiro artigo, os dados coletados foram combinados com informações de estações meteorológicas para isolar as circunstâncias climáticas que regulam a magnitude da ICU. Desta forma dados de temperatura do ar, umidade relativa, pressão, radiação, fluxo do vento, precipitação e cobertura de nuvens foram analisados. A estação INMET foi utilizada como referência para estabelecer as condições climáticas de fundo com as quais a magnitude e a variação sazonal e diurna da UHI poderiam ser medidas. Como resultado, destaca-se que em Santos a sazonalidade da magnitude da ICU está relacionada a (1) variabilidade do teor de umidade na estação de referência no verão (2) pelo clima de estabilidade estática durante o inverno. Em relação à variação diurna da ICU, as LCZs mostraram respostas térmicas distintas que devem ser repensadas para entender o papel da paisagem urbana na estratégia climática da cidade, especialmente em áreas costeiras tropicais. Assim, destaca-se principalmente os resultados encontrados para HRB e CLR2. Enquanto o ambiente urbano com baixo fator de visão do céu (HRB) proporcionou sombreamento mútuo e consequentemente amenizou a temperatura do ar durante o dia, este espaço causa impactos negativos, como maior magnitude da ICU durante à noite e a obstrução da brisa marítima nas demais áreas da cidade. Em relação a CLR2, o ambiente com alto fator de visão do céu contribui para a dispersão da energia térmica e da radiação de ondas longas durante a noite, contudo durante o dia esse tipo de ambiente urbano promove temperaturas mais altas devido à ausência de dispositivos de sombreamento.

Isso é ainda mais intensificado pela falta de áreas verdes, como parques, ou mesmo árvores nas calçadas.

No segundo artigo, para avaliar a variação espacial da TS e da TRM nas LCZs, assim como a influência da vegetação na TRM, utilizamos as imagens termais do LANDSAT 8 e o modelo urbano de simulação SOLWEIG. A diferença térmica entre as LCZs é clara no resultado obtido pela imagem do Landsat 8. Enquanto a HRB possui valores de TS entre 40 - 47°C, a CMR apresentou temperaturas entre 44 - 51°C. Por outro lado, as CLRs apresentaram valores acima de 50°C distribuídos por toda a área. Para o TS calculado usando o SOLWEIG o padrão térmico foi semelhante em todas as LCZs, com os valores mais baixos na HRB e os mais altos nas CLRs. Os resultados de TS mais baixos encontrados na HRB estão relacionados ao sombreamento mútuo dos altos edifícios, já para a CMR pode estar relacionado tanto ao sombreamento de edifícios (entre 3 a 6 andares) quanto às árvores. Já para CLRs, devido à baixa altura dos edifícios (entre 1 e 3 andares na CLR1 e majoritariamente 1 andar na CLR2) as TS além de serem mais altas são espacialmente mais homogêneas se comparadas com as demais LCZs. Em relação à influência da vegetação sobre a TRM, o tamanho do dossel apresentou um poder explicativo geral melhor do que o número de árvores (R^2 de 0,9 e 0,37, respectivamente). Além disso, a importância da vegetação em áreas sem sombreamento de edifícios, normalmente representadas pela CLR, é maior do que em um ambiente complexo como o HRB. Em conclusão, duas abordagens principais devem ser consideradas para reduzir a TRM nas cidades tropicais costeiras: aumentar a vegetação urbana e repensar o design de edifícios altos, de modo a promover conforto ao nível dos pedestres ao longo do dia, como edifícios com fachadas com coberturas ampliadas.

O terceiro artigo investiga a relação entre a desigualdade socioespacial e o conforto térmico de duas LCZs distintas em Santos, HRB e CLR, por meio da combinação da análise da TRM e do PET. Como resultado, podemos observar que o contexto histórico da urbanização de Santos, influenciado por empresas públicas e privadas, definem melhores ambientes urbanos e projetos em áreas com maior valor de terra e, consequentemente, onde a população de alta renda está concentrada. Esse arranjo interfere no microclima urbano, de modo que, a variação espacial da TRM é mais alta na HRB do que na CLR devido à exposição à radiação direta de ondas curtas ao longo do dia. Contudo, áreas expostas ao sol na HRB (paredes) foram consideradas 'hot-spots', especialmente às 14:00 - 15:00 (TRM > 65 ° C). Assim, as diferenças espaço-temporais de TRM são amplamente influenciadas pela densidade e altura do edifício, bem como pela vegetação. Em relação ao conforto térmico, no verão o PET máximo foi estimado acima de 60°C em ambas as LCZs. De fato, durante esta estação, o PET estava claramente acima da faixa de conforto sugerida por Monteiro (2008). No entanto, para algumas áreas da HRB, os

valores permaneceram na faixa "quente", provavelmente devido ao aumento da cobertura de sombra de edifícios e árvores. Assim, o plantio de árvores é obviamente uma estratégia útil para criar sombra e aumentar o conforto térmico em espaços urbanos ao ar livre. Deve ser uma opção a ser considerada em ambas as LCZs, mas com mais urgência na CLR, devido à ausência de sombreamento.

De uma forma geral, pensar o clima urbano como instrumento de planejamento é necessário, visto que, nem sempre as respostas térmicas de áreas próximas são as mesmas dentre da cidade. De tal modo, compreender cada LCZ em sua totalidade pode ser uma das ferramentas mais eficiente para propor projetos que englobem tanto a qualidade ambiental como de conforto térmico dos moradores de cada área. Além disso, fica claro a importância de os planejadores urbanos compreender e integrar os diferentes aspectos que interferem na diferenciação da dinâmica e no comportamento térmico encontrados nas LCZs. Por exemplo, ao repensar a expansão da zona noroeste a partir da verticalização, deve-se levar em consideração a qualidade de vida dos que já residem e dos novos moradores desta região. Visto que, ficou evidente que os moradores da CLR2 são os que sofrem maior desconforto térmico ao longo dos dias, inclusive durante o inverno. Contudo, vale relembrar que, principalmente nesta LCZ, não apenas os tipos de construções, assim como toda a infraestrutura urbana dirigida pelo poder público, disponível (ou não) nesta área (vegetação, espaços abertos permeáveis, ruas e calçadas estreitas), são responsáveis pelas condições climáticas que não favorecem a população residente. Como ressaltado anteriormente, este é um dos processos que acarretam a desigualdade climática entre os citadinos. Destaca-se, desta forma, que não há somente a necessidade de integração entre climatologia urbana e planejamento urbano, mas também o incentivo (e interesse) em propostas e projetos pelo meio público e privado, principalmente em áreas mais vulneráveis, na formação de ambientes urbanos sustentáveis.

REFERÊNCIAS

Acero, J. A; Arrizabalaga, J. (2016). Evaluating the performance of ENVI-met model in diurnal cycles for different meteorological conditions. Theoretical and Applied Climatology. November.

Alexander, P. J; Mills, Gerald; Fealy, R. (2015). Urban Climate Using LCZ data to run an urban energy balance model. Urban Climate, 13, 14–37. https://doi.org/10.1016/j.uclim.2015.05.001

Alves, A. C. N; Andrade, T. C. Q; Nery, J. M. F. G. (2011). A Influência da vegetação e da ocupação do solo no clima urbano: Um exercício analítico sobre a Avenida Paralela. Fórum Patrimônio: Ambiente Construído e Patrimônio Sustentável. Belo Horizonte.

Alfredini, P; Arasaki, E; Pezzoli, A; Fournier, C. P. (2013). Impact of climate changes on the Santos Harbor, São Paulo State (Brazil). Int J Mar Navig Saf Sea. p. 609-617.

Alfredini, P; Arasaki, E; Pezzoli, A; Arcorace, M; Cristofori, E. Exposure of Santos Harbor metropolitan area (Brazil) to wave and storm surge climate changes. Water Qual Expo Health. 2014.

Alfredini, P; Arasaki, E; Pezzoli, A. The impacts of sea level rise in Santos Harbour (Brazil) for next decades. E-proceedings of the 36th IAHR World Congress The Hague, the Netherlands, 2015, p 12.

Bueno, L. M. M; Tangari, V R; Silva, Jm P; Pezzuto, C. C; Montezuma, R. C. M; Rego, A. Q. Paisagem Ambiente: ensaios - n. 30 - São Paulo - p. 123 - 136- 2012. Mudanças climáticas e as formas de ocupação urbana: processo de criação de cenários socioambientais.

Duarte, D. H. S. O impacto da vegetação no microclima em cidades adensadas e seu papel na adaptação aos fenômenos de aquecimento urbano. Contribuições a uma abordagem intersdisciplinar. 2015. Tese (Livre Docência - Departamento de Tecnologia da Arquitetura) – FAUUSP. 167p.

Emmanuel, R; Rosenlund, H; Johansson, E. Urban shading – a design option for the tropics? A study in Colombo, Sri Lanka. International Journal of Climatology. Setembro, 2007.
Fialho, E. S. ILHA DE CALOR: REFLEXÕES ACERCA DE UM CONCEITO. ACTA Geográfica, Boa Vista, Ed. Esp. Climatologia Geográfica, 2012, p.61-76.

Gusson, C. S. Efeito da densidade construída sobre o microclima urbano: construção de diferentes cenários possíveis e seus efeitos no balanço de energia de áreas urbanas. São Paulo, 2014. Dissertação (Mestrado em Arquitetura e Urbanismo) – Faculdade de Arquitetura e Urbanismo, Universidade de São Paulo.

Hammerberg, K; Brousse, O; Martilli, A; Mahdavi, A. (2018). Implications of employing detailed urban canopy parameters for mesoscale climate modelling: A comparison between WUDAPT and GIS databases over Vienna, Austria. International Journal of Climatology. https://doi.org/10.1002/joc.5447

Instituto Brasileiro de Geografia e Estatística – IBGE. Indicadores de desenvolvimento sustentável. Rio de Janeiro: IBGE, 2002.

Järvi, L; Grimmond, C. S. B; Christen, A. (2011). The Surface Urban Energy and Water Balance Scheme (SUEWS): Evaluation in Los Angeles and Vancouver. Journal of Hydrology, 411, 219–237. https://doi.org/10.1016/j.jhydrol.2011.10.001

Krüger, E.L; Minella, F.O; Rasia, F. Impact of urban geometry on outdoor thermal comfort and air quality from field measurements in Curitiba, Brazil. Building and Environment Journal. September, 2010.

Lima, Rejane. Calor aumenta o número de mortes na Baixada. O Estado de São Paulo. São Paulo. 11 fev. 2010. Disponível em: <http://www.estadao.com.br/noticias/cidades,calor-aumenta-numero-de-mortes na-baixada,509652,0.htm.

Landsberg, H. The climate if towns. In: THOMAS, W. L. (Org.) Man's Role in Changing the face of the Earth. Vol. 2, p. 584 606. Tradução por AZEVEDO, T. R. Revista do Departamento de Geografia, FFLCH/USP 18, 2006.

Lombardo, m. a. Ilha de Calor nas Metrópoles: o exemplo de São Paulo. São Paulo: Editora HUCITEC, 1985, 245p.

Masiero, E. Análise da influência de corpos d´água em microclimas urbanos: estudo de caso em são José do Rio Preto, SP. Tese em Engenharia Urbana. Universidade Federal de São Carlos. 2014. São Carlos. 141p.

Mills, G; Ching, J; See, L; Bechtel, B; Feddema, J; Masson, V; Stewart, I; Neophytou, M; O'connor, M; Chen, F; Martilli, A; Grimmond, S; Alexander,P; Foley, M; Gal, T; Wang, X; Mitra, C; Pereira, N; Steeneveld, G.J. 2015. Introduction to the WUDAPT Project. The 9th International Conference on Urban Climate. Toulouse, France.

Nobre, C. et. al. Vulnerabilidade das megacidades brasileiras às mudanças climáticas: A região metropolitana de São Paulo. Junho de 2010. Disponível em http://www.inpe.br/noticias/arquivos/pdf/megacidades.pdf

OBSERVATORIO DO CLIMA. Diretrizes para Formulação de Políticas Públicas em Mudanças Climáticas no Brasil. Organização: Mario Monzoni, Coordenação: Rachel Biderman; Orientação Técnica e Política: Fabio Feldmann. Pesquisadoras Responsáveis: Michelle Muhringer Shayer e Luciana Betiol. 2009

Oke, T. R. Boundary Layer Climates. 2nd ed. Methuen, London, 1987, 435 p.

O'malley, C; Piroozfar, P; Farr, E. R. P; Pomponi, F. Urban Heat Island (UHI) mitigating strategies: A case-based comparative analysis. Sustainable Cities and Society Journal. Junho, 2015.

PAINEL BRASILEIRO DE MUDANÇAS CLIMÁTICAS. Relatórios. Disponível em: http://www.pbmc.coppe.ufrj.br/pt/publicacoes/relatorios-pbmc. Acesso: 03/04/2017.

Perera, N. G. R; Emmanuel, R. A. 2018. "Local Climate Zone" based approach to urban planning in Colombo, Sri Lanka. Urban Climate 23: 188–203

Prata, A. R. Impacto da altura de edifícios nas condições de ventilação natural do meio urbano. 2005. Tese em Arquitetura e Urbanismo. Universidade de São Paulo. São Paulo. 243p.

Rafael, S; Martins, H; Marta-Almeida, M; Sá, E; Coelho, S; Rocha, A; Borrego, C. (2017). Quantification and mapping of urban fluxes under climate change: Application of WRF-SUEWS model to Greater Porto area (Portugal). Environmental Research, 321–334. https://doi.org/10.1016/j.envres.2017.02.033

Schmitz, L. K. Reestruturação urbana e conforto térmico em Curitiba/PR: Diagnóstico, Modelagem e Cenários. 2014. Tese em Geografia. Universidade Federal do Paraná. Curitiba. 298p.

Secretaria de Planejamento e Desenvolvimento Sustentável. Caracterização Socioeconômica de São Paulo Região Metropolitana da Baixada Santista, 2011. Governo do Estado de São Paulo. Disponível em:http://www.planejamento.sp.gov.br/noti_anexo/files/uam/trabalhos/RMBS.pdf

Soares, a. r; silva f. s; santos, m. p; carvalho, h. j. m; santos, m. a. Calibração do software ENVI-met ao clima de João Pessoa - PB: aplicação ao Campus João Pessoa do IFPB. In: 7ª SEMANA DE CIÊNCIA E TECNOLOGIA DO IFPB. Campus João Pessoa. Instituto Federal de Educação, Ciência e Tecnologia. Paraíba, Campus João Pessoa. 2011. 8 p.

Wang, Y; Berardi, U; Akbari, H. Comparing the effects of urban heat island mitigation strategies for Toronto, Canada. Energy & Buildings. Junho, 2015.

Young, A. F. Adaptation actions for integrated climate risk management into urban planning: a new framework from urban typologies to build resilience capacity in Santos (SP). City Territ Archit. 2016.

Zündt, C. Baixada Santista: Uso, Expansão e Ocupação do Solo, Estruturação da Rede Urbana Regional e Metropolização. Campinas: Editora dos textos NEPO, 2006.